Fractional Abelian topological phases of matter for fermions in two-dimensional space

Christopher Mudry

Condensed Matter Theory Group, Paul Scherrer Institute, CH-5232 Villigen PSI, Switzerland

Contents

1
Introduction

During these lectures, I will focus exclusively on two-dimensional realizations of fractional topological insulators. However, before doing so, I need to revisit the definition of non-interacting topological phases of matter for fermions and, for this matter, I would like to attempt to place some of the recurrent concepts that have been used during this school on a time line that starts in 1931.

Topology in physics enters the scene in 1931 when Dirac showed that the existence of magnetic monopoles in quantum mechanics implies the quantization of the electric and magnetic charge. [24]

In the same decade, Tamm and Shockley surmised from the band theory of Bloch that surface states can appear at the boundaries of band insulators (see Fig. 1.1). [115, 110]

The dramatic importance of static and local disorder for electronic quantum transport had been overlooked until 1957 when Anderson showed that sufficiently strong disorder "generically" localizes a bulk electron. [5] That there can be exceptions to this rule follows from reinterpreting the demonstration by Dyson in 1953 that disordered phonons in a linear chain can acquire a diverging density of states at zero energy with the help of bosonization tools in one-dimensional space (see Fig. 1.2). [25]

Following the proposal by Wigner to model nuclear interactions with the help of random matrix theory, Dyson introduced the threefold way in 1963, [26] i.e., the study of the joint probability distribution

$$P(\theta_1, \cdots, \theta_N) \propto \prod_{1 \leq j < k \leq N} \left| e^{\mathrm{i}\theta_j} - e^{\mathrm{i}\theta_k} \right|^{\beta}, \qquad \beta = 1, 2, 4, \tag{1.1}$$

for the eigenvalues of unitary matrices of rank N generated by random Hamiltonians without any symmetry ($\beta = 2$), by random Hamiltonians with time-reversal symmetry corresponding to spin-0 particles ($\beta = 1$), and by random Hamiltonians with time-reversal symmetry corresponding to spin-$1/2$ particles ($\beta = 4$).

Topology acquired a mainstream status in physics as of 1973 with the disovery of Berezinskii and of Kosterlitz and Thousless that topological defects in magnetic classical textures can drive a phase transition. [9, 66, 65] In turn, there is an intimate connection between topological defects of classical background fields in the presence of which electrons propagate and fermionic zero modes, as was demonstrated by Jackiw and Rebbi in 1976 (see Fig. 1.3). [51, 114]

The 70's witnessed the birth of lattice gauge theory as a mean to regularize quantum chromodynamics (QCD_4). Regularizing the standard model on the lattice proved to be more difficult because of the Nielsen-Ninomiya no-go theorem that prohibits defining a theory of chiral

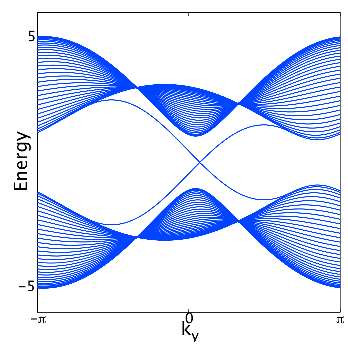

Fig. 1.1 Single-particle spectrum of a Bogoliubov-de-Gennes superconductor in a cylindrical geometry which is the direct sum of a $p_x + \mathrm{i}p_y$ and of a $p_x - \mathrm{i}p_y$ superconductor (after P-Y. Chang, C. Mudry, and S. Ryu, arXiv:1403.6176). The two-fold degenerate dispersion of two chiral edge states are seen to cross the mean-field superconducting gap. There is a single pair of Kramers degenerate edge state that disperses along one edge of the cylinder.

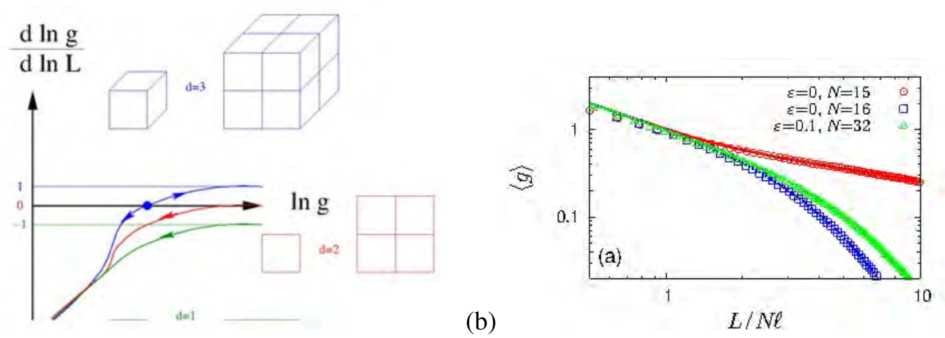

Fig. 1.2 (a) The beta function of the dimensionless conductance g is plotted (qualitatively) as a function of the linear system size L in the orthogonal symmetry class ($\beta = 1$) when space is of dimensionality $d = 1$, $d = 2$, and $d = 3$, respectively. (b) The dependence of the mean Landauer conductance $\langle g \rangle$ for a quasi-one-dimensional wire as a function of the length of the wire L in the symmetry class BD1. The number N of channel is varied as well as the chemical potential ε of the leads. [Taken from P. W. Brouwer, A. Furusaki, C. Mudry, S. Ryu, BUTSURI 60, 935 (2005)]

fermions on a lattice in odd-dimensional space without violating locality or time-reversal symmetry. [90,89,91] This is known as the fermion-doubling problem when regularizing the Dirac equation in d-dimensional space on a d-dimensional lattice.

The 80's opened with a big bang. The integer quantum Hall effect (IQHE) was discovered in 1980 by von Klitzing, Dorda, and Pepper (see Fig. 1.4), [63] while the fractional quantum Hall effect (FQHE) was discovered in 1982 by Tsui, Stormer, and Gossard. [118] At integer fillings of the Landau levels, the non-interacting ground state is unique and the screened Coulomb interaction V_{int} can be treated perturbatively, as long as transitions between Landau levels or outside the confining potential V_{conf} along the magnetic field are suppressed by the

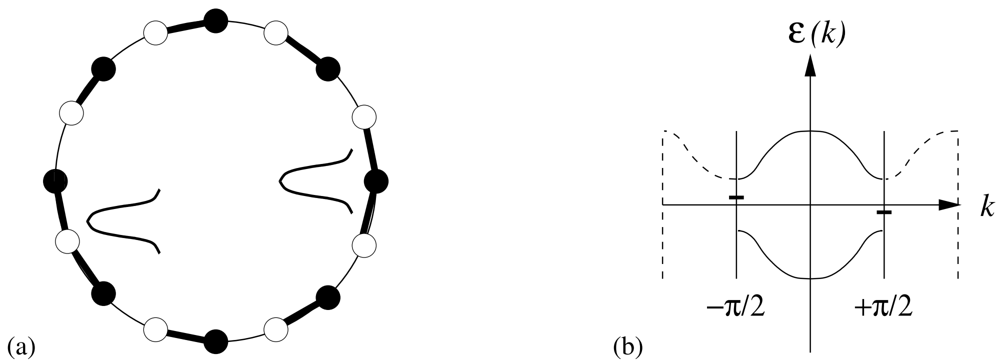

Fig. 1.3 (a) Nearest-neighbor hopping of a spinless fermion along a ring with a real-valued hopping amplitude that is larger on the thick bonds than on the thin bonds. There are two defective sites, each of which are shared by two thick bonds. (b) The single-particle spectrum is gapped at half-filling. There are two bound states within this gap, each exponentially localized around one of the defective sites, whose energy is split from the band center by an energy that decreases exponentially fast with the separation of the two defects.

single-particle gaps $\hbar\,\omega_{\mathrm{c}}$ and V_{conf}, respectively,

$$V_{\mathrm{int}} \ll \hbar\,\omega_{\mathrm{c}} \ll V_{\mathrm{conf}}, \qquad \omega_{\mathrm{c}} = e\,B/(m\,c). \tag{1.2}$$

When Galilean invariance is not broken, the conductivity tensor is then given by the classical Drude formula

$$\lim_{\tau\to\infty} \boldsymbol{j} = \begin{pmatrix} 0 & +\,(B\,R_{\mathrm{H}})^{-1} \\ -\,(B\,R_{\mathrm{H}})^{-1} & 0 \end{pmatrix} \boldsymbol{E}, \qquad R_{\mathrm{H}}^{-1} := -n\,e\,c, \tag{1.3}$$

that relates the (expectation value of the) electronic current density $\boldsymbol{j} \in \mathbb{R}^2$ to an applied electric field $\boldsymbol{E} \in \mathbb{R}^2$ within the plane perpendicular to the applied static and uniform magnetic field $\boldsymbol{B}$ in the ballistic regime ($\tau \to \infty$ is the scattering time). The electronic density, the electronic charge, and the speed of light are denoted n, e, and c, respectively. Moderate disorder is an essential ingredient to observe the IQHE, for it allows the Hall conductivity to develop plateaus at sufficiently low temperatures that are readily visible experimentally (see Fig. 1.4). These plateaus are a consequence of the fact that most single-particle states in a Landau level are localized by disorder, according to Anderson's insight that any quantum interference induced by a static and local disorder almost always lead to localization in one- and two-dimensional space. The caveat "almost" is crucial here, for the very observation of transitions between Landau plateaus implies that not all single-particle Landau levels are localized.

The explanation for the integer quantum Hall effect followed quickly its discovery owing to a very general argument of Laughlin based on gauge invariance that implies that the Hall conductivity must take a fractional value if the longitudinal conductivity vanishes (mobility gap). [67] This argument was complemented by an argument of Halperin stressing the crucial role played by edge states when electrons in the quantum Hall effect are confined to a strip geometry (see Fig. 1.5), [47] while works from Thouless, Kohmoto, Nightingale, den Nijs and

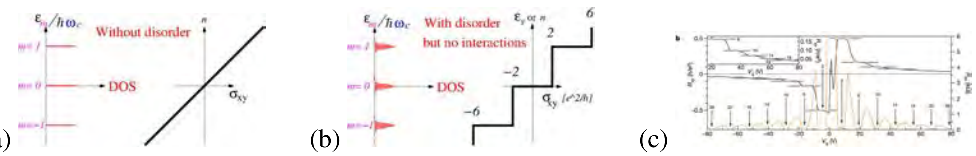

(a) (b) (c)

Fig. 1.4 (a) The Hall conductivity is a linear function of the electron density if Galilean invariance holds. (b) Galilean invariance is broken in the presence of disorder so that plateaus become evident at integral filling fractions of the Landau levels. (c) Graphene deposited on SiO_2/Si, T=1.6 K and B=9 T (inset T=30 mK) support the integer quantum Hall effect at the filling fractions $\nu = \pm 2, \pm 6, \pm 10, \cdots = \pm 2(2n+1)$, $n \in \mathbb{N}$. [Taken from Zhang et al., Nature **438**, 201 (2005)]

Niu demonstrated that the Hall response is, within linear response theory, proportional to the topological invariant

$$C \coloneqq -\frac{\mathrm{i}}{2\pi} \int_0^{2\pi} \mathrm{d}\phi \int_0^{2\pi} \mathrm{d}\varphi \left[\left\langle \frac{\partial \Psi}{\partial \phi} \middle| \frac{\partial \Psi}{\partial \varphi} \right\rangle - \left\langle \frac{\partial \Psi}{\partial \varphi} \middle| \frac{\partial \Psi}{\partial \phi} \right\rangle \right] \tag{1.4}$$

that characterizes the many-body ground state $|\Psi\rangle$ obeying twisted boundary conditions in the quantum Hall effect. [117, 111, 92, 93] Together, these arguments constitute the first example of the bulk-edge correspondence with observable consequences, namely the distinctive signatures of both the integer and the fractional quantum Hall effect.

The transitions between plateaus in the quantum Hall effect are the manifestations at finite temperature and for a system of finite size of a continuous quantum phase transition, i.e., of a singular dependence of the conductivity tensor on the magnetic field (filling fraction) that is rounded by a non-vanishing temperature or by the finite linear size of a sample. In the non-interacting limit, as was the case for the Dyson singularity at the band center, an isolated bulk single-particle state must become critical in the presence of not-too strong disorder. The one-parameter scaling theory of Anderson localization that had been initiated by Wegner and was encoded by a class on non-linear-sigma models (NLSMs) has to be incomplete. [123, 3, 50] Khmelnitskii, on the one hand, and Levine, Libby, and Pruisken, on the other hand, introduced in 1983 a two-parameter scaling theory for the IQHE on phenomenological grounds. [57, 71, 96] They also argued that the NLSM for the IQHE, when augmented by a topological θ term, would reproduce the two-parameter flow diagram (see Fig. 1.6). This remarkable development took place simultaneously with the works on Haldane on encoding the difference between half-integer and integer spin chains (Haldane's conjecture) by the presence of a $\theta = \pi$ topological term in the $O(3)$ NLSM [42, 44] and by the work of Witten [130] on principal chiral models augmented by a Wess-Zumino-Novikow-Witten (WZNW) term.

Deciphering the critical theory for the plateau transition is perhaps the most tantalizing challenge in the theory of Anderson localization. Among the many interesting avenues that have been proposed to reach this goal (that remains elusive so far), Ludwig, Fisher, Shankar, and Grinstein studied random Dirac fermions in two-dimensional space in 1994 (see Fig. 1.7), [75] motivated as they were by the fact that a massive Dirac fermion in two-dimensional space carries the fractional value

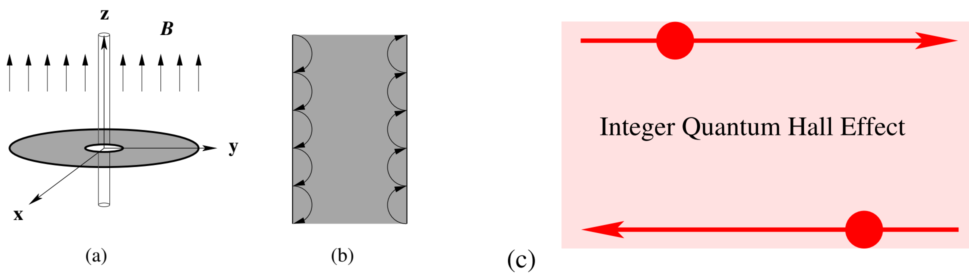

Fig. 1.5 Chiral edges are immune to backscattering within each traffic lane.

$$\sigma_{\rm H}^{\rm Dirac} = \pm \frac{1}{2} \frac{e^2}{h} \tag{1.5}$$

according to Deser, Jackiw, and Templeton [23] and that it is possible to regularize two such massive Dirac fermions on a two-band lattice model realizing a Chern insulator according to Haldane. [45]

The early 90's were also the golden age of mesoscopic physics, the application of random matrix theory to condensed matter physics. The threefold way had been applied successfully to quantum dots and quantum transport in quasi-one-dimensional geometries. Zirnbauer in 1996 and Altland and Zirnbauer in 1997 extended the threefold way of Dyson to the tenfold way by including three symmetry classes of relevance to quantum chromodynamics called the chiral classes, and four symmetry classes of relevance to superconducting quantum dots (see Table 1.1). [133, 4, 49] Quantum transport in quasi-one-dimensional wires belonging to the chiral and superconducting classes was studied by Brouwer, Mudry, Simons, and Altland and by Brouwer, Furusaki, Gruzberg, Mudry, respectively (see Fig. 1.8). [15, 14, 12, 13] Unlike in the threefold way, the three chiral symmetry classes and two of the four superconducting classes (the symmetry classes D and DIII) were shown to realize quantum critical point separating localized phases in quasi-one-dimensional arrays of wires. The diverging nature of the density of states at the band center (the disorder is of vanishing mean) for five of the ten symmetry classes in Table 1.2 is a signature of topologically protected zero modes bound to point defects. These point defects are vanishing values of an order parameter (domain walls) responsible of a spectral if translation symmetry was restored.

Lattice realizations of $\mathbb{Z}_2$ topological band insulators in two-dimensional space were proposed by Kane and Mele in Refs. [54,55] and in three-dimensional space by Refs. [81,99,35]. This theoretical discovery initiated in Refs. [102, 101] the search of Dirac Hamiltonians belonging to the two-dimensional symmetry classes AII and CII from Table 1.1 for which the corresponding NLSM encoding the effects of static and local disorder were augmented by a topological term so as to evade Anderson localization on the boundary of a $d = 3$-dimensional topological insulators. Following this route for all symmetry classes and for all dimensions, Ryu, Schnyder, Furusaki, and Ludwig arrived at the periodic Table 1.3. [106, 107, 103] The same table was derived independently by Kitaev using a mathematical construction known as K theory that he applied to gapped Hamiltonians in the bulk (upon the imposition of periodic boundary conditions, say) in the clean limit. [58] This table specifies in any given dimension d of space, for which symmetry classes it is possible to realize a many-body ground state for non-interacting fermions subject to a static and local disorder such that all bulk states

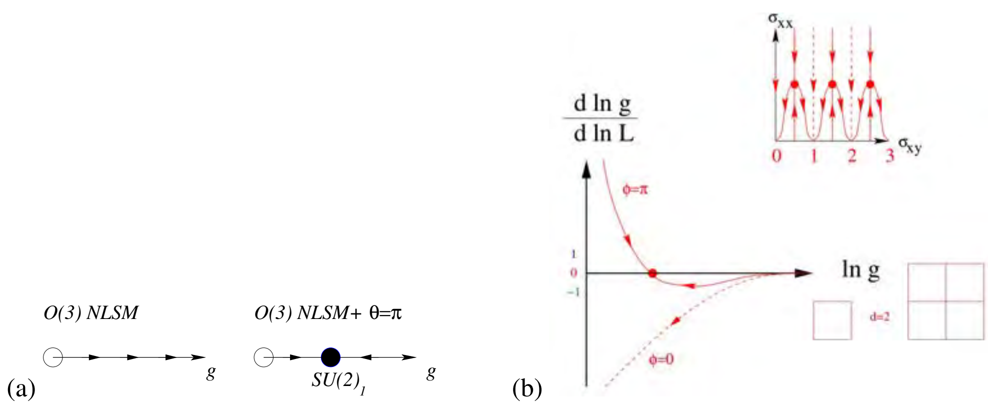

Fig. 1.6 (a) A topological $\theta = \pi$ term modifies the RG flow to strong coupling in the two-dimensional $O(3)$ non-linear-sigma model. There exists a stable critical point at intermediary coupling that realizes the conformal field theory $SU(2)_1$. (b) Pruisken argues that the phenomenological two-parameter flow diagram of Khmelnitskii is a consequence of augmenting the NLSM in the unitary symmetry class by a topological term.

are localized but there exist a certain (topological) number of boundary states, that remain delocalized.

The goals of these lectures are the following.

- First, I would like to rederive the tenfold way for non-interacting fermions in the presence of local interactions and static local disorder.
- Second, I would like to decide if interactions between fermions can produce topological phases of matter with protected boundary states that are not captured by the tenfold way.

This program will be applied in two-dimensional space.

These lectures are organized as follows. Section 2 motivates the tenfold way by deriving it explicitly in quasi-one-dimensional space. Section 3 is a review of Abelian chiral bosonization, the technical tool that allows one to go beyond the tenfold way so as to incorporate the effects of many-body interactions. Abelian chiral bosonization is applied in Sec. 4 to demonstrate the stability of the gapless helical edge states in the symmetry class AII in the presence of disorder and many-body interactions. Abelian chiral bosonization is applied in Sec. 5 to construct microscopically long-ranged entangled phases of two-dimensional quantum matter.

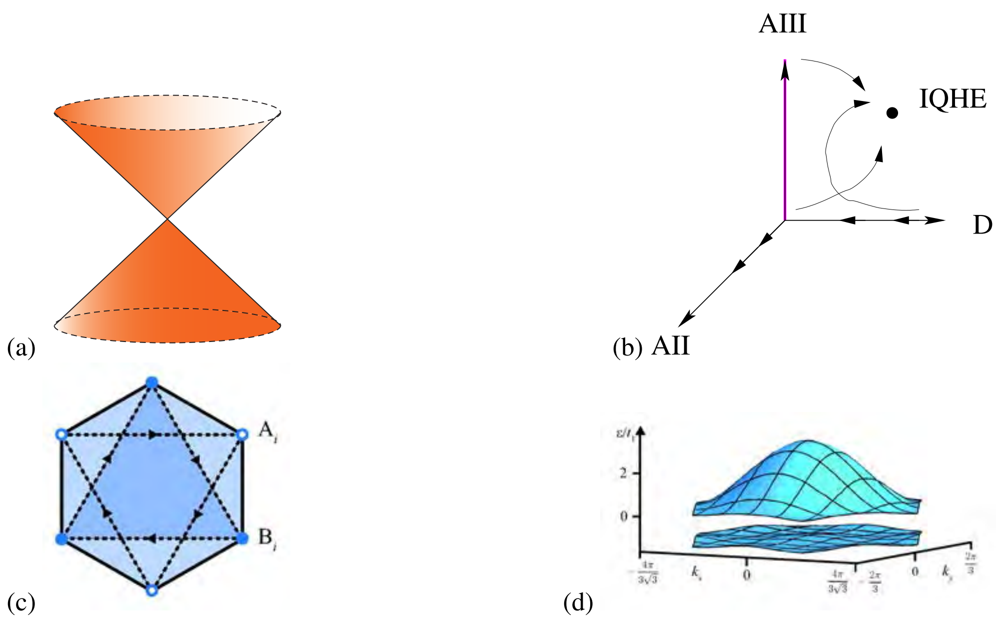

Fig. 1.7 (a) A single (non-degenerate) cone of Dirac fermions in two-dimensional space realizes a critical point between two massive phases of Dirac fermions, each of which carries the Hall conductance $\sigma_{\mathrm{H}}^{\mathrm{Dirac}} = \pm(1/2)$ in units of e^2/h. (b) A generic static and local random perturbation of a single Dirac cone is encoded by three channels. There is a random vector potential that realizes the symmetry class AIII if it is the only one present. There is a random scalar potential that realizes the symmetry class AII if it is the only one present. There is a random mass that realizes the symmetry class D if it is the only one present. It is conjectured in Ref. [75] that in the presence of all three channels, the RG flow to strong coupling (the variance of the disorder in each channel) is to the plateau transition in the universality class of the IQHE. (c) Unit cell of the honeycomb lattice with the pattern of nearest- and next-nearest-neighbor hopping amplitude that realizes a Chen insulators with two bands, shown in panel (d), each of which carries the Chern number ± 1.

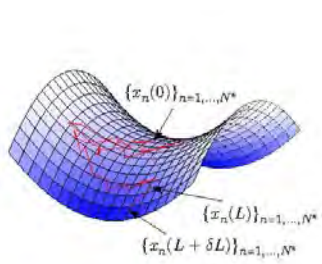

Fig. 1.8 (Taken from Ref. [13]) The “radial coordinate” of the transfer matrix $\mathcal{M}$ from Table 1.2 makes a Brownian motion on an associated non-compact symmetric space.

Table 1.1 Listed are the ten Altland-Zirnbauer (AZ) symmetry classes of single-particle Hamiltonians $\mathcal{H}$, classified according to their behavior under time-reversal symmetry ($\mathcal{T}$), charge-conjugation (or: particle-hole) symmetry ($\mathcal{C}$), as well as "sublattice" (or: "chiral") symmetry ($\mathcal{S}$). The labels T, C, and S, represent the presence/absence of time-reversal, particle-hole, and chiral symmetries, respectively, as well as the types of these symmetries. These operations square to either $\pm$ times the unit operator when they are symmetries. The number 0 indicates that these operations are not symmetries. The column entitled "Hamiltonian" lists, for each of the ten AZ symmetry classes, the symmetric space of which the quantum mechanical time-evolution operator $\exp(\mathrm{i}t\,\mathcal{H})$ is an element. The column "Cartan label" is the name given to the corresponding symmetric space listed in the column "Hamiltonian" in Élie Cartan's classification scheme (dating back to the year 1926). The last column entitled "G/H (fermionic NLSM)" lists the (compact sectors of the) target space of the NLSM describing Anderson localization physics at long wavelength in this given symmetry class.

Cartan label	T	C	S	Hamiltonian	G/H (fermionic NLSM)
A (unitary)	0	0	0	$U(N)$	$U(2n)/U(n)\times U(n)$
AI (orthogonal)	$+1$	0	0	$U(N)/O(N)$	$Sp(2n)/Sp(n)\times Sp(n)$
AII (symplectic)	-1	0	0	$U(2N)/Sp(2N)$	$O(2n)/O(n)\times O(n)$
AIII (ch. unit.)	0	0	$+1$	$U(N+M)/U(N)\times U(M)$	$U(n)$
BDI (ch. orth.)	$+1$	$+1$	$+1$	$O(N+M)/O(N)\times O(M)$	$U(2n)/Sp(2n)$
CII (ch. sympl.)	-1	-1	$+1$	$Sp(N+M)/Sp(N)\times Sp(M)$	$U(2n)/O(2n)$
D (BdG)	0	$+1$	0	$\mathrm{SO}(2N)$	$O(2n)/U(n)$
C (BdG)	0	-1	0	$Sp(2N)$	$Sp(2n)/U(n)$
DIII (BdG)	-1	$+1$	-1	$\mathrm{SO}(2N)/U(N)$	$O(2n)$
CI (BdG)	$+1$	-1	-1	$Sp(2N)/U(N)$	$Sp(2n)$

Table 1.2 Altland-Zirnbauer (AZ) symmetry classes for disordered quantum wires. Symmetry classes are defined by the presence or absence of time-reversal symmetry (TRS) and spin-rotation symmetry (SRS), and by the single-particle spectral symmetries of sublattice symmetry (SLS) (random hopping model at the band center) also known as chiral symmetries, and particle-hole symmetry (PHS) (zero-energy quasiparticles in superconductors). For historical reasons, the first three rows of the table are referred to as the orthogonal (O), unitary (U), and symplectic (S) symmetry classes when the disorder is generic. The prefix "ch" that stands for chiral is added when the disorder respects a SLS as in the next three rows. Finally, the last four rows correspond to dirty superconductors and are named after the symmetric spaces associated to their Hamiltonians. The table lists the multiplicities of the ordinary and long roots $m_{o\pm}$ and m_l of the symmetric spaces associated with the transfer matrix. Except for the three chiral classes, one has $m_{o+} = m_{o-} = m_o$. For the chiral classes, one has $m_{o+} = 0$, $m_{o-} = m_o$. The table also lists the degeneracy D of the transfer matrix eigenvalues, as well as the symbols for the symmetric spaces associated to the transfer matrix $\mathcal{M}$ and the Hamiltonian $\mathcal{H}$. Let g denote the dimensionless Landauer conductance and let $\rho(\varepsilon)$ denote the (self-averaging) density of states (DOS) per unit energy and per unit length. The last three columns list theoretical results for the weak-localization correction δg for $\ell \ll L \ll N\ell$ the disorder average $\overline{\ln g}$ of $\ln g$ for $L \gg N\ell$, and the DOS near $\varepsilon = 0$. The results for $\overline{\ln g}$ and $\rho(\varepsilon)$ in the chiral classes refer to the case of N even. For odd N, $\overline{\ln g}$ and $\rho(\varepsilon)$ are the same as in class D.

Symmetry class	m_o	m_l	D	$\mathcal{M}$	$\mathcal{H}$	δg	$-\overline{\ln g}$	$\rho(\varepsilon)$ for $0 < \varepsilon\tau_c \ll 1$
AI	1	1	2	CI	AI	$-2/3$	$2L/(\gamma\ell)$	ρ_0
A	2	1	2(1)	AIII	A	0	$2L/(\gamma\ell)$	ρ_0
AII	4	1	2	DIII	AII	$+1/3$	$2L/(\gamma\ell)$	ρ_0
BDI	1	0	2	AI	BDI	0	$2m_oL/(\gamma\ell)$	$\rho_0\lvert\ln\lvert\varepsilon\tau_c\rvert\rvert$
AIII	2	0	2(1)	A	AIII	0	$2m_oL/(\gamma\ell)$	$\pi\rho_0\lvert\varepsilon\tau_c\ln\lvert\varepsilon\tau_c\rvert\rvert$
CII	4	0	2	AII	CII	0	$2m_oL/(\gamma\ell)$	$(\pi\rho_0/3)\lvert(\varepsilon\tau_c)^3\ln\lvert\varepsilon\tau_c\rvert\rvert$
CI	2	2	4	C	CI	$-4/3$	$2m_lL/(\gamma\ell)$	$(\pi\rho_0/2)\lvert\varepsilon\tau_c\rvert$
C	4	3	4	CII	C	$-2/3$	$2m_lL/(\gamma\ell)$	$\rho_0\lvert\varepsilon\tau_c\rvert^2$
DIII	2	0	2	D	DIII	$+2/3$	$4\sqrt{L/(2\pi\gamma\ell)}$	$\pi\rho_0/\lvert\varepsilon\tau_c\ln^3\lvert\varepsilon\tau_c\rvert\rvert$
D	1	0	1	BDI	D	$+1/3$	$4\sqrt{L/(2\pi\gamma\ell)}$	$\pi\rho_0/\lvert\varepsilon\tau_c\ln^3\lvert\varepsilon\tau_c\rvert\rvert$

Table 1.3 Classification of topological insulators and superconductors as a function of spatial dimension d and AZ symmetry class, indicated by the "Cartan label" (first column). The definition of the ten AZ symmetry classes of single particle Hamiltonians is given in Table 1.1. The symmetry classes are grouped in two separate lists – the complex and the real cases, respectively – depending on whether the Hamiltonian is complex, or whether one (or more) reality conditions (arising from time-reversal or charge-conjugation symmetries) are imposed on it; the AZ symmetry classes are ordered in such a way that a periodic pattern in dimensionality becomes visible. [58] The symbols $\mathbb{Z}$ and $\mathbb{Z}_2$ indicate that the topologically distinct phases within a given symmetry class of topological insulators (superconductors) are characterized by an integer invariant ($\mathbb{Z}$), or a $\mathbb{Z}_2$ quantity, respectively. The symbol "0" denotes the case when there exists no topological insulator (superconductor), i.e., when all quantum ground states are topologically equivalent to the trivial state.

Real case

Cartan$\backslash d$	0	1	2	3	4	5	6	7	8	9	10	11	$\cdots$
A	$\mathbb{Z}$	0	$\mathbb{Z}$	0	$\mathbb{Z}$	0	$\mathbb{Z}$	0	$\mathbb{Z}$	0	$\mathbb{Z}$	0	$\cdots$
AIII	0	$\mathbb{Z}$	0	$\mathbb{Z}$	0	$\mathbb{Z}$	0	$\mathbb{Z}$	0	$\mathbb{Z}$	0	$\mathbb{Z}$	$\cdots$

Complex case

Cartan$\backslash d$	0	1	2	3	4	5	6	7	8	9	10	11	$\cdots$
AI	$\mathbb{Z}$	0	0	0	$2\mathbb{Z}$	0	$\mathbb{Z}_2$	$\mathbb{Z}_2$	$\mathbb{Z}$	0	0	0	$\cdots$
BDI	$\mathbb{Z}_2$	$\mathbb{Z}$	0	0	0	$2\mathbb{Z}$	0	$\mathbb{Z}_2$	$\mathbb{Z}_2$	$\mathbb{Z}$	0	0	$\cdots$
D	$\mathbb{Z}_2$	$\mathbb{Z}_2$	$\mathbb{Z}$	0	0	0	$2\mathbb{Z}$	0	$\mathbb{Z}_2$	$\mathbb{Z}_2$	$\mathbb{Z}$	0	$\cdots$
DIII	0	$\mathbb{Z}_2$	$\mathbb{Z}_2$	$\mathbb{Z}$	0	0	0	$2\mathbb{Z}$	0	$\mathbb{Z}_2$	$\mathbb{Z}_2$	$\mathbb{Z}$	$\cdots$
AII	$2\mathbb{Z}$	0	$\mathbb{Z}_2$	$\mathbb{Z}_2$	$\mathbb{Z}$	0	0	0	$2\mathbb{Z}$	0	$\mathbb{Z}_2$	$\mathbb{Z}_2$	$\cdots$
CII	0	$2\mathbb{Z}$	0	$\mathbb{Z}_2$	$\mathbb{Z}_2$	$\mathbb{Z}$	0	0	0	$2\mathbb{Z}$	0	$\mathbb{Z}_2$	$\cdots$
C	0	0	$2\mathbb{Z}$	0	$\mathbb{Z}_2$	$\mathbb{Z}_2$	$\mathbb{Z}$	0	0	0	$2\mathbb{Z}$	0	$\cdots$
CI	0	0	0	$2\mathbb{Z}$	0	$\mathbb{Z}_2$	$\mathbb{Z}_2$	$\mathbb{Z}$	0	0	0	$2\mathbb{Z}$	$\cdots$

2
The tenfold way in quasi-one-dimensional space

This section is dedicated to a non-vanishing density of non-interacting fermions hopping between the sites of quasi-one-dimensional lattices or between the sites defining the one-dimensional boundary of a two-dimensional lattice. According to the Pauli exclusion principle, the non-interacting ground state is obtained by filling all the single-particle energy eigenstates up to the Fermi energy fixed by the fermion density. The fate of this single-particle energy eigenstate when a static and local random potential is present is known as the problem of Anderson localization. The effect of disorder on a single-particle extended energy eigenstate state can be threefold:

- The extended nature of the single-particle energy eigenstate is robust to disorder.
- The extended single-particle energy eigenstate is turned into a critical state.
- The extended single-particle energy eigenstate is turned into a localized state.

There are several methods allowing to decide which one of these three outcomes takes place. Irrespectively of the dimensionality d of space, the symmetries obeyed by the static and local random potential matter for the outcome in a dramatic fashion. To illustrate this point, I consider the problem of Anderson localization in quasi-one-dimensional space.

2.1 Symmetries for the case of one one-dimensional channel

For simplicity, consider first the case of an infinitely long one-dimensional chain with the lattice spacing $\mathfrak{a} \equiv 1$ along which a non-vanishing but finite density of spinless fermions hop with the uniform nearest-neighbor hopping amplitude t. If periodic boundary conditions are imposed, the single-particle Hamiltonian is the direct sum over all momenta $-\pi \leq k \leq +\pi$ within the first Brillouin zone of

$$\mathcal{H}(k) \coloneqq -2t\cos k. \tag{2.1}$$

The Fermi energy ε_{F} intersects the dispersion (2.1) at the two Fermi points $\pm k_{\mathrm{F}}$. Linearization of the dispersion (2.1) about these two Fermi points delivers the Dirac Hamiltonian

$$\mathcal{H}_{\mathrm{D}} \coloneqq -\tau_3\,\mathrm{i}\frac{\partial}{\partial x} \tag{2.2a}$$

in the units defined by

$$\hbar \equiv 1, \qquad v_{\mathrm{F}} = 2t\,|\sin k_{\mathrm{F}}| \equiv 1. \tag{2.2b}$$

Here, τ_3 is the third Pauli matrices among the four 2×2 matrices

$$\tau_0 \coloneqq \begin{pmatrix} 1 & 0 \\ 0 & 1 \end{pmatrix}, \qquad \tau_1 \coloneqq \begin{pmatrix} 0 & 1 \\ 1 & 0 \end{pmatrix}, \qquad \tau_2 \coloneqq \begin{pmatrix} 0 & -\mathrm{i} \\ +\mathrm{i} & 0 \end{pmatrix}, \qquad \tau_3 \coloneqq \begin{pmatrix} +1 & 0 \\ 0 & -1 \end{pmatrix}. \tag{2.2c}$$

The momentum eigenstate

$$\Psi_{\mathrm{R},p}(x) \coloneqq e^{+\mathrm{i}p\,x} \begin{pmatrix} 1 \\ 0 \end{pmatrix} \tag{2.3a}$$

is an eigenstate with the single-particle energy $\varepsilon_{\mathrm{R}}(p) = +p$. The momentum eigenstate

$$\Psi_{\mathrm{L},p}(x) \coloneqq e^{+\mathrm{i}p\,x} \begin{pmatrix} 0 \\ 1 \end{pmatrix} \tag{2.3b}$$

is an eigenstate with the single-particle energy $\varepsilon_{\mathrm{L}}(p) = -p$. The plane waves

$$\Psi_{\mathrm{R},p}(x,t) \coloneqq e^{+\mathrm{i}p\,(x-t)} \begin{pmatrix} 1 \\ 0 \end{pmatrix} \tag{2.4a}$$

and

$$\Psi_{\mathrm{L},p}(x,t) \coloneqq e^{+\mathrm{i}p\,(x+t)} \begin{pmatrix} 0 \\ 1 \end{pmatrix} \tag{2.4b}$$

are right-moving and left-moving solutions to the massless Dirac equation

$$\mathrm{i}\frac{\partial}{\partial t}\Psi = \mathcal{H}_{\mathrm{D}}\,\Psi, \tag{2.4c}$$

respectively.

Perturb the massless Dirac Hamiltonian (2.2) with the most generic static and local one-body potential

$$\mathcal{V}(x) \coloneqq a_0(x)\,\tau_0 + m_1(x)\,\tau_1 + m_2(x)\,\tau_2 + a_1(x)\,\tau_3. \tag{2.5}$$

The real-valued function a_0 is a space-dependent chemical potential. It couples to the spinless fermions as the scalar part of the electromagnetic gauge potential does. The real-valued function a_1 is a space-dependent modulation of the Fermi point. It couples to the spinless fermions as the vector part of the electromagnetic gauge potential does. Both a_0 and a_1 multiply Pauli matrices such that each commutes with the massless Dirac Hamiltonian (2.2). Neither channels are confining (localizing). The real-valued functions m_1 and m_2 are space-dependent mass terms, for they multiply Pauli matrices such that each anticommutes with the massless Dirac Hamiltonian and with each other. Either channels are confining (localizing).

Symmetry class A: The only symmetry preserved by

$$\mathcal{H} \coloneqq \mathcal{H}_{\mathrm{D}} + \mathcal{V}(x) \tag{2.6}$$

with $\mathcal{V}$ defined in Eq. (2.5) is the global symmetry under multiplication of all states in the single-particle Hilbert space over which $\mathcal{H}$ acts by the same $U(1)$ phase. Correspondingly, the local two-current

$$J^{\mu}(x,t) \coloneqq \Big(\Psi^{\dagger}\,\Psi, \Psi^{\dagger}\,\tau_3\,\Psi\Big)(x,t), \tag{2.7}$$

obeys the continuity equation

$$\partial_{\mu}\,J^{\mu} = 0, \qquad \partial_0 \coloneqq \frac{\partial}{\partial t}, \qquad \partial_1 \coloneqq \frac{\partial}{\partial x}. \tag{2.8}$$

The family of Hamiltonian (2.6) labeled by the potential $\mathcal{V}$ of the form (2.5) is said to belong to the symmetry class A because of the conservation law (2.8).

One would like to reverse time in the Dirac equation

$$\left(\mathrm{i}\frac{\partial}{\partial t}\Psi\right)(x,t)=\left(\mathcal{H}\,\Psi\right)(x,t) \tag{2.9}$$

where $\mathcal{H}$ is defined by Eq. (2.6). Under reversal of time

$$t=-t', \tag{2.10}$$

the Dirac equation (2.9) becomes

$$\left(-\mathrm{i}\frac{\partial}{\partial t'}\Psi\right)(x,-t')=\left(\mathcal{H}\,\Psi\right)(x,-t'). \tag{2.11}$$

Complex conjugation removes the minus sign on the left-hand side,

$$\left(\mathrm{i}\frac{\partial}{\partial t'}\Psi^{*}\right)(x,-t')=\left(\mathcal{H}\,\Psi\right)^{*}(x,-t'). \tag{2.12}$$

Form invariance of the Dirac equation under reversal of time then follows if one postulates the existence of an unitary 2×2 matrix $\mathcal{U}_{\mathcal{T}}$ and of a phase $0\leq\phi_{\mathcal{T}}<2\pi$ such that (complex conjugation will be denoted by K)

$$\left(\mathcal{U}_{\mathcal{T}}\,\mathsf{K}\right)^{2}=e^{\mathrm{i}\phi_{\mathcal{T}}}\,\tau_{0},\qquad \Psi^{*}(x,-t)=:\mathcal{U}_{\mathcal{T}}\,\Psi_{\mathcal{T}}(x,t),\qquad \mathcal{H}_{\mathcal{T}}:=\mathcal{U}_{\mathcal{T}}^{-1}\,\mathcal{H}^{*}\,\mathcal{U}_{\mathcal{T}}, \tag{2.13a}$$

in which case

$$\left(\mathrm{i}\frac{\partial}{\partial t}\Psi_{\mathcal{T}}\right)(x,t)=\left(\mathcal{H}_{\mathcal{T}}\,\Psi_{\mathcal{T}}\right)(x,t). \tag{2.13b}$$

Time-reversal symmetry then holds if and only if

$$\mathcal{U}_{\mathcal{T}}^{-1}\,\mathcal{H}^{*}\,\mathcal{U}_{\mathcal{T}}=\mathcal{H}. \tag{2.14}$$

Time-reversal symmetry must hold for the massless Dirac equation. By inspection of the right- and left-moving solutions (2.4), one deduces that $\mathcal{U}_{\mathcal{T}}$ must interchange right and left movers. There are two possibilities, either

$$\mathcal{U}_{\mathcal{T}}=\tau_{2},\qquad \phi_{\mathcal{T}}=\pi, \tag{2.15}$$

or

$$\mathcal{U}_{\mathcal{T}}=\tau_{1},\qquad \phi_{\mathcal{T}}=0. \tag{2.16}$$

Symmetry class AII: Imposing time-reversal symmetry using the definition (2.15) restricts the family of Dirac Hamiltonians (2.6) to

$$\mathcal{H}(x):=\ -\mathrm{i}\tau_{3}\,\frac{\partial}{\partial t}+a_{0}(x)\,\tau_{0}. \tag{2.17}$$

The family of Hamiltonian (2.6) labeled by the potential $\mathcal{V}$ of the form (2.17) is said to belong to the symmetry class AII because of the conservation law (2.8) and of the time-reversal symmetry (2.14) with the representation (2.15).

Symmetry class AI: Imposing time-reversal symmetry using the definition (2.16) restricts the family of Dirac Hamiltonians (2.6) to

$$\mathcal{H}(x) := -\mathrm{i}\tau_3 \frac{\partial}{\partial t} + a_0(x)\,\tau_0 + m_1(x)\,\tau_1 + m_2(x)\,\tau_2. \tag{2.18}$$

The family of Hamiltonian (2.6) labeled by the potential $\mathcal{V}$ of the form (2.18) is said to belong to the symmetry class AI because of the conservation law (2.8) and of the time-reversal symmetry (2.14) with the representation (2.16).

Take advantage of the fact that the dispersion relation (2.1) obeys the symmetry

$$\mathcal{H}(k) = -\mathcal{H}(k+\pi). \tag{2.19}$$

This spectral symmetry is a consequence of the fact that the lattice Hamiltonian anticommutes with the local gauge transformation that maps the basis of single-particle localized wave functions

$$\psi_i : \mathbb{Z} \to \mathbb{C}, j \mapsto \psi_i(j) := \delta_{ij} \tag{2.20}$$

into the basis

$$\psi'_i : \mathbb{Z} \to \mathbb{C}, j \mapsto \psi'_i(j) := (-1)^j\,\delta_{ij}. \tag{2.21}$$

Such a spectral symmetry is an example of a sublattice symmetry in condensed matter physics. So far, the chemical potential

$$\varepsilon_{\mathrm{F}} \equiv -2\,t\,\cos k_{\mathrm{F}} \tag{2.22}$$

defined in Eq. (2.1) has been arbitrary. However, in view of the spectral symmetry (2.19), the single-particle energy eigenvalue

$$0 = \varepsilon_{\mathrm{F}} \equiv -2\,t\,\cos k_{\mathrm{F}}, \qquad k_{\mathrm{F}} = \frac{\pi}{2}, \tag{2.23}$$

is special. It is the center of symmetry of the single-particle spectrum (2.1). The spectral symmetry (2.19) is also known as a chiral symmetry of the Dirac equation (2.2a) by which

$$\mathcal{H}_{\mathrm{D}} = -\tau_1\,\mathcal{H}_{\mathrm{D}}\,\tau_1, \tag{2.24}$$

after an expansion to leading order in powers of the deviation of the momenta away from the two Fermi points $\pm\pi/2$.

Symmetry class AIII: If charge conservation holds together with the chiral symmetry

$$\mathcal{H} = -\tau_1\,\mathcal{H}\,\tau_1, \tag{2.25a}$$

then

$$\mathcal{H} = -\tau_3\,\mathrm{i}\partial_x + a_1(x)\,\tau_3 + m_2(x)\,\tau_2 \tag{2.25b}$$

is said to belong to the symmetry class AIII.

Symmetry class CII: It is not possible to write down a 2×2 Dirac equation in the symmetry class CII. For example, if charge conservation holds together with the chiral and time-reversal symmetries

$$\mathcal{H} = -\tau_1\,\mathcal{H}\,\tau_1, \qquad \mathcal{H} = +\tau_2\,\mathcal{H}^*\,\tau_2, \tag{2.26a}$$

respectively, then

$$\mathcal{H} = -\tau_3\,\mathrm{i}\partial_x \tag{2.26b}$$

does not belong to the symmetry class CII, as the composition of the chiral transformation with reversal of time squares to unity instead of minus times unity.

Symmetry class BDI: If charge conservation holds together with the chiral and time-reversal symmetries

$$\mathcal{H} = -\tau_1\,\mathcal{H}\,\tau_1, \qquad \mathcal{H} = +\tau_1\,\mathcal{H}^*\,\tau_1, \tag{2.27a}$$

then

$$\mathcal{H} = -\tau_3\,\mathrm{i}\partial_x + m_2(x)\,\tau_2 \tag{2.27b}$$

is said to belong to the symmetry class BDI.

The global $U(1)$ gauge symmetry responsible for the continuity equation (2.8) demands that one treats the two components of the Dirac spinors as independent. This is not desirable if the global $U(1)$ gauge symmetry is to be restricted to a global $\mathbb{Z}_2$ gauge symmetry, as occurs in a mean-field treatment of superconductivity. If the possibility of restricting the global $U(1)$ to a global $\mathbb{Z}_2$ gauge symmetry is to be accounted for, four more symmetry classes are permissible.

Symmetry class D: Impose a particle-hole symmetry through

$$\mathcal{H} = -\mathcal{H}^*, \tag{2.28a}$$

then

$$\mathcal{H} = -\tau_3\,\mathrm{i}\partial_x + m_2(x)\,\tau_2 \tag{2.28b}$$

is said to belong to the symmetry class D.

Symmetry class DIII: Impose a particle-hole symmetry and time-reversal symmetry through

$$\mathcal{H} = -\mathcal{H}^*, \qquad \mathcal{H} = +\tau_2\,\mathcal{H}^*\,\tau_2, \tag{2.29a}$$

respectively, then

$$\mathcal{H} = -\tau_3\,\mathrm{i}\partial_x \tag{2.29b}$$

is said to belong to the symmetry class DIII.

Symmetry class C: Impose a particle-hole symmetry through

$$\mathcal{H} = -\tau_2\,\mathcal{H}^*\,\tau_2, \tag{2.30a}$$

then

$$\mathcal{H} = a_1(x)\,\tau_3 + m_2(x)\,\tau_2 + m_1(x)\,\tau_1 \tag{2.30b}$$

is said to belong to the symmetry class C. The Dirac kinetic energy is prohibited for a 2×2 Dirac Hamiltonian from the symmetry class C.

Symmetry class CI: Impose a particle-hole symmetry and time-reversal symmetry through

$$\mathcal{H} = -\tau_2\,\mathcal{H}^*\,\tau_2, \qquad \mathcal{H} = +\tau_1\,\mathcal{H}^*\,\tau_1, \tag{2.31a}$$

respectively, then

$$\mathcal{H} = m_2(x)\,\tau_2 + m_1(x)\,\tau_1 \tag{2.31b}$$

is said to belong to the symmetry class CI. The Dirac kinetic energy is prohibited for a 2×2 Dirac Hamiltonian from the symmetry class CI.

2.2 Symmetries for the case of two one-dimensional channels

Imagine two coupled linear chains along which non-interacting spinless fermions are allowed to hop. If the two chains are decoupled and the hopping is a uniform nearest-neighbor hopping along any one of the two chains, then the low-energy and long-wave length effective single-particle Hamiltonian in the vicinity of the chemical potential $\varepsilon_{\mathrm{F}} = 0$ is the tensor product of the massless Dirac Hamiltonian (2.2a) with the 2×2 unit matrix σ_0. Let the three Pauli matrices $\boldsymbol{\sigma}$ act on the same vector space as σ_0 does. For convenience, introduce the sixteen Hermitean 4×4 matrices

$$X_{\mu\nu} := \tau_{\mu} \otimes \sigma_{\nu}, \qquad \mu, \nu = 0, 1, 2, 3. \tag{2.32}$$

Symmetry class A: The generic Dirac Hamiltonian of rank $r = 4$ is

$$\mathcal{H} := -X_{30}\, \mathrm{i}\partial_x + a_{1,\nu}(x)\, X_{3\nu} + m_{2,\nu}(x)\, X_{2\nu} + m_{1,\nu}(x)\, X_{1\nu} + a_{0,\nu}(x)\, X_{0\nu}. \tag{2.33}$$

The summation convention over the repeated index $\nu = 0, 1, 2, 3$ is implied. There are four real-valued parameters for the components $a_{1,\nu}$ with $\mu = 0, 1, 2, 3$ of an $U(2)$ vector potential, eight for the components $m_{1,\nu}$ and $m_{2,\nu}$ with $\mu = 0, 1, 2, 3$ of two independent $U(2)$ masses, and four for the components $a_{0,\nu}$ with $\mu = 0, 1, 2, 3$ of an $U(2)$ scalar potential. As it should be there are 16 real-valued free parameters (functions if one opts to break translation invariance). If all components of the spinors solving the eigenvalue problem

$$\mathcal{H}\, \Psi(x) = \varepsilon\, \Psi(x) \tag{2.34}$$

are independent, the Dirac Hamiltonian (2.33) belongs to the symmetry class A.

In addition to the conservation of the fermion number, one may impose time-reversal symmetry on the Dirac Hamiltonian (2.33) There are two possibilities to do so.

Symmetry class AII: If charge conservation holds together with time-reversal symmetry through

$$\mathcal{H} = +X_{12}\, \mathcal{H}^{*}\; X_{12}, \tag{2.35a}$$

then

$$\mathcal{H} = -X_{30}\, \mathrm{i}\partial_x + \sum_{\nu=1,2,3} a_{1,\nu}(x)\, X_{3\nu} + m_{2,0}(x)\, X_{20} + m_{1,0}(x)\, X_{10} + a_{0,0}(x)\, X_{00} \tag{2.35b}$$

is said to belong to the symmetry class AII.

Symmetry class AI: If charge conservation holds together with time-reversal symmetry through

$$\mathcal{H} = +X_{10}\, \mathcal{H}^{*}\, X_{10}, \tag{2.36a}$$

then

$$\mathcal{H} = -X_{30}\, \mathrm{i}\partial_x + a_{1,2}(x)\, X_{32} + \sum_{\nu=0,1,3} \left[m_{2,\nu}(x)\, X_{2\nu} + m_{1,\nu}(x)\, X_{1\nu} + a_{0,\nu}(x)\, X_{0\nu} \right] \tag{2.36b}$$

is said to belong to the symmetry class AI.

The standard symmetry classes A, AII, and AI can be further constrained by imposing the chiral symmetry. This gives the following three possibilities.

Symmetry class AIII: If charge conservation holds together with the chiral symmetry

$$\mathcal{H} = -X_{10}\,\mathcal{H}\,X_{01}, \tag{2.37a}$$

then

$$\mathcal{H} = -X_{30}\,\mathrm{i}\partial_x + a_{1,\nu}(x)\,X_{3\nu} + m_{2,\nu}(x)\,X_{2\nu} \tag{2.37b}$$

is said to belong to the symmetry class AIII.

Symmetry class CII: If charge conservation holds together with chiral symmetry and time-reversal symmetry

$$\mathcal{H} = -X_{10}\,\mathcal{H}\,X_{10}, \qquad \mathcal{H} = +X_{12}\,\mathcal{H}^{*}\,X_{12}, \tag{2.38a}$$

respectively, then

$$\mathcal{H} = -X_{30}\,\mathrm{i}\partial_x + \sum_{\nu=1,2,3} a_{1,\nu}(x)\,X_{3\nu} + m_{2,0}(x)\,X_{20} \tag{2.38b}$$

is said to belong to the symmetry class CII.

Symmetry class BDI: If charge conservation holds together with chiral symmetry and time-reversal symmetry

$$\mathcal{H} = -X_{10}\,\mathcal{H}\,X_{10}, \qquad \mathcal{H} = +X_{10}\mathcal{H}^{*}\,X_{10}, \tag{2.39a}$$

respectively, then

$$\mathcal{H} = -X_{30}\,\mathrm{i}\partial_x + a_{1,2}(x)\,X_{32} + \sum_{\nu=0,1,3} m_{2,\nu}(x)\,X_{2\nu} \tag{2.39b}$$

is said to belong to the symmetry class BDI.

Now, we move to the four Bogoliubov-de-Gennes (BdG) symmetry classes by relaxing the condition that all components of a spinor on which the Hamiltonian acts be independent. This means that changing each component of a spinor by a multiplicative global phase factor is not legitimate anymore. However, changing each component of a spinor by a global sign remains legitimate. The contraints among the components of a spinor come about by imposing a particle-hole symmetry.

Symmetry class D: Impose particle-hole symmetry through

$$\mathcal{H} = -\mathcal{H}^{*}, \tag{2.40a}$$

then

$$\mathcal{H} = -X_{30}\,\mathrm{i}\partial_x + a_{1,2}(x)\,X_{32} + \sum_{\nu=0,1,3} m_{2,\nu}(x)\,X_{2\nu} + m_{1,2}(x)\,X_{12} + a_{0,2}(x)\,X_{02} \tag{2.40b}$$

is said to belong to the symmetry class D.

Symmetry class DIII: Impose particle-hole symmetry and time-reversal symmetry through

$$\mathcal{H} = -\mathcal{H}^{*}, \qquad \mathcal{H} = +X_{20}\,\mathcal{H}^{*}\,X_{20}, \tag{2.41a}$$

respectively, then

$$\mathcal{H} = -X_{30}\,\mathrm{i}\partial_x + a_{1,2}(x)\,X_{32} + m_{1,2}(x)\,X_{12} \tag{2.41b}$$

is said to belong to the symmetry class DIII.

Symmetry class C: Impose particle-hole symmetry through

$$\mathcal{H} = -X_{02}\,\mathcal{H}^*\,X_{02}, \tag{2.42a}$$

respectively, then

$$\mathcal{H} = -X_{30}\,\mathrm{i}\partial_x + \sum_{\nu=1,2,3} a_{1,\nu}(x)\,X_{3\nu} + m_{2,0}(x)\,X_{20} + \sum_{\nu=1,2,3}\left[m_{1,\nu}(x)\,X_{1\nu} + a_{0,\nu}(x)\,X_{0\nu}\right] \tag{2.42b}$$

is said to belong to the symmetry class C.

Symmetry class CI: Impose particle-hole symmetry and time-reversal symmetry through

$$\mathcal{H} = -X_{02}\,\mathcal{H}^*\,X_{02}, \qquad \mathcal{H} = +X_{10}\,\mathcal{H}^*\,X_{10}, \tag{2.43a}$$

respectively, then

$$\mathcal{H} = -X_{30}\,\mathrm{i}\partial_x + a_{1,2}(x)\,X_{32} + m_{2,0}(x)\,X_{20} + m_{1,1}(x)\,X_{11} + m_{1,3}(x)\,X_{13} + a_{0,3}(x)\,X_{03} \tag{2.43b}$$

is said to belong to the symmetry class CI.

2.3 Definition of the minimum rank

In Secs. 2.1 and 2.2, we have imposed ten symmetry restrictions corresponding to the tenfold way introduced by Altland and Zirnbauer to Dirac Hamiltonians with Dirac matrices of rank $r = 2$ and $r = 4$, respectively. These Dirac Hamiltonians describe the propagation of single-particle states in one-dimensional space. All ten symmetry classes shall be called the Altland-Zirnbauer (AZ) symmetry classes.

Observe that some of the AZ symmetries can be very restrictive for the Dirac Hamiltonians with Dirac matrices of small rank r. For example, it is not possible to write down a Dirac Hamiltonian of rank $r = 2$ in the symmetry class CII, the symmetry classes C and CI do not admit a Dirac kinetic energy of rank $r = 2$, and the symmetry classes AII and DIII do not admit Dirac masses in their Dirac Hamiltonians of rank $r = 2$.

This observation suggests the definition of the minimum rank r_{min} for which the Dirac Hamiltonian describing the propagation in d-dimensional space for a given AZ symmetry class admits a Dirac mass. Hence, r_{min} depends implicitly on the dimensionality of space and on the AZ symmetry class. In one-dimensional space, we have found that

$$\begin{aligned}
&r^{\mathrm{A}}_{\mathrm{min}} = 2, \qquad r^{\mathrm{AII}}_{\mathrm{min}} = 4, \qquad r^{\mathrm{AI}}_{\mathrm{min}} = 2,\\
&r^{\mathrm{AIII}}_{\mathrm{min}} = 2, \qquad r^{\mathrm{CII}}_{\mathrm{min}} = 4, \qquad r^{\mathrm{BDI}}_{\mathrm{min}} = 2,\\
&r^{\mathrm{D}}_{\mathrm{min}} = 2, \qquad r^{\mathrm{DIII}}_{\mathrm{min}} = 4, \qquad r^{\mathrm{C}}_{\mathrm{min}} = 4, \qquad r^{\mathrm{CI}}_{\mathrm{min}} = 4.
\end{aligned} \tag{2.44}$$

The usefulness of this definition is the following.

First, Anderson localization in a given AZ symmetry class is impossible for any random Dirac Hamiltonian with Dirac matrices of rank r smaller than r_{min}. This is the case for the symmetry classes AII and DIII for a Dirac Hamiltonian of rank $r = 2$ in one-dimensional space. The lattice realization of these Dirac Hamiltonians is along the boundary of a two-dimensional insulator in the symmetry classes AII and DIII when the bulk realizes a topologically non-trivial insulating phase owing to the fermion doubling problem. This is why an odd number of helical pairs of edge states in the symmetry class AII and an odd number of helical pairs of Majorana edge states in the symmetry class DIII can evade Anderson localization. The limit $r = 2$ for the Dirac Hamiltonians encoding one-dimensional propagation in the symmetry classes AII and DIII are the signatures for the topologically non-trivial entries of the group $\mathbb{Z}_2$ in column $d = 2$ from Table 1.3. For the symmetry classes A and D, we can consider the limit $r = 1$ as a special limit that shares with a Dirac Hamiltonian the property that it is a first-order differential operator in space, but, unlike a Dirac Hamiltonian, this limit does no treat right- and left-movers on equal footing (and thus breaks time-reversal symmetry explicitly). Such a first-order differential operator encodes the propagation of right movers on the inner boundary of a two-dimensional ring (the Corbino geometry of Fig. 1.5) while its complex conjugate encodes the propagation of left movers on the outer boundary of a two-dimensional ring or vice versa. For the symmetry class C, one must consider two copies of opposite spins of the $r = 1$ limit of class D. The limit $r = 1$ for Dirac Hamiltonians encoding one-dimensional propagation in the symmetry classes A, D, and C are realized on the boundary of two-dimensional insulating phases supporting the integer quantum Hall effect, the thermal integer quantum Hall effect, and the spin-resolved thermal integer quantum Hall effect, respectively. The limits $r = 1$ for the Dirac Hamiltonians encoding one-dimensional propagation in the symmetry classes A, D, and C are the signatures for the non-trivial entries ± 1 and ± 2 of the groups $\mathbb{Z}$ and $2\mathbb{Z}$ in column $d = 2$ from Table 1.3, respectively.

Second, one can always define the quasi-d-dimensional Dirac Hamiltonian

$$\mathcal{H}(\boldsymbol{x}) := -\mathrm{i}(\boldsymbol{\alpha} \otimes I) \cdot \frac{\partial}{\partial \boldsymbol{x}} + \mathcal{V}(\boldsymbol{x}), \tag{2.45a}$$

where $\boldsymbol{\alpha}$ and β are a set of matrices that anticommute pairwise and square to the unit $r_{\min} \times r_{\min}$ matrix, I is a unit $N \times N$ matrix, and

$$\mathcal{V}(\boldsymbol{x}) = m(\boldsymbol{x})\, \beta \otimes I + \cdots \tag{2.45b}$$

with $\cdots$ representing all other masses, vector potentials, and scalar potentials allowed by the AZ symmetry class. For one-dimensional space, the stationary eigenvalue problem

$$\mathcal{H}(x)\, \Psi(x;\varepsilon) = \varepsilon\, \Psi(x;\varepsilon) \tag{2.46}$$

with the given "initial value" $\Psi(y;\varepsilon)$ is solved through the transfer matrix

$$\Psi(x;\varepsilon) = \mathcal{M}(x|y;\varepsilon)\, \Psi(y;\varepsilon) \tag{2.47a}$$

where

$$\mathcal{M}(x|y;\varepsilon) := \mathcal{P}_{x'}\, \exp\left(\int_y^x \mathrm{d}x'\, \mathrm{i}(\alpha \otimes I)\, [\varepsilon - \mathcal{V}(x')] \right). \tag{2.47b}$$

The symbol $\mathcal{P}_{x'}$ represents path ordering. The limit $N \to \infty$ with all entries of $\mathcal{V}$ independently and identically distributed (iid) up to the AZ symmetry constraints, (averaging over the disorder is denoted by an overline)

$$\overline{\mathcal{V}_{ij}(x)} \propto \mathsf{v}_{ij}, \quad \overline{[\mathcal{V}_{ij}(x) - \mathsf{v}_{ij}]\, [\mathcal{V}_{kl}(y) - \mathsf{v}_{kl}]} \propto \mathrm{g}^2\, e^{-|x-y|/\xi_{\mathrm{dis}}}, \tag{2.48}$$

for $i, j, k, l = 1, \cdots, r_{\min} N$ defines the thick quantum wire limit.

The consequences of Eq. (2.47) are the following. First, the local symmetries defining the symmetry classes A, AII, and AI obeyed by $\varepsilon - \mathcal{V}(x')$ carry through to the transfer matrix at any single-particle energy ε. The local unitary spectral symmetries defining the symmetry classes AIII, CII, and BDI and the local anti-unitary spectral symmetries defining the symmetry classes D, DIII, C, and CI carry through to the transfer matrix at the single-particle energy $\varepsilon = 0$. Second, the diagonal matrix entering the polar decomposition of the transfer matrix at the band center $\varepsilon = 0$ is related to the non-compact symmetric spaces from the column $\mathcal{M}$ in Table 1.2. Third, the composition law obeyed by the transfer matrix that encodes enlarging the length of a disordered wire coupled to perfect leads is matrix multiplication. It is then possible to derive a Fokker-Planck equation for the joint probability obeyed by the radial coordinates on the non-compact symmetric spaces from the column $\mathcal{M}$ in Table 1.2 as the length L of of a disordered wire coupled to perfect leads is increased. In this way, the moments of the dimensionless Landauer conductance g in the columns δg and $-\overline{\ln g}$ can be computed (see Table 1.2). An infinitesimal increase in the length of the disordered region for one of the ten symmetry classes induces an infinitesimal Brownian motion (see Fig. 1.8) of the Lyapunov exponents that is solely controlled by the multiplicities of the ordinary, long, and short roots of the corresponding classical semi-simple Lie algebra under suitable assumptions on the disorder (locality, weakness, and isotropy between all channels). When the transfer matrix describes the stability of the metallic phase in the thick quantum wire limit of non-interacting fermions perturbed by static one-body random potentials with local correlations and of vanishing means in the bulk of a quasi-one-dimensional lattice model, the multiplicities of the short root entering the Brownian motion of the Lyapunov exponents always vanish. However, when the transfer matrix describes the quasi-one-dimensional boundary of a two-dimensional topological band insulator moderately perturbed by static one-body random potentials with local correlations, the multiplicities of the short roots is nonvanishing in the Brownian motion of the Lyapunov exponents in the five AZ symmetry classes A, AII, D, DIII, and C. Correspondingly, the conductance is of order one along the infinitely long boundary, i.e., the insulating bulk supports extended edge states. These extended edge states can be thought of as realizing a quasi-one-dimensional ballistic phase of quantum matter robust to disorder.

2.4 Topological spaces for the normalized Dirac masses

To study systematically the effects of static and local disorder on the insulating phases of quasi-d-dimensional phases, it is very useful to explore the topological properties of the normalized Dirac masses entering a generic random Dirac Hamiltonian of the form (2.45) within any given AZ symmetry class. This approach allows to construct the periodic Table 1.3. [1] Deriving columns $d = 1, \cdots, 8$ from Table 1.3 can be achieved by brute force if one constructs the generic Dirac Hamiltonian with Dirac matrices of rank r_{min} belonging to any one of the ten AZ symmetry classes and repeat this construction with Dirac matrices or rank $2r_{\text{min}}$, $3r_{\text{min}}$, and so on. It then becomes apparent that for any dimension d:

1. Five of the ten AZ symmetry classes accommodate one normalized Dirac matrix up to a sign when the Dirac matrices have the rank $r = r_{\text{min}}$. These are the symmetry classes that realize topologically distinct localized phases of d-dimensional quantum matter.
   (a) Three of these symmetry classes are characterized by having one normalized Dirac mass matrix that commutes with all other Dirac matrices when $r = N\, r_{\text{min}}$ with

$N = 2, 3, \cdots$. These are the entries with the group $\mathbb{Z}$ (or $2\mathbb{Z}$ when there is a degeneracy of 2) in the periodic Table 1.3. Mathematically, the group $\mathbb{Z}$ is the zeroth homotopy group of the normalized Dirac masses in the limit $N \to \infty$.

(b) Two of these symmetry classes are characterized by the fact that the sum of all mass terms can be associated to a $2N \times 2N$ Hermitean and antisymmetric matrix for any $r = r_{\min} N$ with $N = 1, 2, \cdots$. The sign ambiguity of the Pfaffian of this matrix indexes the two group elements in the entries with the group $\mathbb{Z}_2$ from the periodic Table 1.3. Mathematically, the group $\mathbb{Z}_2$ is the zeroth homotopic group of the normalized Dirac masses for N sufficiently large.

2. The topological space of normalized Dirac masses is compact and path connected for the remaining five symmetry classes, i.e., its zeroth homotopy group is the trivial one. No Dirac mass is singled out. The localized phase of matter is topologically trivial.

The observed periodicity of two for the complex classes and of eight for the real classes in Table 1.3 follows from the Bott periodicity in K theory.

3

Fractionalization from Abelian bosonization

3.1 Introduction

Abelian bosonization is attributed to Coleman, [22] Mandelstam, [77] and Luther and Peschel, [76] respectively. Here, we follow the more general formulation of Abelian bosonization given by Haldane in Ref. [46], as it lends itself to a description of one-dimensional quantum effective field theories arising in the low-energy sector along the boundary in space of $(2+1)$-dimensional topological quantum field theories.

3.2 Definition

Define the quantum Hamiltonian (in units with the electric charge e, the speed of light c, and $\hbar$ set to one)

$$\begin{aligned}\widehat{H} &\coloneqq \int\limits_{0}^{L} \mathrm{d}x\,\left[\frac{1}{4\pi}\,V_{ij}\,\left(D_x\,\hat{u}_i\right)\left(D_x\,\hat{u}_j\right)+A_0\left(\frac{q_i}{2\pi}\,K^{-1}_{ij}\left(D_x\,\hat{u}_j\right)\right)\right](t,x),\\ D_x\,\hat{u}_i(t,x) &\coloneqq \left(\partial_x\,\hat{u}_i+q_i\,A_1\right)(t,x).\end{aligned} \tag{3.1a}$$

The indices $i,j=1,\cdots,N$ label the bosonic modes. Summation is implied for repeated indices. The N real-valued quantum fields $\hat{u}_i(t,x)$ obey the equal-time commutation relations

$$\left[\hat{u}_i(t,x),\hat{u}_j(t,y)\right] \coloneqq \mathrm{i}\pi\left[K_{ij}\,\mathrm{sgn}(x-y)+L_{ij}\right] \tag{3.1b}$$

for any pair $i,j=1,\cdots,N$. The function $\mathrm{sgn}(x)=-\mathrm{sgn}(-x)$ gives the sign of the real variable x and will be assumed to be periodic with periodicity L. The $N\times N$ matrix K is symmetric, invertible, and integer valued. Given the pair $i,j=1,\cdots,N$, any of its matrix elements thus obey

$$K_{ij}=K_{ji}\in\mathbb{Z},\qquad K^{-1}_{ij}=K^{-1}_{ji}\in\mathbb{Q}. \tag{3.1c}$$

The $N\times N$ matrix L is anti-symmetric

$$L_{ij}=-L_{ji}=\begin{cases}0, & \text{if } i=j,\\ \mathrm{sgn}(i-j)\left(K_{ij}+q_i\,q_j\right), & \text{otherwise},\end{cases} \tag{3.1d}$$

for $i,j=1,\cdots,N$. The sign function $\mathrm{sgn}(i)$ of any integer i is here not made periodic and taken to vanish at the origin of $\mathbb{Z}$. The external scalar gauge potential $A_0(t,x)$ and vector gauge potential $A_1(t,x)$ are real-valued functions of time t and space x coordinates. They are also chosen to be periodic under $x \mapsto x+L$. The $N \times N$ matrix V is symmetric and positive definite

$$V_{ij} = V_{ji} \in \mathbb{R}, \qquad v_i\, V_{ij}\, v_j > 0, \qquad i,j = 1,\cdots,N, \tag{3.1e}$$

for any nonvanishing vector $v = (v_i) \in \mathbb{R}^N$. The charges q_i are integer valued and satisfy

$$(-1)^{K_{ii}} = (-1)^{q_i}, \qquad i = 1,\cdots,N. \tag{3.1f}$$

Finally, we shall impose the boundary conditions

$$\hat{u}_i(t,x+L) = \hat{u}_i(t,x) + 2\pi n_i, \qquad n_i \in \mathbb{Z}, \tag{3.1g}$$

and

$$(\partial_x\, \hat{u}_i)\,(t,x+L) = (\partial_x\, \hat{u}_i)\,(t,x), \tag{3.1h}$$

for any $i = 1,\cdots,N$.

3.3 Chiral equations of motion

For any $i,j = 1,\cdots,N$, one verifies with the help of the equal-time commutation relations

$$\left[\hat{u}_i(t,x), D_y\, \hat{u}_j(t,y)\right] = -2\pi\mathrm{i}\, K_{ij}\, \delta(x-y) \tag{3.2}$$

that the equations of motions are

$$\begin{aligned} \mathrm{i}\,(\partial_t\, \hat{u}_i)\,(t,x) \coloneqq&\ \left[\hat{u}_i(t,x), \widehat{H}\right] \\ =&\ -\mathrm{i}K_{ij}\, V_{jk}\,(\partial_x\, \hat{u}_k + q_k\, A_1)\,(t,x) - \mathrm{i}q_i\, A_0(t,x). \end{aligned} \tag{3.3}$$

Introduce the covariant derivatives

$$D_\mu\, \hat{u}_k \coloneqq \left(\partial_\mu\, \hat{u}_k + q_k\, A_\mu\right), \qquad \partial_0 \equiv \partial_t, \qquad \partial_1 \equiv \partial_x, \tag{3.4}$$

for $\mu = 0,1$ and $k = 1,\cdots,N$. The equations of motion

$$0 = \delta_{ik}\, D_0\, \hat{u}_k + K_{ij}\, V_{jk}\, D_1\, \hat{u}_k \tag{3.5}$$

are chiral. Doing the substitutions $\hat{u}_i \mapsto \hat{v}_i$ and $K \mapsto -K$ everywhere in Eq. (3.1) delivers the chiral equations of motions

$$0 = \delta_{ik}\, D_0\, \hat{v}_k - K_{ij}\, V_{jk}\, D_1\, \hat{v}_k, \tag{3.6}$$

with the opposite chirality. Evidently, the chiral equations of motion (3.5) and (3.6) are first-order differential equations, as opposed to the Klein-Gordon equations of motion obeyed by a relativistic quantum scalar field.

3.4 Gauge invariance

The chiral equations of motion (3.5) and (3.6) are invariant under the local $U(1)$ gauge symmetry

$$\begin{aligned} \hat{u}_i(t,x) &=: \hat{u}'_i(t,x) + q_i\,\chi(t,x), \\ A_0(t,x) &=: A'_0(t,x) - (\partial_t\,\chi)\,(t,x), \\ A_1(t,x) &=: A'_1(t,x) - (\partial_x\,\chi)\,(t,x), \end{aligned} \tag{3.7a}$$

for any real-valued function χ that satisfies the periodic boundary conditions

$$\chi(t,x+L) = \chi(t,x). \tag{3.7b}$$

Functional differentiation of Hamiltonian (3.1a) with respect to the gauge potentials allows to define the two-current with the components

$$\begin{aligned} \hat{J}^0(t,x) &:= \frac{\delta\widehat{H}}{\delta A_0(t,x)} \\ &= \frac{1}{2\pi}\,q_i\,K^{-1}_{ij}\,\left(D_1\,\hat{u}_j\right)(t,x) \end{aligned} \tag{3.8a}$$

and

$$\begin{aligned} \hat{J}^1(t,x) &:= \frac{\delta\widehat{H}}{\delta A_1(t,x)} \\ &= \frac{1}{2\pi}\,q_i\,V_{ij}\,\left(D_1\,\hat{u}_j\right)(t,x) + \frac{1}{2\pi}\,\left(q_i\,K^{-1}_{ij}\,q_j\right)A_0(t,x). \end{aligned} \tag{3.8b}$$

Introduce the short-hand notation

$$\sigma_{\mathrm{H}} := \frac{1}{2\pi}\,\left(q_i\,K^{-1}_{ij}\,q_j\right) \in \frac{1}{2\pi}\,\mathbb{Q} \tag{3.9}$$

for the second term on the right-hand side of Eq. (3.8b). The subscript stands for Hall as we shall shortly interpret σ_{H} as a dimensionless Hall conductance.

The transformation law of the two-current (3.8) under the local gauge transformation (3.7) is

$$\hat{J}^0(t,x) = \hat{J}^{0\,\prime}(t,x) \tag{3.10a}$$

and

$$\hat{J}^1(t,x) = \hat{J}^{1\,\prime}(t,x) - \sigma_{\mathrm{H}}\,(\partial_t\chi)\,(t,x). \tag{3.10b}$$

The two-current (3.8) is only invariant under gauge transformations (3.7) that are static when $\sigma_{\mathrm{H}} \neq 0$.

With the help of

$$\left[D_x\,\hat{u}_i(t,x), D_y\,\hat{u}_j(t,y)\right] = -2\pi\mathrm{i}\,K_{ij}\,\delta'(x-y) \tag{3.11}$$

for $i,j=1,\cdots,N$, one verifies that the total derivative of $\hat{J}^0(t,x)$ is

$$\begin{aligned}\frac{\partial\,\hat{J}^0}{\partial t} &= -\,\mathrm{i}\left[\hat{J}^0,\widehat{H}\right] + \sigma_H\,\frac{\partial\,A_1}{\partial t}\\ &= -\,\frac{\partial\,\hat{J}^1}{\partial x} + \sigma_H\,\frac{\partial\,A_1}{\partial t}.\end{aligned} \tag{3.12}$$

There follows the continuity equation

$$\partial_\mu\,\hat{J}^\mu = 0 \tag{3.13}$$

provided A_1 is time independent or $\sigma_H = 0$. The continuity equation (3.13) delivers a conserved total charge if and only if A_0 and A_1 are both static for arbitrary $\sigma_H \neq 0$.

For any non-vanishing σ_{H}, the continuity equation

$$\partial_\mu\,\hat{J}^\mu = \sigma_H\,\frac{\partial\,A_1}{\partial t} \tag{3.14}$$

is anomalous as soon as the vector gauge potential A_1 is time dependent. The edge theory (3.1) is said to be chiral when $\sigma_{\mathrm{H}} \neq 0$, in which case the continuity equation (3.14) is anomalous. The anomalous continuity equation (3.14) is form covariant under any smooth gauge transformation (3.7). The choice of gauge may be fixed by the condition

$$\frac{\partial\,A_0}{\partial x} = 0 \tag{3.15a}$$

for which the anomalous continuity equation (3.14) then becomes

$$\left(\partial_\mu\,\hat{J}^\mu\right)(t,x) = +\sigma_H\,E(t,x), \tag{3.15b}$$

where

$$E(t,x) \coloneqq +\left(\frac{\partial\,A_1}{\partial t}\right)(t,x) \equiv -\left(\frac{\partial\,A^1}{\partial t}\right)(t,x) \tag{3.15c}$$

represents the electric field in this gauge.

To interpret the anomalous continuity equation (3.15) of the bosonic chiral edge theory (3.1), we recall that x is a compact coordinate because of the periodic boundary conditions (3.1g), (3.1f), and (3.7). For simplicity, we assume

$$E(t,x) = E(t). \tag{3.16}$$

The interval $0 \le x \le L$ is thought of as a circle of perimeter L centered at the origin of the three-dimensional Euclidean space as shown in Fig. 3.1. The vector potential $A^1(t)$ and the electric field $E(t) = -\left(\frac{\partial\,A^1}{\partial t}\right)(t)$ along the circle of radius $R \equiv L/(2\pi)$ are then the polar

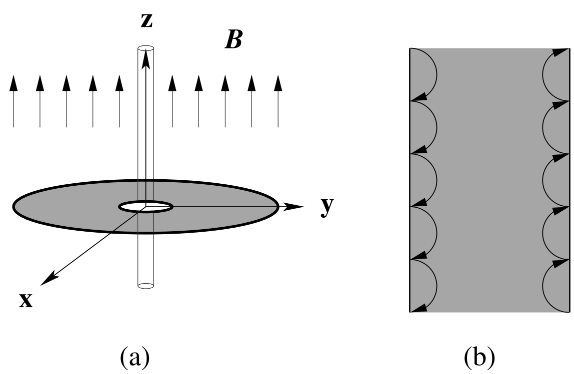

Fig. 3.1 (a) A ring of outer radius $R \equiv L/(2\pi)$ and inner radius r in which electrons are confined. A uniform and static magnetic field $\boldsymbol{B}$ normal to the ring is present. The hierarchy $\ell_B \ll r \ll R$ of length scales is assumed, where $\ell_B \equiv \hbar c/|e\,B|$ is the magnetic length. A time-dependent vector potential $\boldsymbol{A}(t,\boldsymbol{r})$ is induced by a time-dependent flux supported within a solenoid of radius $r_{\mathrm{sln}} \ll r$. This Corbino geometry has a cylindrical symmetry. (b) The classical motion of electrons confined to a plane normal to a uniform static magnetic field is circular. In the limit $R \to \infty$ holding R/r fixed, the Corbino disk turns into a Hall bar. An electron within a magnetic length of the boundary undergoes a classical skipping orbit. Upon quantization, a classical electron undergoing a skipping orbit turns into a chiral electron. Upon bosonization, a chiral electron turns into a chiral boson.

components of a three-dimensional gauge field $A^{\mu}(t,\boldsymbol{r}) = (A^0,\boldsymbol{A})(t,\boldsymbol{r})$ in a cylindrical geometry with the electro-magnetic fields

$$\boldsymbol{E}(t,\boldsymbol{r}) = -(\boldsymbol{\nabla}\,A^0)(t,\boldsymbol{r}) - (\partial_t\,\boldsymbol{A})(t,\boldsymbol{r}), \qquad \boldsymbol{B}(t,\boldsymbol{r}) = (\boldsymbol{\nabla}\wedge\boldsymbol{A})(t,\boldsymbol{r}). \tag{3.17}$$

The dimensionless Hall conductance σ_{H} encodes the linear response of spin-polarized electrons confined to move along this circle in the presence of a uniform and static magnetic field normal to the plane that contains this circle. The time-dependent anomalous term on the right-hand side of the anomalous continuity equation (3.15b) is caused by a solenoid of radius $r_{\mathrm{sln}} \ll r \ll R$ in a puncture of the plane that contains the circle of radius r_{sln} supporting a time-dependent flux. The combination of this time-dependent flux with the uniform static magnetic field exerts a Lorentz force on spin-polarized electrons moving along circles in the ring with the inner edge of radius r and the outer edge of radius R. This Lorentz force causes a net transfer of charge between the inner and outer edges

$$\frac{1}{L}\int\limits_0^T \mathrm{d}t\,Q(T) \coloneqq \int\limits_0^T \mathrm{d}t\,\langle \hat{J}^0(t)\rangle = \sigma_{\mathrm{H}}\int\limits_0^T \mathrm{d}t\,E(t) \tag{3.18}$$

during the adiabatic evolution with period T of the normalized many-body ground state of the outer edge, provided we may identify the anomalous continuity equation (3.15b) with that of chiral spin-polarized electrons propagating along the outer edge in Fig. 3.1. Hereto, separating the many-body ground state at the outer edge from all spin-polarized electrons supported between the inner and outer edge requires the existence of an energy scale separating it from many-body states in which these bulk spin-polarized electrons participate and by demanding that the inverse of this energy scale, a length scale, is much smaller than $R-r$. This energy scale is brought about by the uniform and static magnetic field $\boldsymbol{B}$ in Fig. 3.1. That none of this pumped charge is lost in the shaded region of the ring follows if it is assumed that the spin-polarized electrons are unable to transport (dissipatively) a charge current across any circle of radius less than R and greater than r. The Hall conductance in the Corbino geometry of Fig. 3.1 is then a rank two anti-symmetric tensor proportional to the rank two Levi-Civita anti-symmetric tensor with σ_{H} the proportionality constant in units of e^2/h. The charge density and current density for the ring obey a continuity equation as full gauge invariance is restored in the ring.

The chiral bosonic theory (3.1) is nothing but a theory for chiral electrons at the outer edge of the Corbino disk, as we still have to demonstrate. Chiral fermions are a fraction of the original fermion (a spin-polarized electron). More precisely, low-energy fermions have been split into one half that propagate on the outer edge and another half that propagate on the inner edge of the Corbino disk. The price for this fractionalization is an apparent breakdown of gauge invariance and charge conservation, when each chiral edge is treated independently from the other. Manifest charge conservation and gauge invariance are only restored if all low-energy degrees of freedom from the Corbino disk are treated on equal footing.

3.5 Conserved topological charges

Turn off the external gauge potentials

$$A_0(t,x)=A_1(t,x)=0. \tag{3.19}$$

For any $i=1,\cdots,N$, define the operator

$$\begin{aligned}\widehat{\mathcal{N}}_i(t) &\coloneqq \frac{1}{2\pi}\int\limits_0^L \mathrm{d}x\,\left(\partial_x\hat{u}_i\right)(t,x)\\ &=\frac{1}{2\pi}\left[\hat{u}_i(t,L)-\hat{u}_i(t,0)\right].\end{aligned} \tag{3.20}$$

This operator is conserved if and only if

$$\left(\partial_x\hat{u}_i\right)(t,x)=\left(\partial_x\hat{u}_i\right)(t,x+L),\qquad 0\le x\le L, \tag{3.21}$$

for

$$\mathrm{i}\left(\partial_t\widehat{\mathcal{N}}_i\right)(t)=-\frac{\mathrm{i}}{2\pi}K_{ik}V_{kl}\big[\left(\partial_x\hat{u}_l\right)(t,L)-\left(\partial_x\hat{u}_l\right)(t,0)\big]. \tag{3.22}$$

Furthermore, if we demand that there exists an $n_i\in\mathbb{Z}$ such that

$$\hat{u}_i(t,x+L)=\hat{u}_i(t,x)-2\pi n_i, \tag{3.23}$$

it then follows that

$$\widehat{\mathcal{N}}_i=n_i. \tag{3.24}$$

The N conserved topological charges $\mathcal{N}_i$ with $i = 1, \cdots, N$ commute pairwise, for

$$\begin{aligned}\left[\widehat{\mathcal{N}}_i, \widehat{\mathcal{N}}_j\right] &= \frac{1}{2\pi} \int\limits_0^L \mathrm{d}y \, \left[\widehat{\mathcal{N}}_i, \left(\partial_y \hat{u}_j\right)(y)\right] \\ &= \frac{1}{2\pi} \int\limits_0^L \mathrm{d}y \, \partial_y \left[\widehat{\mathcal{N}}_i, \hat{u}_j(y)\right],\end{aligned} \tag{3.25}$$

whereby $j = 1, \cdots, N$ and

$$\left[\widehat{\mathcal{N}}_i, \hat{u}_j(y)\right] = \mathrm{i} K_{ij} \tag{3.26}$$

is independent of y.

The local counterpart to the global conservation of the topological charge is

$$\partial_t \, \hat{\rho}_i^{\text{top}} + \partial_x \, \hat{j}_i^{\text{top}} = 0, \tag{3.27a}$$

where the local topological density operator is defined by

$$\hat{\rho}_i^{\text{top}}(t,x) := \frac{1}{2\pi} \left(\partial_x \hat{u}_i\right)(t,x) \tag{3.27b}$$

and the local topological current operator is defined by

$$\hat{j}_i^{\text{top}}(t,x) := \frac{1}{2\pi} K_{ik} \, V_{kl} \, \left(\partial_x \hat{u}_l\right)(t,x) \tag{3.27c}$$

for $i = 1, \cdots, N$. The local topological density operator obeys the equal-time algebra

$$\left[\hat{\rho}_i^{\text{top}}(t,x), \hat{\rho}_j^{\text{top}}(t,y)\right] = -\frac{\mathrm{i}}{2\pi} \, K_{ij} \, \partial_x \delta(x-y) \tag{3.28a}$$

for any $i, j = 1, \cdots, N$. The local topological current operator obeys the equal-time algebra

$$\left[\hat{j}_i^{\text{top}}(t,x), \hat{j}_j^{\text{top}}(t,y)\right] = -\frac{\mathrm{i}}{2\pi} K_{ik} V_{kl} \, K_{jk'} V_{k'l'} \, K_{ll'} \, \partial_x \delta(x-y) \tag{3.28b}$$

for any $i, j = 1, \cdots, N$. Finally,

$$\left[\hat{\rho}_i^{\text{top}}(t,x), \hat{j}_j^{\text{top}}(t,y)\right] = -\frac{\mathrm{i}}{2\pi} \, K_{jk} \, V_{kl} \, K_{il} \, \partial_x \delta(x-y) \tag{3.28c}$$

for any $i, j = 1, \cdots, N$.

Introduce the local charges and currents

$$\hat{\rho}_i(t,x) := K_{ij}^{-1} \hat{\rho}_j^{\text{top}}(t,x) \tag{3.29a}$$

and

$$\hat{j}_i(t,x) := K_{ij}^{-1} \hat{j}_j^{\text{top}}(t,x), \tag{3.29b}$$

respectively, for any $i=1,\cdots,N$. The continuity equation (3.27a) is unchanged under this linear transformation,

$$\partial_t\,\hat{\rho}_i+\partial_x\,\hat{j}_i=0, \tag{3.29c}$$

for any $i=1,\cdots,N$. The topological current algebra (3.28) transforms into

$$\begin{aligned}
\left[\hat{\rho}_i(t,x),\hat{\rho}_j(t,y)\right]&=-\frac{\mathrm{i}}{2\pi}\,K^{-1}_{ij}\,\partial_x\delta(x-y), && (3.30\text{a})\\
\left[\hat{j}_i(t,x),\hat{j}_j(t,y)\right]&=-\frac{\mathrm{i}}{2\pi}\,V_{ik}\,V_{jl}\,K_{kl}\,\partial_x\delta(x-y), && (3.30\text{b})\\
\left[\hat{\rho}_i(t,x),\hat{j}_j(t,y)\right]&=-\frac{\mathrm{i}}{2\pi}\,V_{ij}\,\partial_x\delta(x-y), && (3.30\text{c})
\end{aligned}$$

for any $i,j=1,\cdots,N$.

At last, if we contract the continuity equation (3.29c) with the integer-valued charge vector, we obtain the flavor-global continuity equation

$$\partial_t\,\hat{\rho}+\partial_x\,\hat{j}=0, \tag{3.31a}$$

where the local flavor-global charge operator is

$$\hat{\rho}(t,x):=\,q_i\,K^{-1}_{ij}\,\hat{\rho}^{\mathrm{top}}_j(t,x) \tag{3.31b}$$

and the local flavor-global current operator is

$$\hat{j}(t,x):=\,q_i\,K^{-1}_{ij}\,\hat{j}^{\mathrm{top}}_j(t,x). \tag{3.31c}$$

The flavor-resolved current algebra (3.30) turns into the flavor-global current algebra

$$\begin{aligned}
\left[\hat{\rho}(t,x),\hat{\rho}(t,y)\right]&=-\frac{\mathrm{i}}{2\pi}\left(q_i\,K^{-1}_{ij}\,q_j\right)\,\partial_x\delta(x-y), && (3.32\text{a})\\
\left[\hat{j}(t,x),\hat{j}(t,y)\right]&=-\frac{\mathrm{i}}{2\pi}\left(q_i\,V_{ik}\,K_{kl}\,V_{lj}\,q_j\right)\,\partial_x\delta(x-y), && (3.32\text{b})\\
\left[\hat{\rho}(t,x),\hat{j}(t,y)\right]&=-\frac{\mathrm{i}}{2\pi}\left(q_i\,V_{ij}\,q_j\right)\,\partial_x\delta(x-y). && (3.32\text{c})
\end{aligned}$$

3.6 Quasi-particle and particle excitations

When Eq. (3.19) holds, there exist N conserved global topological (i.e., integer valued) charges $\widehat{\mathcal{N}}_i$ with $i=1,\cdots,N$ defined in Eq. (3.20) that commute pairwise. Define the N global charges

$$\widehat{Q}_i:=\int\limits_0^L\mathrm{d}x\,\hat{\rho}_i(t,x)=K^{-1}_{ij}\,\widehat{\mathcal{N}}_j,\qquad i=1,\cdots,N. \tag{3.33}$$

These charges shall shortly be interpreted as the elementary Fermi-Bose charges.

For any $i = 1, \cdots, N$, define the pair of vertex operators

$$\widehat{\Psi}^{\dagger}_{\text{q-p},i}(t,x) := e^{-\mathrm{i}K^{-1}_{ij}\,\hat{u}_j(t,x)} \tag{3.34a}$$

and

$$\widehat{\Psi}^{\dagger}_{\text{f-b},i}(t,x) := e^{-\mathrm{i}\delta_{ij}\,\hat{u}_j(t,x)}, \tag{3.34b}$$

respectively. The quasi-particle vertex operator $\widehat{\Psi}^{\dagger}_{\text{q-p},i}(t,x)$ is multi-valued under a shift by 2π of all $\hat{u}_j(t,x)$ where $j = 1, \cdots, N$. The Fermi-Bose vertex operator $\widehat{\Psi}^{\dagger}_{\text{f-b},i}(t,x)$ is single-valued under a shift by 2π of all $\hat{u}_j(t,x)$ where $j = 1, \cdots, N$.

For any pair $i, j = 1, \cdots, N$, the commutator (3.26) delivers the identities

$$\left[\widehat{\mathcal{N}}_i, \widehat{\Psi}^{\dagger}_{\text{q-p},j}(t,x)\right] = \delta_{ij}\,\widehat{\Psi}^{\dagger}_{\text{q-p},j}(t,x), \quad \left[\widehat{\mathcal{N}}_i, \widehat{\Psi}^{\dagger}_{\text{f-b},j}(t,x)\right] = K_{ij}\,\widehat{\Psi}^{\dagger}_{\text{f-b},j}(t,x), \tag{3.35}$$

and

$$\left[\widehat{Q}_i, \widehat{\Psi}^{\dagger}_{\text{q-p},j}(t,x)\right] = K^{-1}_{ij}\,\widehat{\Psi}^{\dagger}_{\text{q-p},j}(t,x), \quad \left[\widehat{Q}_i, \widehat{\Psi}^{\dagger}_{\text{f-b},j}(t,x)\right] = \delta_{ij}\,\widehat{\Psi}^{\dagger}_{\text{f-b},j}(t,x), \tag{3.36}$$

respectively. The quasi-particle vertex operator $\widehat{\Psi}^{\dagger}_{\text{q-p},i}(t,x)$ is an eigenstate of the topological number operator $\widehat{\mathcal{N}}_i$ with eigenvalue one. The Fermi-Bose vertex operator $\widehat{\Psi}^{\dagger}_{\text{f-b},i}(t,x)$ is an eigenstate of the charge number operator $\widehat{Q}_i$ with eigenvalue one.

The Baker-Campbell-Hausdorff formula implies that

$$e^{\hat{A}}\,e^{\hat{B}} = e^{\hat{A}+\hat{B}}\,e^{+(1/2)[\hat{A},\hat{B}]} = e^{\hat{B}}\,e^{\hat{A}}\,e^{[\hat{A},\hat{B}]} \tag{3.37}$$

whenever two operators $\hat{A}$ and $\hat{B}$ have a $\mathbb{C}$-number as their commutator.

A first application of the Baker-Campbell-Hausdorff formula to any pair of quasi-particle vertex operator at equal time t but two distinct space coordinates $x \neq y$ gives

$$\widehat{\Psi}^{\dagger}_{\text{q-p},i}(t,x)\,\widehat{\Psi}^{\dagger}_{\text{q-p},j}(t,y) = e^{-\mathrm{i}\pi\,\Theta^{\text{q-p}}_{ij}}\,\widehat{\Psi}^{\dagger}_{\text{q-p},j}(t,y)\,\widehat{\Psi}^{\dagger}_{\text{q-p},i}(t,x), \tag{3.38a}$$

where

$$\Theta^{\text{q-p}}_{ij} := K^{-1}_{ji}\,\mathrm{sgn}(x-y) + \left(K^{-1}_{ik}\,K^{-1}_{jl}\,K_{kl} + q_k\,K^{-1}_{ik}\,K^{-1}_{jl}\,q_l\right)\mathrm{sgn}(k-l). \tag{3.38b}$$

Here and below, it is understood that

$$\mathrm{sgn}(k-l) = 0 \tag{3.39}$$

when $k = l = 1, \cdots, N$. Hence, the quasi-particle vertex operators obey neither bosonic nor fermionic statistics since $K^{-1}_{ij} \in \mathbb{Q}$.

The same exercise applied to the Fermi-Bose vertex operators yields

$$\widehat{\Psi}^{\dagger}_{\text{f-b},i}(t,x)\,\widehat{\Psi}^{\dagger}_{\text{f-b},j}(t,y) = \begin{cases} (-1)^{K_{ii}}\,\widehat{\Psi}^{\dagger}_{\text{f-b},i}(t,y)\,\widehat{\Psi}^{\dagger}_{\text{f-b},i}(t,x), & \text{if } i = j, \\ \\ (-1)^{q_i\,q_j}\,\widehat{\Psi}^{\dagger}_{\text{f-b},j}(t,y)\,\widehat{\Psi}^{\dagger}_{\text{f-b},i}(t,x), & \text{if } i \neq j, \end{cases} \tag{3.40}$$

when $x \neq y$. The self statistics of the Fermi-Bose vertex operators is carried by the diagonal matrix elements $K_{ii} \in \mathbb{Z}$. The mutual statistics of any pair of Fermi-Bose vertex operators labeled by $i \neq j$ is carried by the product $q_i\,q_j \in \mathbb{Z}$ of the integer-valued charges q_i and q_j. Had we not assumed that K_{ij} with $i \neq j$ are integers, the mutual statistics would not be Fermi-Bose because of the non-local term $K_{ij}\mathrm{sgn}\,(x-y)$.

A third application of the Baker-Campbell-Hausdorff formula allows to determine the boundary conditions

$$\widehat{\Psi}^{\dagger}_{\text{q-p},i}(t,x+L) = \widehat{\Psi}^{\dagger}_{\text{q-p},i}(t,x)\,e^{-2\pi\mathrm{i}\,K^{-1}_{ij}\widehat{\mathcal{N}}_j}\,e^{-\pi\mathrm{i}\,K^{-1}_{ii}} \tag{3.41}$$

and

$$\widehat{\Psi}^{\dagger}_{\text{f-b},i}(t,x+L) = \widehat{\Psi}^{\dagger}_{\text{f-b},i}(t,x)\,e^{-2\pi\mathrm{i}\,\widehat{\mathcal{N}}_i}\,e^{-\pi\mathrm{i}\,K_{ii}} \tag{3.42}$$

obeyed by the quasi-particle and Fermi-Bose vertex operators, respectively.

This discussion closes with the following definitions. Introduce the operators

$$\widehat{Q} \coloneqq q_i\,\widehat{Q}_i, \quad \widehat{\Psi}^{\dagger}_{\text{q-p},\boldsymbol{m}} \coloneqq e^{-\mathrm{i}m_i K^{-1}_{ij}\hat{u}_j(t,x)}, \qquad \widehat{\Psi}^{\dagger}_{\text{f-b},\boldsymbol{m}} \coloneqq e^{-\mathrm{i}m_i\delta_{ij}\hat{u}_j(t,x)} \tag{3.43}$$

where $\boldsymbol{m} \in \mathbb{Z}^N$ is the vector with the integer-valued components m_i for any $i = 1, \cdots, N$. The N charges q_i with $i = 1, \cdots, N$ that enter Hamiltonian (3.1a) can also be viewed as the components of the vector $\boldsymbol{q} \in \mathbb{Z}^N$. Define the functions

$$\begin{aligned} q : \mathbb{Z}^N &\to \mathbb{Z}, \\ \boldsymbol{m} &\mapsto q(\boldsymbol{m}) \coloneqq q_i\,m_i \equiv \boldsymbol{q}\cdot\boldsymbol{m}, \end{aligned} \tag{3.44a}$$

and

$$\begin{aligned} K : \mathbb{Z}^N &\to \mathbb{Z}, \\ \boldsymbol{m} &\mapsto K(\boldsymbol{m}) \coloneqq m_i\,K_{ij}\,m_j. \end{aligned} \tag{3.44b}$$

On the one hand, for any distinct pair of space coordinate $x \neq y$, we deduce from Eqs. (3.36), (3.38), and (3.41) that

$$\left[\widehat{Q}, \widehat{\Psi}^{\dagger}_{\text{q-p},\boldsymbol{m}}(t,x)\right] = \left(q_i\,K^{-1}_{ij}\,m_j\right)\widehat{\Psi}^{\dagger}_{\text{q-p},\boldsymbol{m}}(t,x), \tag{3.45a}$$

$$\widehat{\Psi}^{\dagger}_{\text{q-p},\boldsymbol{m}}(t,x)\,\widehat{\Psi}^{\dagger}_{\text{q-p},\boldsymbol{n}}(t,y) = e^{-\mathrm{i}\pi\,m_i\,\Theta^{\text{q-p}}_{ij}\,n_j}\,\widehat{\Psi}^{\dagger}_{\text{q-p},\boldsymbol{n}}(t,y)\,\widehat{\Psi}^{\dagger}_{\text{q-p},\boldsymbol{m}}(t,x), \tag{3.45b}$$

$$\widehat{\Psi}^{\dagger}_{\text{q-p},\boldsymbol{m}}(t,x+L) = \widehat{\Psi}^{\dagger}_{\text{q-p},\boldsymbol{m}}(t,x)\,e^{-2\pi\mathrm{i}\,m_i\,K^{-1}_{ij}\,\widehat{\mathcal{N}}_j}\,e^{-\pi\mathrm{i}\,m_i\,K^{-1}_{ij}\,m_j}, \tag{3.45c}$$

respectively. On the other hand, for any distinct pair of space coordinate $x \neq y$, we deduce from Eqs. (3.36), (3.40), and (3.42) that

$$\left[\widehat{Q}, \widehat{\Psi}^{\dagger}_{\text{f-b},\boldsymbol{m}}(t,x)\right] = q(\boldsymbol{m})\,\widehat{\Psi}^{\dagger}_{\text{f-b},\boldsymbol{m}}(t,x), \tag{3.46a}$$

$$\widehat{\Psi}^{\dagger}_{\text{f-b},\boldsymbol{m}}(t,x)\,\widehat{\Psi}^{\dagger}_{\text{f-b},\boldsymbol{n}}(t,y) = e^{-\mathrm{i}\pi\,m_i\,\Theta^{\text{f-b}}_{ij}\,n_j}\,\widehat{\Psi}^{\dagger}_{\text{f-b},\boldsymbol{n}}(t,y)\,\widehat{\Psi}^{\dagger}_{\text{f-b},\boldsymbol{m}}(t,x), \tag{3.46b}$$

$$\widehat{\Psi}^{\dagger}_{\text{f-b},\boldsymbol{m}}(t,x+L) = \widehat{\Psi}^{\dagger}_{\text{f-b},\boldsymbol{m}}(t,x)\,e^{-2\pi\mathrm{i}\,m_i\widehat{\mathcal{N}}_i}\,e^{-\pi\mathrm{i}\,m_i K_{ij} m_j}, \tag{3.46c}$$

respectively, where

$$\Theta^{\text{f-b}}_{ij} \coloneqq K_{ij}\,\mathrm{sgn}(x-y) + \left(K_{ij} + q_i\,q_j\right)\,\mathrm{sgn}(i-j). \tag{3.46d}$$

The integer quadratic form $K(\boldsymbol{m})$ is thus seen to dictate whether the vertex operator $\widehat{\Psi}^{\dagger}_{\text{f-b},\boldsymbol{m}}(t,x)$ realizes a fermion or a boson. The vertex operator $\widehat{\Psi}^{\dagger}_{\text{f-b},\boldsymbol{m}}(t,x)$ realizes a fermion if and only if

$$K(\boldsymbol{m}) \text{ is an odd integer} \tag{3.47}$$

or a boson if and only if

$$K(\boldsymbol{m}) \text{ is an even integer.} \tag{3.48}$$

Because of assumption (3.1f),

$$(-1)^{K(\boldsymbol{m})} = (-1)^{q(\boldsymbol{m})}. \tag{3.49}$$

Hence, the vertex operator $\widehat{\Psi}^{\dagger}_{\text{f-b},\boldsymbol{m}}(t,x)$ realizes a fermion if and only if

$$q(\boldsymbol{m}) \text{ is an odd integer} \tag{3.50}$$

or a boson if and only if

$$q(\boldsymbol{m}) \text{ is an even integer.} \tag{3.51}$$

3.7 Bosonization rules

We are going to relate the theory of chiral bosons (3.1) without external gauge fields to a massless Dirac Hamiltonian. To this end, we proceed in three steps.

Step 1: Make the choices

$$N = 2, \qquad i,j = 1,2 \equiv -,+, \tag{3.52a}$$

and

$$K := \begin{pmatrix} +1 & 0 \\ 0 & -1 \end{pmatrix}, \qquad V := \begin{pmatrix} +1 & 0 \\ 0 & +1 \end{pmatrix}, \qquad \boldsymbol{q} = \begin{pmatrix} 1 \\ 1 \end{pmatrix}, \tag{3.52b}$$

in Eq. (3.1). With this choice, the free bosonic Hamiltonian on the real line is

$$\widehat{H}_{\mathrm{B}} = \int\limits_{\mathbb{R}} \mathrm{d}x\, \frac{1}{4\pi} \left[(\partial_x \hat{u}_-)^2 + (\partial_x \hat{u}_+)^2 \right], \tag{3.53a}$$

where

$$[\hat{u}_-(t,x), \hat{u}_-(t,y)] = +\mathrm{i}\pi\, \mathrm{sgn}(x-y), \tag{3.53b}$$

$$[\hat{u}_+(t,x), \hat{u}_+(t,y)] = -\mathrm{i}\pi\, \mathrm{sgn}(x-y), \tag{3.53c}$$

$$[\hat{u}_-(t,x), \hat{u}_+(t,y)] = +\mathrm{i}\pi. \tag{3.53d}$$

There follows the chiral equations of motion [recall Eq. (3.3)]

$$\partial_t\, \hat{u}_- = -\partial_x\, \hat{u}_-, \qquad \partial_t\, \hat{u}_+ = +\partial_x\, \hat{u}_+, \tag{3.54}$$

obeyed by the right-mover $\hat{u}_-$ and the left-mover $\hat{u}_+$

$$\left[\hat{\rho}(t,x),\hat{\rho}(t,y)\right]=0, \tag{3.55a}$$

$$\left[\hat{j}(t,x),\hat{j}(t,y)\right]=0, \tag{3.55b}$$

$$\left[\hat{\rho}(t,x),\hat{j}(t,y)\right]=-\frac{\mathrm{i}}{\pi}\partial_x\delta(x-y), \tag{3.55c}$$

obeyed by the density

$$\hat{\rho}=+\frac{1}{2\pi}\left(\partial_x\,\hat{u}_- -\partial_x\,\hat{u}_+\right)\equiv\hat{j}_- +\hat{j}_+ \tag{3.55d}$$

and the current density [1]

$$\hat{j}=+\frac{1}{2\pi}\left(\partial_x\,\hat{u}_- +\partial_x\,\hat{u}_+\right)\equiv\hat{j}_- -\hat{j}_+, \tag{3.55e}$$

and the identification of the pair of vertex operators [recall Eq. (3.34b)]

$$\hat{\psi}^\dagger_- := \sqrt{\frac{1}{4\pi\,\mathfrak{a}}}\,e^{-\mathrm{i}\hat{u}_-},\qquad \hat{\psi}^\dagger_+ := \sqrt{\frac{1}{4\pi\,\mathfrak{a}}}\,e^{+\mathrm{i}\hat{u}_+}, \tag{3.56}$$

with a pair of creation operators for fermions. The multiplicative prefactor $1/\sqrt{4\pi}$ is a matter of convention and the constant $\mathfrak{a}$ carries the dimension of length, i.e., the fermion fields carries the dimension of $1/\sqrt{\text{length}}$. By construction, the chiral currents

$$\hat{j}_- := +\frac{1}{2\pi}\,\partial_x\,\hat{u}_-,\qquad \hat{j}_+ := -\frac{1}{2\pi}\,\partial_x\,\hat{u}_+, \tag{3.57}$$

obey the chiral equations of motion

$$\partial_t\,\hat{j}_- = -\partial_x\,\hat{j}_-,\qquad \partial_t\,\hat{j}_- = +\partial_x\,\hat{j}_-, \tag{3.58}$$

i.e., they depend solely on $(t-x)$ and $(t+x)$, respectively. As with the chiral fields $\hat{u}_-$ and $\hat{u}_+$, the chiral currents $\hat{j}_-$ and $\hat{j}_+$ are right-moving and left-moving solutions, respectively, of the Klein-Gordon equation

$$(\partial_t^2-\partial_x^2)\,f(t,x)=(\partial_t-\partial_x)\,(\partial_t+\partial_x)\,f(t,x)=0. \tag{3.59}$$

Step 2: Define the free Dirac Hamiltonian

$$\widehat{H}_{\mathrm{D}} := \int\limits_{\mathbb{R}}\mathrm{d}x\,\hat{\psi}^\dagger\,\gamma^0\,\gamma^1\,\mathrm{i}\partial_x\,\hat{\psi}\equiv\int\limits_{\mathbb{R}}\mathrm{d}x\,\hat{\bar{\psi}}\,\gamma^1\,\mathrm{i}\partial_x\,\hat{\psi}, \tag{3.60a}$$

where

$$\left\{\hat{\psi}(t,x),\hat{\psi}^\dagger(t,y)\right\}=\tau_0\,\delta(x-y) \tag{3.60b}$$

delivers the only non-vanishing equal-time anti-commutators. If we define the chiral projections ($\gamma_5\equiv-\gamma^5\equiv-\gamma^0\gamma^1$)

[1] Notice that the chiral equations of motion implies that $\hat{j}=-\frac{1}{2\pi}\left(\partial_t\,\hat{u}_- -\partial_t\,\hat{u}_+\right)$.

$$\hat{\psi}^{\dagger}_{\mp} := \hat{\psi}^{\dagger}\,\frac{1}{2}(1\mp\gamma_5), \qquad \hat{\psi}_{\mp} := \frac{1}{2}(1\mp\gamma_5)\,\hat{\psi}\,, \tag{3.61a}$$

there follows the chiral equations of motion

$$\partial_t\,\hat{\psi}_- = -\partial_x\,\hat{\psi}_-, \qquad \partial_t\,\hat{\psi}_+ = +\partial_x\,\hat{\psi}_+. \tag{3.61b}$$

The annihilation operator $\hat{\psi}_-$ removes a right-moving fermion. The annihilation operator $\hat{\psi}_+$ removes a left-moving fermion. Moreover, the Lagrangian density

$$\mathcal{L}_{\mathrm{D}} := \hat{\psi}^{\dagger}\,\gamma^0\,\mathrm{i}\gamma^{\mu}\,\partial_{\mu}\,\hat{\psi} \tag{3.62}$$

obeys the additive decomposition

$$\mathcal{L}_{\mathrm{D}} = \hat{\psi}^{\dagger}_{-}\,\mathrm{i}(\partial_0+\partial_1)\,\hat{\psi}_- + \hat{\psi}^{\dagger}_{+}\,\mathrm{i}(\partial_0-\partial_1)\,\hat{\psi}_+ \tag{3.63}$$

with the two independent chiral currents

$$\hat{j}_{\mathrm{D}-} := 2\,\hat{\psi}^{\dagger}_{-}\,\hat{\psi}_-, \qquad \hat{j}_{\mathrm{D}+} := 2\,\hat{\psi}^{\dagger}_{+}\,\hat{\psi}_+, \tag{3.64a}$$

obeying the independent conservation laws

$$\partial_t\,\hat{j}_{\mathrm{D}-} = -\partial_x\,\hat{j}_{\mathrm{D}-}, \qquad \partial_t\,\hat{j}_{\mathrm{D}+} = +\partial_x\,\hat{j}_{\mathrm{D}+}. \tag{3.64b}$$

Finally, it can be shown that if the chiral currents are normal ordered with respect to the filled Fermi sea with a vanishing chemical potential, then the only non-vanishing equal-time commutators are

$$\left[\hat{j}_{\mathrm{D}-}(t,x),\hat{j}_{\mathrm{D}-}(t,y)\right] = -\frac{\mathrm{i}}{2\pi}\,\partial_x\,\delta(x-y), \tag{3.65a}$$

and

$$\left[\hat{j}_{\mathrm{D}+}(t,x),\hat{j}_{\mathrm{D}+}(t,y)\right] = +\frac{\mathrm{i}}{2\pi}\,\partial_x\,\delta(x-y). \tag{3.65b}$$

Step 3: The Dirac chiral current algebra (3.65) is equivalent to the bosonic chiral current algebra (3.55). This equivalence is interpreted as the fact that (i) the bosonic theory (3.53) is equivalent to the Dirac theory (3.60), and (ii) there is a one-to-one correspondence between the following operators acting on their respective Fock spaces. To establish this one-to-one correspondence, we introduce the pair of bosonic fields

$$\hat{\phi}(x^0,x^1) := \hat{u}_-(x^0-x^1) + \hat{u}_+(x^0+x^1), \tag{3.66a}$$

$$\hat{\theta}(x^0,x^1) := \hat{u}_-(x^0-x^1) - \hat{u}_+(x^0+x^1). \tag{3.66b}$$

Now, the relevant one-to-one correspondence between operators in the Dirac theory for fermions and operators in the chiral bosonic theory is given in Table 3.1.

Table 3.1 Abelian bosonization rules in two-dimensional Minkowski space. The conventions of relevance to the scalar mass $\hat{\bar{\psi}}\,\hat{\psi}$ and the pseudo-scalar mass $\hat{\bar{\psi}}\,\gamma_5\,\hat{\psi}$ are $\hat{\bar{\psi}} = \hat{\psi}^\dagger\,\gamma^0$ with $\hat{\psi}^\dagger = (\hat{\psi}^\dagger_-, \hat{\psi}^\dagger_+)$, whereby $\gamma^0 = \tau_1$ and $\gamma^1 = \mathrm{i}\tau_2$ so that $\gamma^5 = -\gamma_5 = -\gamma^0\,\gamma^1 = \tau_3$.

	Fermions	Bosons
Kinetic energy	$\hat{\bar{\psi}}\,\mathrm{i}\gamma^\mu\,\partial_\mu\,\hat{\psi}$	$\frac{1}{8\pi}\,(\partial^\mu\,\hat{\phi})(\partial_\mu\,\hat{\phi})$
Current	$\hat{\bar{\psi}}\,\gamma^\mu\,\hat{\psi}$	$\frac{1}{2\pi}\,\epsilon^{\mu\nu}\,\partial_\nu\,\hat{\phi}$
Chiral currents	$2\,\hat{\psi}^\dagger_\mp\,\hat{\psi}_\mp$	$\pm\frac{1}{2\pi}\partial_x\,\hat{u}_\mp$
Right and left movers	$\hat{\psi}^\dagger_\mp$	$\sqrt{\frac{1}{4\pi\,\mathfrak{a}}}\,e^{\mp\mathrm{i}\hat{u}_\mp}$
Backward scattering	$\hat{\psi}^\dagger_-\,\hat{\psi}_+$	$\frac{1}{4\pi\,\mathfrak{a}}\,e^{-\mathrm{i}\hat{\phi}}$
Cooper pairing	$\hat{\psi}^\dagger_-\,\hat{\psi}^\dagger_+$	$\frac{1}{4\pi\,\mathfrak{a}}\,e^{-\mathrm{i}\hat{\theta}}$
Scalar mass	$\hat{\psi}^\dagger_-\,\hat{\psi}_+ + \hat{\psi}^\dagger_+\,\hat{\psi}_-$	$\frac{1}{2\pi\,\mathfrak{a}}\,\cos\hat{\phi}$
Pseudo-scalar mass	$\hat{\psi}^\dagger_-\,\hat{\psi}_+ - \hat{\psi}^\dagger_+\,\hat{\psi}_-$	$\frac{-\mathrm{i}}{2\pi\,\mathfrak{a}}\,\sin\hat{\phi}$

3.8 From the Hamiltonian to the Lagrangian formalism

What is the Minkowski path integral that is equivalent to the quantum theory defined by Eq. (3.1)? In other words, we seek the path integrals

$$Z^{(\pm)} := \int \mathcal{D}[u]\,e^{\mathrm{i}S^{(\pm)}[u]} \tag{3.67a}$$

with the Minkowski action

$$S^{(\pm)}[u] := \int\limits_{-\infty}^{+\infty} \mathrm{d}t\,L^{(\pm)}[u] \equiv \int\limits_{-\infty}^{+\infty} \mathrm{d}t \int\limits_{0}^{L} \mathrm{d}x\,\mathcal{L}^{(\pm)}[u](t,x) \tag{3.67b}$$

such that one of the two Hamiltonians

$$H^{(\pm)} := \int\limits_{0}^{L} \mathrm{d}x \left[\Pi^{(\pm)}_i\,(\partial_t\,u_i) - \mathcal{L}^{(\pm)}[u]\right] \tag{3.68}$$

can be identified with $\widehat{H}$ in Eq. (3.1a) after elevating the classical fields

$$u_i(t,x) \tag{3.69a}$$

and

$$\Pi_i^{(\pm)}(t,x) := \frac{\delta\,\mathcal{L}^{(\pm)}}{\delta(\partial_t\,u_i)(t,x)} \tag{3.69b}$$

entering $\mathcal{L}^{(\pm)}[u]$ to the status of quantum fields $\hat{u}_i(t,x)$ and $\hat{\Pi}_j^{(\pm)}(t,y)$ upon imposing the equal-time commutation relations

$$\left[\hat{u}_i(t,x), \hat{\Pi}_j^{(\pm)}(t,y)\right] = \pm\frac{\mathrm{i}}{2}\,\delta_{ij}\,\delta(x-y) \tag{3.69c}$$

for any $i,j = 1,\cdots,N$. The unusual factor $\pm 1/2$ (instead of 1) on the right-hand side of the commutator between pairs of canonically conjugate fields arises because each scalar field u_i with $i = 1,\cdots,N$ is chiral, i.e., it represents "one-half" of a canonical scalar field.

We try

$$\mathcal{L}^{(\pm)} := \frac{1}{4\pi}\left[\mp(\partial_x\,u_i)\,K_{ij}^{-1}\left(\partial_t\,u_j\right) - (\partial_x\,u_i)\,V_{ij}\left(\partial_x\,u_j\right)\right] \tag{3.70a}$$

with the chiral equations of motion

$$\begin{aligned}
0 &= \partial_\mu\,\frac{\delta\,\mathcal{L}^{(\pm)}}{\delta\,\partial_\mu\,u_i} - \frac{\delta\,\mathcal{L}^{(\pm)}}{\delta\,u_i} \\
&= \partial_t\,\frac{\delta\,\mathcal{L}^{(\pm)}}{\delta\,\partial_t\,u_i} + \partial_x\,\frac{\delta\,\mathcal{L}^{(\pm)}}{\delta\,\partial_x\,u_i} - \frac{\delta\,\mathcal{L}^{(\pm)}}{\delta\,u_i} \\
&= \frac{1}{4\pi}\,\Big(\mp K_{ji}^{-1}\,\partial_t\,\partial_x \mp K_{ij}^{-1}\,\partial_x\,\partial_t - 2V_{ij}\,\partial_x\,\partial_x\Big)\,u_j \\
&= \mp\,\frac{K_{ij}^{-1}}{2\pi}\,\partial_x\,\Big(\delta_{jl}\,\partial_t \pm K_{jk}\,V_{kl}\,\partial_x\Big)\,u_l
\end{aligned} \tag{3.70b}$$

for any $i = 1,\cdots,N$. Observe that the term that mixes time t and space x derivatives only becomes imaginary in Euclidean time $\tau = \mathrm{i}t$.

Proof The canonical momentum $\Pi_i^{(\pm)}$ to the field u_i is

$$\Pi_i^{(\pm)}(t,x) := \frac{\delta\,\mathcal{L}^{(\pm)}}{\delta\,(\partial_t\,u_i)(t,x)} = \mp\frac{1}{4\pi}\,K_{ij}^{-1}\,\left(\partial_x\,u_j\right)(t,x) \tag{3.71}$$

for any $i = 1,\cdots,N$ owing to the symmetry of the matrix K. Evidently, the Legendre transform

$$\mathcal{H}^{(\pm)} := \Pi_i^{(\pm)}\,\left(\partial_t\,u_i\right) - \mathcal{L}^{(\pm)} \tag{3.72}$$

delivers

$$\mathcal{H}^{(\pm)} = \frac{1}{4\pi}\,\left(\partial_x\,u_i\right)\,V_{ij}\,\left(\partial_x\,u_j\right). \tag{3.73}$$

The right-hand side does not depend on the chiral index $\pm$. We now quantize the theory by elevating the classical fields u_i to the status of operators $\hat{u}_i$ obeying the algebra (3.1b). This gives a quantum theory that meets all the demands of the quantum chiral edge theory (3.1) in all compatibility with the canonical quantization rules (3.69c), for

$$\begin{aligned}
\left[\hat{u}_i(t,x), \hat{\Pi}^{(\pm)}_j(t,y)\right] &= \mp \frac{1}{4\pi} K^{-1}_{jk}\, \partial_y \left[\hat{u}_i(t,x), \hat{u}_k(t,y)\right] \\
\overset{\text{Eq. (3.1b)}}{} &= \mp \frac{1}{4\pi} K^{-1}_{jk}\, (\pi \mathrm{i}) K_{ik}\, (-2)\delta(x-y) \\
\overset{K_{ik}\,=\,K_{ki}}{} &= \pm \frac{\mathrm{i}}{2} K^{-1}_{jk}\, K_{ki}\, \delta(x-y) \\
&= \pm \frac{\mathrm{i}}{2}\, \delta_{ij}\, \delta(x-y)
\end{aligned} \tag{3.74}$$

where $i, j = 1, \cdots, N$. □

Finally, analytical continuation to Euclidean time

$$\tau = \mathrm{i}t \tag{3.75a}$$

allows to define the finite-temperature quantum chiral theory through the path integral

$$Z^{(\pm)}_{\beta} := \int \mathcal{D}[u]\, \exp\left(- \int_0^{\beta} \mathrm{d}\tau \int_0^{L} \mathrm{d}x\, \mathcal{L}^{(\pm)} \right), \tag{3.75b}$$

$$\begin{aligned}
\mathcal{L}^{(\pm)} := \frac{1}{4\pi} &\left[(\pm)\mathrm{i}\, (\partial_x u_i)\; K^{-1}_{ij}\; \left(\partial_\tau u_j\right) + (\partial_x u_i)\; V_{ij}\; \left(\partial_x u_j\right) \right] \\
&+ J \left(\frac{q_i}{2\pi} K^{-1}_{ij}\, (\partial_x u_j) \right),
\end{aligned} \tag{3.75c}$$

in the presence of an external source field J that couples to the charges q_i like a scalar potential would do.

3.9 Applications to polyacetylene

Consider the Dirac Hamiltonian

$$\widehat{H}_{\mathrm{D}} := \widehat{H}_{\mathrm{D}\,0} + \widehat{H}_{\mathrm{D}\,1}, \tag{3.76a}$$

where the free-field and massless contribution is

$$\widehat{H}_{\mathrm{D}\,0} := \int_{\mathbb{R}} \mathrm{d}x\, \left(\hat{\psi}^{\dagger}_{+}\, \mathrm{i}\partial_x\, \hat{\psi}_{+} - \hat{\psi}^{\dagger}_{-}\, \mathrm{i}\partial_x\, \hat{\psi}_{-} \right), \tag{3.76b}$$

while

$$\widehat{H}_{\mathrm{D}\,1} := \int_{\mathbb{R}} \mathrm{d}x\, \left[\phi_1 \left(\hat{\psi}^{\dagger}_{-}\, \hat{\psi}_{+} + \hat{\psi}^{\dagger}_{+}\, \hat{\psi}_{-} \right) + \mathrm{i}\phi_2 \left(\hat{\psi}^{\dagger}_{-}\, \hat{\psi}_{+} - \hat{\psi}^{\dagger}_{+}\, \hat{\psi}_{-} \right) \right] \tag{3.76c}$$

couples the Dirac field to two real-valued and classical scalar fields ϕ_1 and ϕ_2. The only non-vanishing equal-time anti-commutators are given by Eq. (3.60b).

According to the bosonization rules from Table 3.1 and with the help of the polar decomposition

$$\phi_1(t,x) = |\boldsymbol{\phi}(t,x)|\,\cos\varphi(t,x), \quad \phi_2(t,x) = |\boldsymbol{\phi}(t,x)|\,\sin\varphi(t,x), \tag{3.77}$$

the many-body bosonic Hamiltonian that is equivalent to the Dirac Hamiltonian (3.76) is

$$\widehat{H}_{\mathrm{B}} := \widehat{H}_{\mathrm{B}\,0} + \widehat{H}_{\mathrm{B}\,1}, \tag{3.78a}$$

where

$$\widehat{H}_{\mathrm{B}\,0} := \int\limits_{\mathbb{R}} \mathrm{d}x\, \frac{1}{8\pi} \left[\widehat{\Pi}^2 + \left(\partial_x \hat{\phi}\right)^2\right], \tag{3.78b}$$

while

$$\widehat{H}_{\mathrm{B}\,1} := \int\limits_{\mathbb{R}} \mathrm{d}x\, \frac{1}{2\pi\,\mathfrak{a}}\, |\boldsymbol{\phi}|\, \cos\left(\hat{\phi} - \varphi\right). \tag{3.78c}$$

Here, the canonical momentum

$$\widehat{\Pi}(t,x) := \left(\partial_t\, \hat{\phi}\right)(t,x) \tag{3.79a}$$

shares with $\hat{\phi}(t,x)$ the only non-vanishing equal-time commutator

$$\left[\hat{\phi}(t,x), \widehat{\Pi}(t,y)\right] = \mathrm{i}\delta(x-y). \tag{3.79b}$$

Hamiltonian (3.78) is interacting, and its interaction (3.78c) can be traced to the mass contributions in the non-interacting Dirac Hamiltonian (3.76). The interaction (3.78c) is minimized when the operator identity

$$\hat{\phi}(t,x) = \varphi(t,x) + \pi \tag{3.80}$$

holds. This identity can only be met in the limit

$$|\boldsymbol{\phi}(t,x)| \to \infty \tag{3.81}$$

for all time t and position x in view of the algebra (3.79) and the competition with the contributions (3.78b) and (3.78c).

Close to the limit (3.81), the bosonization formula for the conserved current

$$\hat{\bar{\psi}}\,\gamma^{\mu}\,\hat{\psi} \to \frac{1}{2\pi}\,\epsilon^{\mu\nu}\,\partial_{\nu}\hat{\phi} \tag{3.82}$$

simplifies to

$$\frac{1}{2\pi}\,\epsilon^{\mu\nu}\,\partial_{\nu}\hat{\phi} \approx \frac{1}{2\pi}\,\epsilon^{\mu\nu}\,\partial_{\nu}\varphi. \tag{3.83}$$

On the one hand, the conserved charge

$$\widehat{Q} := \int\limits_{\mathbb{R}} \mathrm{d}x\, \left(\hat{\bar{\psi}}\,\gamma^0\,\hat{\psi}\right)(t,x) \to \frac{\epsilon^{01}}{2\pi}\,\left[\hat{\phi}(t,x=+\infty) - \hat{\phi}(t,x=-\infty)\right] \tag{3.84}$$

for the static profile $\varphi(x)$ is approximately given by

$$\widehat{Q} \approx \frac{\epsilon^{01}}{2\pi}\,\left[\varphi(x=+\infty)-\varphi(x=-\infty)\right]. \tag{3.85}$$

On the other hand, the number of electrons per period $T=2\pi/\omega$ that flows across a point x

$$\hat{I} := \int_0^T \mathrm{d}t\,\left(\hat{\bar{\psi}}\,\gamma^1\,\hat{\psi}\right)(t,x) \to \frac{\epsilon^{10}}{2\pi}\,\left[\hat{\phi}(T,x)-\hat{\phi}(0,x)\right] \tag{3.86}$$

for the uniform profile $\varphi(t)=\omega\,t$ is approximately given

$$\hat{I} \approx \frac{\epsilon^{10}}{2\pi}\,\omega\,T = \epsilon^{10}. \tag{3.87}$$

Results (3.85) and (3.87) are sharp operator identities in the limit (3.81). The small parameter in both expansions is $1/m$ where $m := \lim_{x\to\infty}|\boldsymbol{\phi}(t,x)|$.

4

Stability analysis for the edge theory in the symmetry class AII

4.1 Introduction

The hallmark of the integer quantum effect (IQHE) in an open geometry is the localized nature of all two-dimensional (bulk) states while an integer number of chiral edge states freely propagate along the one-dimensional boundaries. [63, 67, 47] These chiral edge states are immune to the physics of Anderson localization as long as backward scattering between edge states of opposite chiralities is negligible. [67, 47]

Many-body interactions among electrons can be treated perturbatively in the IQHE provided the characteristic many-body energy scale is less than the single-particle gap between Landau levels. This is not true anymore if the chemical potential lies within a Landau level as the non-interacting many-body ground state is then macroscopically degenerate. The lifting of this extensive degeneracy by the many-body interactions is a non-perturbative effect. At some "magic" filling fractions that deliver the fractional quantum Hall effect (FQHE), [118, 113, 68, 43] a screened Coulomb interaction selects a finitely degenerate family of ground states, each of which describes a featureless liquid separated from excitations by an energy gap in a closed geometry. Such a ground state is called an incompressible fractional Hall liquid. The FQHE is an example of topological order. [125, 124, 129] In an open geometry, there are branches of excitations that disperse across the spectral gap of the two-dimensional bulk, but these excitations are localized along the direction normal to the boundary while they propagate freely along the boundary. [129, 126, 128, 127] Contrary to the IQHE, these excitations need not all share the same chirality. However, they are nevertheless immune to the physics of Anderson localization provided scattering induced by the disorder between distinct edges in an open geometry is negligible.

The integer quantum Hall effect (IQHE) is the archetype of a two-dimensional topological band insulator. The two-dimensional $\mathbb{Z}_2$ topological band insulator is a close relative of the IQHE that occurs in semi-conductors with sufficiently large spin-orbit coupling but no breaking of time-reversal symmetry. [54, 55, 11, 10, 64] As with the IQHE, the smoking gun for the $\mathbb{Z}_2$ topological band insulator is the existence of gapless Kramers degenerate pairs of edge states that are delocalized along the boundaries of an open geometry as long as disorder-induced scattering between distinct boundaries is negligible. In contrast to the IQHE, it is the odd parity in the number of Kramers pairs of edge states that is robust to the physics of Anderson localization.

A simple example of a two-dimensional $\mathbb{Z}_2$ topological band insulator can be obtained by putting together two copies of an IQHE system with opposite chiralities for up and down

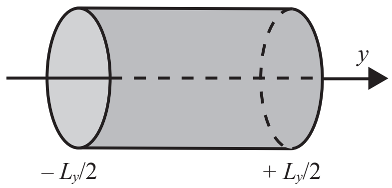

Fig. 4.1 Cylindrical geometry for a two-dimensional band insulator. The cylinder axis is labeled by the coordinate y. Periodic boundary conditions are imposed in the transverse direction labeled by the coordinate x. There is an edge at $y = -L_y/2$ and another one at $y = +L_y/2$. Bulk states have a support on the shaded surface of the cylinder. Edge states are confined in the y direction to the vicinity of the edges $y = \pm L_y/2$. Topological band insulators have the property that there are edge states freely propagating in the x direction even in the presence of disorder with the mean free path ℓ provided the limit $\ell/L_y \ll 1$ holds.

spins. For instance, one could take two copies of Haldane's model, [45] each of which realizes an integer Hall effect on the honeycomb lattice, but with Hall conductance differing by a sign. In this case the spin current is conserved, a consequence of the independent conservation of the up and down currents, and the spin Hall conductance inherits its quantization from the IQHE of each spin species. This example thus realizes an integer quantum spin Hall effect (IQSHE). However, although simple, this example is not generic. The $\mathbb{Z}_2$ topological band insulator does not necessarily have conserved spin currents, let alone quantized responses.

Along the same line of reasoning, two copies of a FQHE system put together, again with opposite chiralities for up and down particles, would realize a fractional quantum spin Hall effect (FQSHE), as proposed by Bernevig and Zhang. [11] (See also Refs. [33] and [48].) Levin and Stern in Ref. [70] proposed to characterize two-dimensional fractional topological liquids supporting the FQSHE by the criterion that their edge states are stable against disorder provided that they do not break time-reversal symmetry spontaneously.

In this chapter, the condition that projection about some quantization axis of the electron spin from the underlying microscopic model is a good quantum number is *not* imposed. Only time-reversal symmetry is assumed to hold. The generic cases of fractional topological liquids with time-reversal symmetry from the special cases of fractional topological liquids with time-reversal symmetry *and* with residual spin-1/2 $U(1)$ rotation symmetry will thus be distinguished. In the former cases, the electronic spin is not a good quantum number. In the latter cases, conservation of spin allows the FQSHE.

The subclass of incompressible time-reversal-symmetric liquids that we construct here is closely related to Abelian Chern-Simons theories. Other possibilities that are not discussed, may include non-Abelian Chern Simons theories, [34,80] or theories that include, additionally, conventional local order parameters (Higgs fields). [100]

The relevant effective action for the Abelian Chern-Simons theory is of the form [124, 129, 126, 127]

$$S := S_0 + S_e + S_s, \tag{4.1a}$$

where

$$S_0 := -\int \mathrm{d}t\, \mathrm{d}^2\boldsymbol{x}\; \epsilon^{\mu\nu\rho}\, \frac{1}{4\pi} K_{ij}\; a^i_\mu\; \partial_\nu\, a^j_\rho, \tag{4.1b}$$

$$S_e \coloneqq \int \mathrm{d}t\,\mathrm{d}^2\boldsymbol{x}\;\epsilon^{\mu\nu\rho}\,\frac{e}{2\pi}\,Q_i\,A_\mu\partial_\nu\,a^i_\rho, \tag{4.1c}$$

and

$$S_s \coloneqq \int \mathrm{d}t\,\mathrm{d}^2\boldsymbol{x}\;\epsilon^{\mu\nu\rho}\,\frac{s}{2\pi}\,S_i\,B_\mu\partial_\nu\,a^i_\rho. \tag{4.1d}$$

The indices i and j run from 1 to $2N$ and any pair thereof labels an integer-valued matrix element K_{ij} of the symmetric and invertible $2N \times 2N$ matrix K. The indices μ, ν, and ρ run from 0 to 2. They either label the component x_μ of the coordinates $(t, \boldsymbol{x})$ in (2+1)-dimensional space and time or the component $A_\mu(t, \boldsymbol{x})$ of an external electromagnetic gauge potential, or the component $B_\mu(t, \boldsymbol{x})$ of an external gauge potential that couples to the spin-1/2 degrees of freedom along some quantization axis, or the components of $2N$ flavors of dynamical Chern-Simons fields $a^i_\mu(t, \boldsymbol{x})$. The integer-valued component Q_i of the $2N$-dimensional vector Q represents the i-th electric charge in units of the electronic charge e and obeys the compatibility condition

$$(-1)^{Q_i} = (-1)^{K_{ii}} \tag{4.1e}$$

for any $i = 1, \cdots, 2N$ in order for bulk quasiparticles or, in an open geometry, quasiparticles on edges to obey a consistent statistics. The integer-valued component S_i of the $2N$-dimensional vector S represents the i-th spin charge in units of the spin charge s along some conserved quantization axis. The operation of time reversal is the map

$$A_\mu(t, \boldsymbol{x}) \mapsto +g^{\mu\nu}\,A_\nu(-t, \boldsymbol{x}), \tag{4.2a}$$

$$B_\mu(t, \boldsymbol{x}) \mapsto -g^{\mu\nu}\,b_\nu(-t, \boldsymbol{x}), \tag{4.2b}$$

$$a^i_\mu(t, \boldsymbol{x}) \mapsto -g^{\mu\nu} a^{i+N}_\nu(-t, \boldsymbol{x}), \tag{4.2c}$$

for $i = 1, \cdots, N$. Here, $g_{\mu\nu} = \mathrm{diag}(+1, -1, -1)$ is the Lorentz metric in $(2{+}1)$-dimensional space and time. It will be shown that time-reversal symmetry imposes that the matrix K is of the block form

$$K = \begin{pmatrix} \kappa & \Delta \\ \Delta^{\mathsf{T}} & -\kappa \end{pmatrix}, \tag{4.3a}$$

$$\kappa^{\mathsf{T}} = \kappa, \quad \Delta^{\mathsf{T}} = -\Delta, \tag{4.3b}$$

where κ and Δ are $N \times N$ matrices, while the integer-charge vectors Q and S are of the block forms

$$Q = \begin{pmatrix} \varrho \\ \varrho \end{pmatrix}, \qquad S = \begin{pmatrix} \varrho \\ -\varrho \end{pmatrix}. \tag{4.3c}$$

The K matrix together with the charge vector Q and spin vector S that characterize the topological field theory with the action (4.1a) define the charge filling fraction, a rational number,

$$\nu_e \coloneqq Q^{\mathsf{T}}\,K^{-1}\,Q \tag{4.4a}$$

and the spin filling fraction, another rational number,

$$\nu_s \coloneqq \frac{1}{2}\, Q^{\mathsf{T}}\, K^{-1}\, S, \tag{4.4b}$$

respectively. The block forms of K and Q in Eq. (4.3) imply that

$$\nu_e = 0. \tag{4.4c}$$

The "zero charge filling fraction" (4.4c) states nothing but the fact that there is no charge Hall conductance when time-reversal symmetry holds. On the other hand, time-reversal symmetry of the action (4.1a) is compatible with a non-vanishing FQSHE as measured by the non-vanishing quantized spin-Hall conductance

$$\sigma_{\mathrm{sH}} \coloneqq \frac{e}{2\pi} \times \nu_s. \tag{4.4d}$$

The origin of the FQSHE in the action (4.1a) is the $U(1) \times U(1)$ gauge symmetry when $(2+1)$-dimensional space and time has the same topology as a manifold without boundary. It is always assumed that the $U(1)$ symmetry associated with charge conservation holds in this lecture. However, we shall not do the same with the $U(1)$ symmetry responsible for the conservation of the "spin" quantum number.

The special cases of the FQSHE treated in Refs. [11] and [70] correspond to imposing the condition

$$\Delta = 0 \tag{4.5}$$

on the K matrix in Eq. (4.3a). This restriction is, however, not necessary to treat either the FQSHE or the generic case when there is no residual spin-1/2 $U(1)$ symmetry in the underlying microscopic model.

The effective topological field theory (4.1) with the condition for time-reversal symmetry (4.3) is made of $2N$ Abelian Chern-Simons fields. As is the case with the FQHE, when two-dimensional space is a manifold without boundary of genus one, i.e., when two-dimensional space is topologically equivalent to a torus, it is characterized by distinct topological sectors. [125, 124, 129] All topological sectors are in one-to-one correspondence with a finite number $\mathcal{N}_{\mathrm{GS}}$ of topologically degenerate ground states of the underlying microscopic theory. [125, 124, 129] This degeneracy is nothing but the magnitude of the determinant K in Eq. (4.1a), which is, because of the block structure (4.3a), in turn given by

$$\begin{aligned} \mathcal{N}_{\mathrm{GS}} &= \left| \det \begin{pmatrix} \kappa & \Delta \\ \Delta^{\mathsf{T}} & -\kappa \end{pmatrix} \right| \\ &= \left| \det \begin{pmatrix} \Delta^{\mathsf{T}} & -\kappa \\ \kappa & \Delta \end{pmatrix} \right| \\ &= \left| \mathrm{Pf} \begin{pmatrix} \Delta^{\mathsf{T}} & -\kappa \\ \kappa & \Delta \end{pmatrix} \right|^2 \\ &= (\text{integer})^2 . \end{aligned} \tag{4.6}$$

To reach the last line, the fact that the K matrix is integer valued was used. It is thus predicted that the class of two-dimensional time-reversal-symmetric fractional topological liquids, whose universal properties are captured by Eqs. (4.1) and (4.3), are characterized by a topological ground state degeneracy that is always the square of an integer, even if $\Delta \neq 0$, when space is topologically equivalent to a torus. (Notice that the condition that Δ is antisymmetric implies that non-vanishing Δ can only occur for $N > 1$.)

The stability of the edge states associated with the bulk Chern-Simons action (4.1) obeying the condition for the time-reversal symmetry (4.3) is discussed in detail. A single one-dimensional edge is considered and an interacting quantum field theory for $1 \leq N_{\mathrm{K}} \leq N$ pairs of Kramers degenerate electrons subject to strong disorder that preserves time-reversal symmetry is constructed. (The integer $2N_{\mathrm{K}}$ is the number of odd charges entering the charge vector Q. [2]) The conditions under which at least one Kramers degenerate pair of electrons remains gapless in spite of the interactions and disorder are identified. This approach is here inspired by the stability analysis of the edge states performed for the single-layer FQHE by Haldane in Ref. [46] (see also Refs. [53] and [82]), by Naud et al. in Refs. [84] and [85] for the bilayer FQHE, and specially that by Levin and Stern in Ref. [70] for the FQSHE and that in Ref. [88]. As for the FQSHE, our analysis departs from the analysis of Haldane in that we impose time-reversal symmetry. In this lecture, we also depart from Ref. [70] by considering explicitly the effects of the off-diagonal elements Δ in the K-matrix. Such terms are generically present for any realistic underlying microscopic model independently of whether this underlying microscopic model supports or not the FQSHE. When considering the stability of the edge theory, we allow the residual spin-1/2 $U(1)$ symmetry responsible for the FQSHE to be broken by interactions among the edge modes or by a disorder potential. Hence, we seek a criterion for the stability of the edge theory that does not rely on the existence of a quantized spin Hall conductance in the bulk as was done in Ref. [70].

The stability of the edge states against disorder hinges on whether the integer

$$R := r\, \varrho^{\mathsf{T}} \, (\kappa - \Delta)^{-1} \, \varrho \tag{4.7}$$

is odd (stable) or even (unstable). The vector ϱ together with the matrices κ and Δ were defined in Eq. (4.3). The integer r is the smallest integer such that all the N components of the vector $r\,(\kappa - \Delta)^{-1}\,\varrho$ are integers. One can quickly check a few simple examples. First, observe that, in the limit $\Delta = 0$, we recover the criterion derived in Ref. [70]. Second, when we impose a residual spin-1/2 $U(1)$ symmetry by appropriately restricting the interactions between edge channels, $\nu_{\uparrow} = -\nu_{\downarrow} = \varrho^{\mathsf{T}}(\kappa - \Delta)^{-1}\,\varrho$ can be interpreted as the Hall conductivity σ_{xy} in units of e^2/h for each of the separately conserved spin components along the spin quantization axis. The integer r has the interpretation of the number of fluxes needed to pump a unit of charge, or the inverse of the "minimum charge" of Ref. [70]. Further restricting to the case when $\kappa = \mathbb{1}_N$ gives $R = N$, i.e., we have recovered the same criterion as for the two-dimensional non-interacting $\mathbb{Z}_2$ topological band insulator.

When there is no residual spin-$1/2$ $U(1)$ symmetry, one can no longer relate the index R to a physical spin Hall conductance. Nevertheless, the index R defined in Eq. (4.7) discriminates in all cases whether there is or not a remaining branch of gapless modes dispersing along the edge.

4.2 Definitions

Consider an interacting model for electrons in a two-dimensional cylindrical geometry as is depicted in Fig. 4.1. Demand that (i) charge conservation and time-reversal symmetry are the only intrinsic symmetries of the microscopic quantum Hamiltonian, (ii) neither are broken spontaneously by the many-body ground state, and (iii), if periodic boundary conditions are assumed along the y coordinate in Fig. 4.1, then there is at most a finite number of degenerate many-body ground states and each many-body ground state is separated from its tower of many-body excited states by an energy gap. Had the condition that time-reversal symmetry holds been relaxed, the remaining assumptions would be realized for the FQHE.

In the open geometry of Fig. 4.1, the only possible excitations with an energy smaller than the bulk gap in the closed geometry of a torus must be localized along the y coordinate in the vicinities of the edges at $\pm L_y/2$. If L_y is much larger than the characteristic linear extension into the bulk of edge states, the two edges decouple from each other. It is then meaningful to define a low-energy and long-wavelength quantum field theory for the edge states propagating along any one of the two boundaries in Fig. 4.1, which we take to be of length L each.

The low-energy and long-wavelength effective quantum field theory for the edge that we are going to construct is inspired by the construction by Wen of the chiral Luttinger edge theory for the FQHE. [126, 124, 127] As for the FQHE, this time-reversal symmetric boundary quantum field theory has a correspondence to the effective time-reversal symmetric bulk topological quantum-field theory built out of $2N$ Abelian Chern-Simon fields.

The simplest class of quantum Hamiltonians that fulfills requirements (i)–(iii) can be represented in terms of $2N$ real-valued chiral scalar quantum fields $\widehat{\Phi}_i(t,x)$ with $i = 1,\ldots,2N$ that form the components of the quantum vector field $\widehat{\Phi}(t,x)$. After setting the electric charge e, the speed of light c, and $\hbar$ to unity, the Hamiltonian for the system is given by [1]

$$\widehat{H} := \widehat{H}_0 + \widehat{H}_{\mathrm{int}}, \tag{4.8a}$$

where

$$\widehat{H}_0 := \int\limits_0^L \mathrm{d}x\, \frac{1}{4\pi} \left(\partial_x \widehat{\Phi}^{\mathsf{T}}\right)(t,x)\, V(x)\, \left(\partial_x \widehat{\Phi}\right)(t,x), \tag{4.8b}$$

with $V(x)$ a $2N \times 2N$ symmetric and positive definite matrix that accounts, in this bosonic representation, for the screened density-density interactions between electrons. The theory is quantized according to the equal-time commutators

$$\left[\widehat{\Phi}_i(t,x), \widehat{\Phi}_j(t,x')\right] = -\mathrm{i}\pi \left[K^{-1}_{ij}\, \mathrm{sgn}(x-x') + \Theta_{ij}\right], \tag{4.8c}$$

where K is a $2N \times 2N$ symmetric and invertible matrix with integer-valued matrix elements, and the Θ matrix accounts for Klein factors that ensure that charged excitations in the theory (vertex operators) satisfy the proper commutation relations. Fermionic or bosonic charged excitations are represented by the normal ordered vertex operators

$$\widehat{\Psi}^{\dagger}_T(t,x) := \,:e^{-\mathrm{i}\, T_i\, K_{ij}\, \widehat{\Phi}_j(t,x)}:, \tag{4.8d}$$

where the integer-valued $2N$-dimensional vector T determines the charge (and statistics) of the operator. The operator that measures the total charge density is

[1]Do the linear transformation $\hat{u}_i \equiv K_{ij}\, \widehat{\Phi}_j$ in Eq. (3.1), where we recall that the matrix K and its inverse K^{-1} are symmetric so that we may write $\Theta_{ij} \equiv K^{-1}_{ii'}\, L_{i'j'}\, K^{-1}_{j'j}$.

$$\hat{\rho}(t,x) = \frac{1}{2\pi}\, Q_i \left(\partial_x \widehat{\Phi}_i\right)(t,x), \tag{4.8e}$$

where the integer-valued $2N$-dimensional charge vector Q, together with the K-matrix, specify the universal properties of the edge theory. The charge q_T of the vertex operator in Eq. (4.8d) follows from its commutation with the charge density operator in Eq. (4.8e), yielding $q_T = T^{\mathsf{T}}\, Q$.

Tunneling of electronic charge among the different edge branches is accounted for by

$$\widehat{H}_{\mathrm{int}} := -\int_0^L \mathrm{d}x \sum_{T\in\mathbb{L}} h_T(x) : \cos\left(T^{\mathsf{T}} K\, \widehat{\Phi}(t,x) + \alpha_T(x)\right) : . \tag{4.8f}$$

The real functions $h_T(x) \geq 0$ and $0 \leq \alpha_T(x) \leq 2\pi$ encode information about the disorder along the edge when position dependent. The set

$$\mathbb{L} := \left\{ T \in \mathbb{Z}^{2N} \,\middle|\, T^{\mathsf{T}}\, Q = 0 \right\}, \tag{4.8g}$$

encodes all the possible charge neutral tunneling processes (i.e., those that just rearrange charge among the branches). This charge neutrality condition implies that the operator $\hat{\Psi}^{\dagger}_T(t,x)$ that makes up Eq. (4.8f) is bosonic, for it has even charge. Observe that set $\mathbb{L}$ forms a lattice. Consequently, if T belongs to $\mathbb{L}$ so does $-T$. In turn, relabeling T to $-T$ in $\widehat{H}_{\mathrm{int}}$ implies that $h_T(x) = +h_{-T}(x)$ whereas $\alpha_T(x) = -\alpha_{-T}(x)$.

The theory (4.8) is inherently encoding interactions. The terms $\widehat{H}_0$ and $\widehat{H}_{\mathrm{int}}$ encode single-particle *as well as* many-body interactions with matrix elements that preserve and break translation symmetry, respectively. Recovering the single-particle kinetic energy of N Kramers degenerate pairs of electrons from Eq. (4.8b) corresponds to choosing the matrix V to be proportional to the unit $2N \times 2N$ matrix with the proportionality constant fixed by the condition that the scaling dimension of each electron is $1/2$ at the bosonic free-field fixed point defined by Hamiltonian $\widehat{H}_0$. Of course, to implement the fermionic statistics for all $2N$ fermions, one must also demand that all diagonal entries of K are odd integers in some basis. [2]

4.3 Time-reversal symmetry of the edge theory

The operation of time-reversal on the $\widehat{\Phi}$ fields is defined by

$$\mathcal{T}\, \widehat{\Phi}(t,x)\, \mathcal{T}^{-1} := \Sigma_1\, \widehat{\Phi}(-t,x) + \pi K^{-1}\, \Sigma_{\downarrow}\, Q, \tag{4.9a}$$

where

$$\Sigma_1 = \begin{pmatrix} 0 & \mathbb{1} \\ \mathbb{1} & 0 \end{pmatrix} \qquad \Sigma_{\downarrow} = \begin{pmatrix} 0 & 0 \\ 0 & \mathbb{1} \end{pmatrix}. \tag{4.9b}$$

This definition ensures that the fermionic and bosonic vertex operators defined in Eq. (4.8d) are properly transformed under reversal of time. More precisely, one can then construct a pair of fermionic operators $\hat{\Psi}^{\dagger}_1$ and $\hat{\Psi}^{\dagger}_2$ of the form (4.8d) by suitably choosing a pair of vectors T_1 and T_2, respectively, in such a way that the operation of time-reversal maps $\hat{\Psi}^{\dagger}_1$ into $+\hat{\Psi}^{\dagger}_2$ whereas it maps $\hat{\Psi}^{\dagger}_2$ into $-\hat{\Psi}^{\dagger}_1$. Thus, it is meaningful to interpret the block structure displayed in Eq. (4.9b) as arising from the upper or lower projection along some spin-1/2 quantization axis.

Time-reversal symmetry on the chiral edge theory (4.8) demands that

$$V = +\Sigma_1 \, V \, \Sigma_1, \tag{4.10a}$$

$$K = -\Sigma_1 \, K \, \Sigma_1, \tag{4.10b}$$

$$Q = \Sigma_1 \, Q, \tag{4.10c}$$

$$h_T(x) = h_{\Sigma_1 T}(x), \tag{4.10d}$$

$$\alpha_T(x) = \left(-\alpha_{\Sigma_1 \, T}(x) + \pi T^{\mathsf{T}} \, \Sigma_{\downarrow} \, Q\right) \mod 2\pi. \tag{4.10e}$$

Proof The first two conditions, Eqs. (4.10a) and (4.10b), follow from the requirement that $\widehat{H}_0$ be time-reversal invariant. In particular, the decomposition

$$K = \begin{pmatrix} \kappa & \Delta \\ \Delta^{\mathsf{T}} & -\kappa \end{pmatrix} \qquad \kappa^{\mathsf{T}} = \kappa, \quad \Delta^{\mathsf{T}} = -\Delta, \tag{4.11}$$

where κ and Δ are $N \times N$ matrices, follows from Eq. (4.10b) and $K = K^{\mathsf{T}}$.

The third condition, Eq. (4.10c), states that the charge density is invariant under time reversal. In particular, the decomposition

$$Q = \begin{pmatrix} \varrho \\ \varrho \end{pmatrix} \tag{4.12}$$

follows.

Finally, $\mathcal{T} \widehat{H}_{\mathrm{int}} \mathcal{T}^{-1} = \widehat{H}_{\mathrm{int}}$ requires that

$$\begin{aligned}
&\sum_{T \in \mathbb{L}} h_T(x) \, \cos\left(T^{\mathsf{T}} \, K \, \widehat{\Phi}(t,x) + \alpha_T(x)\right) = \\
&\sum_{T \in \mathbb{L}} \mathcal{T} \, \left[h_T(x) \, \cos\left(T^{\mathsf{T}} \, K \, \widehat{\Phi}(t,x) + \alpha_T(x)\right)\right] \mathcal{T}^{-1} = \\
&\sum_{T \in \mathbb{L}} h_T(x) \, \cos\left(-\left(\Sigma_1 \, T\right)^{\mathsf{T}} K \, \widehat{\Phi}(-t,x) + \alpha_T(x) - \pi T^{\mathsf{T}} \, \Sigma_{\downarrow} \, Q\right) = \\
&\sum_{T \in \mathbb{L}} h_{\Sigma_1 \, T}(x) \, \cos\left(-T^{\mathsf{T}} K \, \widehat{\Phi}(-t,x) + \alpha_{\Sigma_1 \, T}(x) - \pi (\Sigma_1 \, T)^{\mathsf{T}} \, \Sigma_{\downarrow} \, Q\right) = \\
&\sum_{T \in \mathbb{L}} h_{\Sigma_1 T}(x) \, \cos\left(T^{\mathsf{T}} K \, \widehat{\Phi}(-t,x) - \alpha_{\Sigma_1 \, T}(x) + \pi (\Sigma_1 T)^{\mathsf{T}} \, \Sigma_{\downarrow} \, Q\right),
\end{aligned} \tag{4.13}$$

as the conditions needed to match the two trigonometric expansions. This leads to the last two relations, Eqs. (4.10d) and (4.10e). **qed**

Disorder parametrized by $h_T(x) = +h_{-T}(x)$ and $\alpha_T(x) = -\alpha_{-T}(x)$ and for which the matrix T obeys

$$\Sigma_1\, T = -T, \tag{4.14a}$$

and

$$T^{\mathsf{T}}\, \Sigma_{\downarrow}\, Q \text{ is an odd integer,} \tag{4.14b}$$

cannot satisfy the condition (4.10e) for time-reversal symmetry. Such disorder is thus prohibited to enter $\widehat{H}_{\mathrm{int}}$ in Eq. (4.8f), for it would break explicitly time-reversal symmetry otherwise. Moreover, we also prohibit any ground state that provides $\exp\left(\mathrm{i}T^{\mathsf{T}}\, K\, \widehat{\Phi}(t,x)\right)$ with an expectation value when T satisfies Eq. (4.14), for it would break spontaneously time-reversal symmetry otherwise.

4.4 Pinning the edge fields with disorder potentials: the Haldane criterion

Solving the interacting theory (4.8) is beyond the scope of this lecture. What can be done, however, is to identify those fixed points of the interacting theory (4.8) that are pertinent to the question of whether or not some edge modes remain extended along the edge in the limit of strong disorder $h_T(x) \to \infty$ for all tunneling matrices $T \in \mathbb{L}$ entering the interaction (4.8f).

This question is related to the one posed and answered by Haldane in Ref. [46] for Abelian FQH states and which, in the context of this lecture, would be as follows. Given an interaction potential caused by *weak* disorder on the edges as defined by Hamiltonian (4.8f), what are the tunneling vectors $T \in \mathbb{L}$ that can, in principle, describe relevant perturbations that will cause the system to flow to a strong coupling fixed point characterized by $h_T \to \infty$ away from the fixed point $\widehat{H}_0$? (See Ref. [131] for an answer to this weak-coupling question in the context of the IQSHE and $\mathbb{Z}_2$ topological band insulators.) By focusing on the strong coupling limit from the outset, we avoid the issue of following the renormalization group flow from weak to strong coupling. Evidently, this point of view presumes that the strong coupling fixed point is stable and that no intermediary fixed point prevents it from being reached.

To identify the fixed points of the interacting theory (4.8) in the strong coupling limit (strong disorder limit) $h_T \to \infty$, we ignore the contribution $\widehat{H}_0$ and restrict the sum over the tunneling matrices in $\widehat{H}_{\mathrm{int}}$ to a subset $\mathbb{H}$ of $\mathbb{L}$ ($\mathbb{H} \subset \mathbb{L}$) with a precise definition of $\mathbb{H}$ that will follow in Eq. (4.21). For any choice of $\mathbb{H}$, there follows the strong-coupling fixed point Hamiltonian

$$\widehat{H}_{\mathbb{H}} := -\int_0^L \mathrm{d}x \sum_{T\in\mathbb{H}} h_T(x) : \cos\left(T^{\mathsf{T}} K\, \widehat{\Phi}(x) + \alpha_T(x)\right) : . \tag{4.15}$$

Assume that a fixed point Hamiltonian (4.15) is stable if and only if the set $\mathbb{H}$ is "maximal". The study of the renormalization group flows relating the weak, moderate (if any), and the strong fixed points in the infinite-dimensional parameter space spanned by the non-universal data V, $h_T(x)$, and $\alpha_T(x)$ is again beyond the scope of this lecture.

One might wonder why we cannot simply choose $\mathbb{H} = \mathbb{L}$. This is a consequence of the chiral equal-time commutation relations (4.8c), as emphasized by Haldane in Ref. [46], that prevent the simultaneous locking of the phases of all the cosines through the condition

$$\partial_x \left(T^{\mathsf{T}}\, K\, \widehat{\Phi}(t,x) + \alpha_T(x)\right) = C_T(x) \tag{4.16}$$

for some time-independent and real-valued function $C_T(x)$ on the canonical momentum

$$(4\pi)^{-1}\, K\, (\partial_x \widehat{\Phi})(t,x) \tag{4.17}$$

that is conjugate to $\widehat{\Phi}(t,x)$, when applied to the ground state. The locking condition (4.16) removes a pair of chiral bosonic modes with opposite chiralities from the gapless degrees of freedom of the theory. However, even in the strong-coupling limit, there are quantum fluctuations as a consequence of the chiral equal-time commutation relations (4.8c) that prevent minimizing the interaction $\widehat{H}_{\mathrm{int}}$ by minimizing separately each contribution to the trigonometric expansion (4.8f). Finding the ground state in the strong coupling limit is a strongly frustrated problem of optimization.

To construct a maximal set $\mathbb{H}$, demand that any $T \in \mathbb{H}$ must satisfy the locking condition (4.16). Furthermore, require that the phases of the cosines entering the fixed point Hamiltonian (4.15) be constants of motion

$$\left[\partial_x \left(T^{\mathsf{T}}\, K\, \widehat{\Phi}(t,x)\right), \widehat{H}_{\mathbb{H}}\right] = 0\ . \tag{4.18}$$

To find the tunneling vectors $T \in \mathbb{H}$, one thus needs to consider the following commutator

$$\begin{aligned} \int\limits_0^L \mathrm{d}x' \, \Big[\partial_x \left(T^{\mathsf{T}}\, K\, \widehat{\Phi}(t,x)\right),\ h_{T'}(x')\, \cos\left(T'^{\,\mathsf{T}}\, K\, \widehat{\Phi}(t,x') + \alpha_{T'}(x')\right)\Big] = \\ -\,\mathrm{i}\, 2\pi\, T^{\mathsf{T}}\, K\, T'\ \ h_{T'}(x)\ \sin\left(T'^{\,\mathsf{T}}\, K\, \widehat{\Phi}(t,x) + \alpha_{T'}(x)\right), \end{aligned} \tag{4.19}$$

and demand that it vanishes. This is achieved if $T^{\mathsf{T}}\, K\, T' = 0$. Equation (4.19) implies that any set $\mathbb{H}$ is composed of the charge neutral vectors satisfying

$$T^{\mathsf{T}}\, K\, T' = 0. \tag{4.20}$$

It is by choosing a set $\mathbb{H}$ to be "maximal" that we shall obtain the desired Haldane criterion for stability.

4.5 Stability criterion for edge modes

Section 4.1 presented and briefly discussed the criteria for at least one branch of edge excitations to remain delocalized even in the presence of strong disorder. Here these criteria are proved.

The idea is to count the maximum possible number of edge modes that can be pinned (localized) along the edge by tunneling processes. The set of pinning processes must satisfy

$$T^{\mathsf{T}}\, Q = 0 \qquad T^{\mathsf{T}}\, K\, T' = 0, \tag{4.21}$$

which defines a set $\mathbb{H}$ introduced in Sec. 4.4. (Note, however, that $\mathbb{H}$ is not uniquely determined from this condition.) Define the real extension $\mathbb{V}$ of a set $\mathbb{H}$, by allowing the tunneling vectors

T that satisfy Eq. (4.21) to take real values instead of integer values. Notice that $\mathbb{V}$ is a vector space over the real numbers. Demand that $\mathbb{H}$ forms a lattice that is as dense as the lattice $\mathbb{L}$ by imposing

$$\mathbb{V} \cap \mathbb{L} = \mathbb{H}. \tag{4.22}$$

For any vector $T \in \mathbb{V}$, consider the vector $K\,T$. It follows from Eq. (4.21) that $K\,T \perp T', \forall T' \in \mathbb{V}$. So K maps the space $\mathbb{V}$ into an orthogonal space $\mathbb{V}^{\perp}$. Since K is invertible, we have $\mathbb{V}^{\perp} = K\,\mathbb{V}$ as well as $\mathbb{V} = K^{-1}\,\mathbb{V}^{\perp}$, and thus $\dim\,\mathbb{V} = \dim\,\mathbb{V}^{\perp}$. Since $\dim \mathbb{V} + \dim \mathbb{V}^{\perp} \leq 2N$, it follows that $\dim \mathbb{V} \leq N$. Therefore (as could be anticipated physically) the maximum number of Kramers pairs of edge modes that can be pinned is N. If that happens, the edge has no gapless delocalized mode.

Next, we look at the conditions for which the maximum dimension N is achieved in order to establish a contradiction.

Assume that $\dim \mathbb{V} = \dim \mathbb{V}^{\perp} = N$. It follows that $\mathbb{V} \oplus \mathbb{V}^{\perp} = \mathbb{R}^{2N}$, exhausting the space of available vectors. In this case the charge vector $Q \in \mathbb{V}^{\perp}$ because of Eq. (4.21). Consequently, $K^{-1}\,Q \in \mathbb{V}$. We can then construct an integer vector $\bar{T} \parallel K^{-1}\,Q$ by scaling $K^{-1}\,Q$ with the minimum integer r that accomplishes this. (This is always possible because K^{-1} is a matrix with rational entries and Q is a vector of integers.) Because the inverse of K is not known, it seems hopeless to write $K^{-1}\,Q$ in closed form. However, K^{-1} must anticommutes with Σ_1 given that K anticommutes with Σ_1, while Σ_1 squares to the unit matrix. Hence, $K^{-1}\,Q$ is an eigenstate of Σ_1 with eigenvalue -1. Now,

$$\bar{T} \coloneqq r \begin{pmatrix} +(\kappa-\Delta)^{-1}\,\varrho \\ -(\kappa-\Delta)^{-1}\,\varrho \end{pmatrix} \tag{4.23}$$

is also an eigenstate of Σ_1 with eigenvalue -1. This suggests that we may use $\bar{T}$ instead of $K^{-1}\,Q$. Indeed, the existence of $(\kappa-\Delta)^{-1}$ follows from $\det K \neq 0$ and

$$\det K = (-1)^{N}\left[\det(\kappa-\Delta)\right]^{2}. \tag{4.24}$$

Moreover, one verifies that $\bar{T}$ is orthogonal to the charge vector Q and that $K\,\bar{T}$ is orthogonal to $\bar{T}$.

Equipped with $\bar{T}$, we construct the integer

$$R \coloneqq -\bar{T}^{\mathsf{T}}\,\Sigma_{\downarrow}\,Q. \tag{4.25}$$

It is the parity of this integer number that will allow us to establish a contradiction, i.e., it is the parity of R that determines if it is possible or not to localize all the modes with the N tunneling operators. To establish the contradiction, we employ Eq. (4.10e) together with the fact that $\Sigma_1\,\bar{T} = -\bar{T}$. In other words,

$$\begin{aligned} \pi R &= -\,\pi \bar{T}^{\mathsf{T}}\,\Sigma_{\downarrow}\,Q \\ &= \Big(-\,\alpha_{\bar{T}}(x) - \alpha_{\Sigma_1\,\bar{T}}(x)\Big) \mod 2\pi \\ &= \Big(-\,\alpha_{\bar{T}}(x) - \alpha_{-\bar{T}}(x)\Big) \mod 2\pi \\ &= 0 \mod 2\pi, \end{aligned} \tag{4.26}$$

where in the last line $\alpha_{T}(x) = -\alpha_{-T}(x)$ for all $T \in \mathbb{L}$ was used. If $\bar{T}$ satisfies Eq. (4.26), then R must be an even integer. If Eq. (4.26) is violated (i.e., R is an odd integer) then $\bar{T}$ is not allowed to enter $\widehat{H}_{\rm int}$ for it would otherwise break time-reversal symmetry [thus $h_{\bar{T}}(x) = 0$ must always hold in this case to prevent $\bar{T}$ from entering $\widehat{H}_{\rm int}$]. One therefore arrives at the condition that

- If the maximum number of edge modes are localized or gaped, then R must be even.

A corollary is that

- If R is odd, at least one edge branch is gapless and delocalized.

It remains to prove that if R is even, then one can indeed reach the maximum dimension N for the space of pinning vectors. This is done by construction. Take all eigenvectors of Σ_1 with $+1$ eigenvalue. Choose $(N-1)$ of such vectors, all those orthogonal to Q. For the last one, choose $\bar{T}$. One can check that these N vectors satisfy Eq. (4.21) with the help of $\Sigma_1\, K\, \Sigma_1 = -K$ [listed in Eq. (4.10b)] and of $\bar{T} \parallel K^{-1}Q$. Now, the $(N-1)$ vectors $\Sigma_1 T = +T$ are of the form $T^{\mathsf{T}} = (t^{\mathsf{T}}, t^{\mathsf{T}})$, where we need to satisfy $T^{\mathsf{T}} Q = 2t^{\mathsf{T}} \varrho = 0$. This leads to $T^{\mathsf{T}}\, \Sigma_{\downarrow}\, Q$ even, and then Eq. (4.10e) brings no further conditions whatsoever. So we can take all these $(N-1)$ tunneling vectors. Finally, we take $\bar{T}$ as constructed above, which is a legitimate choice since R is assumed even and thus consistent with Eq. (4.26). Hence, we have constructed the N tunneling vectors that gap or localize all edge modes, and can state that

- If R is even, then the maximum number of edge modes are localized or gaped.

As a by-product, we see that it is always possible to localize along the boundary at least all but one Kramers degenerate pair of edge states via the $(N-1)$ tunneling vectors that satisfy $\Sigma_1 T = +T$. Thus, either one or no Kramers degenerate pair of edge state remains delocalized along the boundary when translation invariance is strongly broken along the boundary.

4.6 The stability criterion for edge modes in the FQSHE

What is the fate of the stability criterion when we impose the residual spin-$1/2$ $U(1)$ symmetry in the model so as to describe an underlying microscopic model that supports the FQSHE? The residual spin-$1/2$ $U(1)$ symmetry is imposed on the interacting theory (4.8) by positing the existence of a spin vector $S = -\Sigma_1\, S \in \mathbb{Z}^{2N}$ associated to a conserved $U(1)$ spin current. This spin vector is the counterpart to the charge vector $Q = +\Sigma_1\, Q \in \mathbb{Z}^{2N}$. The condition

$$S = -\Sigma_1\, S \tag{4.27a}$$

is required for compatibility with time-reversal symmetry and is the counterpart to Eq. (4.10c). Compatibility with time-reversal symmetry of Q and S thus imply that they are orthogonal, $Q^{\mathsf{T}}\, S = 0$. If we restrict the interaction (4.8f) by demanding that the tunneling matrices obey

$$T^{\mathsf{T}}\, S = 0, \tag{4.27b}$$

we probe the stability of the FQSHE described by $\hat{H}_0$ when perturbed by $\hat{H}_{\rm int}$.[2]

[2] It is important to observe that the quadratic Hamiltonian (4.8b) has a much larger symmetry group than the interacting Hamiltonian (4.8f). For example, $\widehat{H}_0$ commutes with the transformation

To answer this question we supplement the condition $T^{\mathsf{T}}Q = 0$ on tunneling vectors that belong to $\mathbb{L}$ and $\mathbb{H}$, by $T^{\mathsf{T}}S = 0$. By construction, S is orthogonal to Q. Hence, it remains true that $\mathbb{H}$ is made of at most N linearly independent tunneling vectors.

The strategy for establishing the condition for the strong coupling limit of $\hat{H}_{\mathrm{int}}$ to open a mobility gap for all the extended modes of $\hat{H}_0$ thus remains to construct the largest set $\mathbb{H}$ out of as few tunneling vectors with $T = -\Sigma_1\, T$ as possible, since these tunneling vectors might spontaneously break time-reversal symmetry.

As before, there are $(N-1)$ linearly independent tunneling vectors with $T = +\Sigma_1\, T$, while the tunneling matrix $\bar{T}$ from Eq. (4.23) must belong to any $\mathbb{H}$ with N linearly independent tunneling vectors.

At this stage, we need to distinguish the case

$$\bar{T}^{\mathsf{T}}\, S = 0 \tag{4.28a}$$

from the case

$$\bar{T}^{\mathsf{T}}\, S \neq 0. \tag{4.28b}$$

In the former case, the spin neutrality condition (4.27b) holds for $\bar{T}$ and thus the stability criterion is unchanged for the FQSHE. In the latter case, the spin neutrality condition (4.27b) is violated so that $\hat{H}_{\mathrm{int}}$ is independent of any tunneling matrix proportional to $\bar{T}$. Thus, when Eq. (4.28b) holds, as could be the case when $\kappa \propto \mathbb{1}_N$ and $\Delta = 0$ say, the FQSHE carried by at least one Kramers pair of edge states of $\hat{H}_0$ is robust to the strong coupling limit of the time-reversal symmetric and residual spin-$1/2$ U(1) symmetric perturbation $\hat{H}_{\mathrm{int}}$.

$$\widehat{\Phi}(t,x) \longrightarrow \widehat{\Phi}(t,x) + \pi K^{-1}\,\Sigma_{\downarrow}\, S.$$

One verifies that the transformation law of a Kramers doublet of fermions under this transformation is the one expected from a rotation about the quantization axis of the residual spin-1/2 U(1) symmetry provided the parities of the components of S are the same as those of Q. Hence, $\widehat{H}_0$ has, by construction, the residual spin-1/2 U(1) symmetry even though a generic microscopic model with time-reversal symmetry does not. This residual spin-1/2 U(1) symmetry of $\widehat{H}_0$ is broken by $\widehat{H}_{\mathrm{int}}$, unless one imposes the additional constraint (4.27b) on the tunneling matrices $T \in \mathbb{L}$ allowed to enter the interacting theory defined in Eq. (4.8).

5

Construction of two-dimensional topological phases from coupled wires

5.1 Introduction

One accomplishment in the study of topological phases of matter has been the theoretical prediction and experimental discovery of two-dimensional topological insulators. [54, 55, 11, 10, 64] The integer quantum Hall effect (IQHE) is an early example of how states can be classified into distinct topological classes using an integer, the Chern number, to express the quantized Hall conductivity. [63, 67, 117] In the IQHE, the number of delocalized edge channels is proportional to the quantized Hall conductivity through the Chern number. More recently, it has been found that the symmetry under reversal of time protects the parity in the number of edge modes in (bulk) insulators with strong spin-orbit interactions in two and three dimensions. [54, 35] Correspondingly, these systems are characterized by a $\mathbb{Z}_2$ topological invariant.

The discovery of $\mathbb{Z}_2$ topological insulators initiated a search for a classification of phases of fermionic matter that are distinct by some topological attribute. For non-interacting electrons, a complete classification, the tenfold way, has been accomplished in arbitrary dimensions. [106, 107, 103, 58] In this scheme, three discrete symmetries that act locally in position space – time-reversal symmetry (TRS), particle-hole symmetry (PHS), and chiral or sublattice symmetry (SLS) – play a central role when defining the quantum numbers that identify the topological insulating fermionic phases of matter within one of the ten symmetry classes (see columns 1-3 from Table 5.1).

The tenfold way is believed to be robust to a perturbative treatment of short-ranged electron-electron interactions for the following reasons. First, the unperturbed ground state in the clean limit and in a closed geometry is non-degenerate. It is given by the filled bands of a band insulator. The band gap provides a small expansion parameter, namely the ratio of the characteristic interacting energy scale to the band gap. Second, the quantized topological invariant that characterizes the filled bands, provided its definition and topological character survives the presence of electron-electron interactions as is the case for the symmetry class A in two spatial dimensions, cannot change in a perturbative treatment of short-range electron-electron interactions. [41]

On the other hand, the fate of the tenfold way when electron-electron interactions are strong is rather subtle. [28, 41, 78, 122] For example, short-range interactions can drive the system through a topological phase transition at which the energy gap closes. [97, 16] They may also break spontaneously a defining symmetry of the topological phase. Even when short-range interactions neither spontaneously break the symmetries nor close the gap, it may be that two phases from the non-interacting tenfold way cease to be distinguishable in the presence of interactions. Indeed, it was shown for the symmetry class BDI in one dimension by Fidkowski and Kitaev that the non-interacting $\mathbb{Z}$ classification is too fine in that it must be replaced by a $\mathbb{Z}_8$ classification when generic short-range interactions are allowed. How to construct a counterpart to the tenfold way for interacting fermion (and boson) systems has thus attracted a lot of interest. [39, 95, 108, 18, 19, 29, 119, 40, 73, 17, 74]

The fractional quantum Hall effect (FQHE) is the paradigm for a situation by which interactions select topologically ordered ground states of a very different kind than the non-degenerate ground states from the tenfold way. On a closed two-dimensional manifold of genus g, interactions can stabilize incompressible many-body ground states with a g-dependent degeneracy. Excited states in the bulk must then carry fractional quantum numbers (see Ref. [128] and references therein). Such phases of matter, that follow the FQHE paradigm, appear in the literature under different names: fractional topological insulators, long-range entangled phases, topologically ordered phases, or symmetry enriched topological phases. In this section, the terminology long-range entangled (LRE) phase is used for all phases with nontrivial g-dependent ground state degeneracy. All other phases, i.e., those that follow the IQHE paradigm, are called short-range entangled (SRE) phases. (In doing so, the terminology of Ref. [73] is borrowed. It differs slightly from the one used in Ref. [18]. The latter counts all chiral phases irrespective of their ground state degeneracy as LRE.)

While there are nontrivial SRE and LRE phases in the absence of any symmetry constraint, many SRE and LRE phases are defined by some symmetry they obey. If this symmetry is broken, the topological attribute of the phase is not well defined any more. However, there is a sense in which LRE phases are more robust than SRE phases against a weak breaking of the defining symmetry. The topological attributes of LRE phases are not confined to the boundary in space between two distinct topological realizations of these phases, as they are for SRE phases. They also characterize intrinsic bulk properties such as the existence of gapped deconfined fractionalized excitations. Hence, whereas gapless edge states are gapped by any breaking of the defining symmetry, topological bulk properties are robust to a weak breaking of the defining symmetry as long as the characteristic energy scale for this symmetry breaking is small compared to the bulk gap in the LRE phase, for a small breaking of the protecting symmetry does not wipe out the gapped deconfined fractionalized bulk excitations.

The purpose of this section is to implement a classification scheme for interacting electronic systems in two spatial dimensions that treats SRE and LRE phases on equal footing. To this end, a coupled wire construction for each of the symmetry classes from the tenfold way is used. This approach has been pioneered in Refs. [132] and [69] for the IQHE and in Refs. [56] and [116] for the FQHE (see also related work in Refs. [112, 79, 61, 62, 109, 121]).

The main idea is here the following. To begin with, non-chiral Luttinger liquids are placed in a periodic array of coupled wires. In doing so, forward-scattering two-body interactions are naturally accounted for within each wire. Back-scatterings (i.e., tunneling) within a given wire or between neighboring wires are assumed to be the dominant energy scales. Imposing symmetries constrains these allowed tunnelings. Whether a given arrangement of tunnelings truly gaps out all bulk modes, except for some non-gapped edge states on the first and last wire, is verified with the help of a condition that applies to the limit of strong tunneling. This condition is nothing but the Haldane criterion of Sec. 4.4. [46] It will be shown that, for a proper choice of the tunnelings, all bulk modes are gapped. Moreover, in five out of the ten symmetry classes

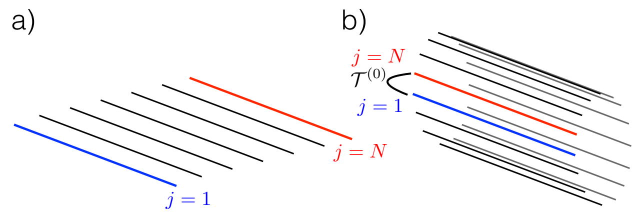

Fig. 5.1 (Taken from Ref. [86]) The boundary conditions determine whether a topological phase has protected gapless modes or not. (a) With open boundary conditions, gapless modes exist near the wires $j = 1$ and $j = N$, the scattering between them is forbidden by imposing locality in the limit $N \to \infty$. (b) Periodic boundary conditions allow the scattering vector $\mathcal{T}^{(0)}$ that gaps modes which were protected by locality before.

of the tenfold way, there remain gapless edge states in agreement with the tenfold way. It is the character of the tunnelings that determines if this wire construction selects a SRE or a LRE phase. Hence, this construction, predicated as it is on the strong tunneling limit, generalizes the tenfold way for SRE phases to LRE phases. Evidently, this edge-centered classification scheme does not distinguish between LRE phases of matter that do not carry protected gapless edge modes at their interfaces. For example, some fractional, time-reversal-symmetric, incompressible and topological phases of matter can have fractionalized excitations in the bulk, while not supporting protected gapless modes at their boundaries. [126, 104, 83]

The section is inspired from Ref. [86]. It is organized as follows. The array of Luttinger liquids is defined in Sec. 5.2. The Haldane criterion, which plays an essential role for the stability analysis of the edge theory, is reviewed in Sec. 5.3.3. All five SRE entries of Table 5.1 are derived in Sec. 5.4, while all five LRE entries of Table 5.1 are derived in Sec. 5.5.

The main result of this section is Table 5.1. For each of the symmetry classes A, AII, D, DIII, and C entering Table 5.1, the ground state supports propagating gapless edge modes localized on the first and last wire that are immune to local and symmetry-preserving perturbations. The first column labels the symmetry classes according to the Cartan classification of symmetric spaces. The second column dictates if the operations for reversal of time ($\widehat{\Theta}$ with the single-particle representation Θ), exchange of particles and holes ($\widehat{\Pi}$ with the single-particle representation Π), and reversal of chirality ($\widehat{C}$ with the single-particle representation C) are the generators of symmetries with their single-particle representations squaring to $+1$, -1, or are not present in which case the entry 0 is used. (A chiral symmetry is present if there exists a chiral operator $\widehat{C}$ that is antiunitary and commutes with the Hamiltonian. The single-particle representation C of $\widehat{C}$ is a unitary operator that anticommutes with the single-particle Hamiltonian. In a basis in which C is strictly block off diagonal, C reverses the chirality. This chirality is unrelated to the direction of propagation of left and right movers which is also called chirality in these lectures.) The third column is the set to which the topological index from the tenfold way, defined as it is in the non-interacting limit, belongs to. The fourth column is a pictorial representation of the interactions (a set of tunnelings vectors T) for the two-dimensional array of quantum wires that delivers short-range entangled (SRE) gapless edge states. A wire is represented by a colored box with the minimum number of channels compatible with the symmetry class. Each channel in a wire is either a right mover ($\otimes$) or a

Table 5.1 Realization of a two-dimensional array of quantum wires in each symmetry class of the tenfold way.

	Θ^2	Π^2	C^2		SRE topological phase	LRE topological phase
A	0	0	0	$\mathbb{Z}$	Fig. 5.2(a)	Fig. 5.2(b)
AIII	0	0	$+$		NONE	
AII	$-$	0	0	$\mathbb{Z}_2$	Fig. 5.2(c)	Fig. 5.2(d)
DIII	$-$	$+$	$-$	$\mathbb{Z}_2$	Fig. 5.2(e)	Fig. 5.2(f)
D	0	$+$	0	$\mathbb{Z}$	Fig. 5.2(g)	Fig. 5.2(h)
BDI	$+$	$+$	$+$		NONE	
AI	$+$	0	0		NONE	
CI	$+$	$-$	$-$		NONE	
C	0	$-$	0	$\mathbb{Z}$	Fig. 5.2(i)	Fig. 5.2(j)
CII	$-$	$-$	$+$		NONE	

left mover ($\odot$) that may or may not carry a spin quantum number ($\uparrow, \downarrow$) or a particle (yellow color) or hole (black color) attribute. The lines describe tunneling processes within a wire or between consecutive wires in the array that are of one-body type when they do not carry an arrow or of strictly many-body type when they carry an arrow. Arrows point toward the sites on which creation operators act and away from the sites on which annihilation operators act. For example in the symmetry class A, the single line connecting two consecutive wires in the SRE column represents a one-body backward scattering by which left and right movers belonging to consecutive wires are coupled. The lines have been omitted for the fifth (LRE) column, only the tunneling vectors are specified.

5.2 Definitions

Consider an array of N parallel wires that stretch along the x direction of the two-dimensional embedding Euclidean space (see Fig. 5.1). Label a wire by the Latin letter $i = 1, \cdots, N$. Each wire supports fermions that carry an even integer number M of internal degrees of freedom

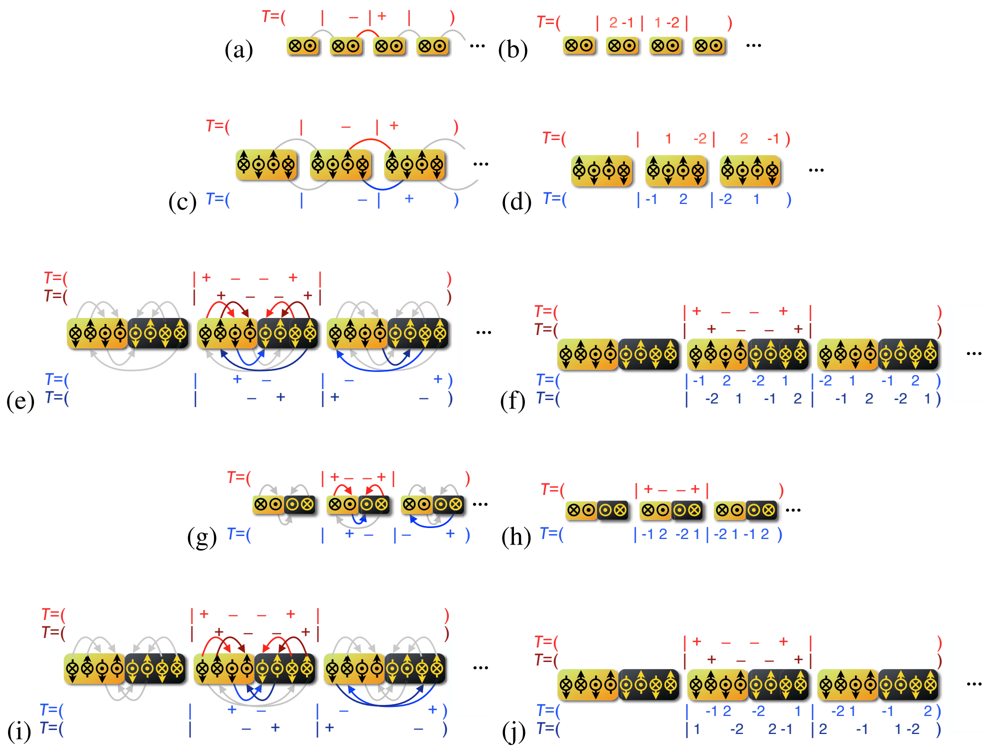

Fig. 5.2 Figures entering Table 5.1.

that discriminate between left- and right-movers, the projection along the spin-$1/2$ quantization axis, and particle-hole quantum numbers, among others (e.g., flavors). Label these internal degrees of freedom by the Greek letter $\gamma = 1, \cdots, M$. Combine those two indices in a collective index $\mathsf{a} \equiv (i, \gamma)$. Correspondingly, introduce the $M \times N$ pairs of creation $\hat{\psi}^{\dagger}_{\mathsf{a}}(x)$ and annihilation $\hat{\psi}_{\mathsf{a}}(x)$ field operators obeying the fermionic equal-time algebra

$$\left\{\hat{\psi}_{\mathsf{a}}(x), \hat{\psi}^{\dagger}_{\mathsf{a}'}(x')\right\} = \delta_{\mathsf{a},\mathsf{a}'}\,\delta(x - x') \tag{5.1a}$$

with all other anticommutators vanishing and the collective labels $\mathsf{a}, \mathsf{a}' = 1, \cdots, M \times N$. The notation

$$\widehat{\Psi}^{\dagger}(x) \equiv \left(\hat{\psi}^{\dagger}_{1}(x) \cdots \hat{\psi}^{\dagger}_{MN}(x)\right), \quad \widehat{\Psi}(x) \equiv \begin{pmatrix} \hat{\psi}_{1}(x) \\ \vdots \\ \hat{\psi}_{MN}(x) \end{pmatrix}, \tag{5.1b}$$

is used for the operator-valued row ($\widehat{\Psi}^{\dagger}$) and column ($\widehat{\Psi}$) vector fields. Assume that the many-body quantum dynamics of the fermions supported by this array of wires is governed by the Hamiltonian $\hat{H}$, whereby interactions within each wire are dominant over interactions between wires so that $\hat{H}$ may be represented as N coupled Luttinger liquids, each one of which is composed of M interacting fermionic channels.

By assumption, the $M \times N$ fermionic channels making up the array may thus be bosonized as was explained in chapters 3 and 4. Within Abelian bosonization, [87] this is done by postulating first the $MN \times MN$ matrix

$$\mathcal{K} \equiv (\mathcal{K}_{\mathsf{aa}'}) \tag{5.2a}$$

to be symmetric with integer-valued entries. Because an array of identical wires – each of which having its quantum dynamics governed by that of a Luttinger liquid – is assumed, it is natural to choose $\mathcal{K}$ to be reducible,

$$\mathcal{K}_{\mathsf{aa}'} = \delta_{ii'}\, K_{\gamma\gamma'}, \quad \gamma, \gamma' = 1, \cdots, M, \quad i, i' = 1, \cdots, N. \tag{5.2b}$$

A second $MN \times MN$ matrix is then defined by

$$\mathcal{L} \equiv (\mathcal{L}_{\mathsf{aa}'}) \tag{5.3a}$$

where

$$\mathcal{L}_{\mathsf{aa}'} \coloneqq \operatorname{sgn}(\mathsf{a} - \mathsf{a}')\, (\mathcal{K}_{\mathsf{aa}'} + \mathcal{Q}_{\mathsf{a}}\, \mathcal{Q}_{\mathsf{a}'})\,, \qquad \mathsf{a}, \mathsf{a}' = 1, \cdots, MN, \tag{5.3b}$$

depends on the integer-valued charge vector $\mathcal{Q} \equiv (\mathcal{Q}_{\mathsf{a}})$ in addition to the matrix $\mathcal{K} \equiv (\mathcal{L}_{\mathsf{aa}'})$. The MN compatibility conditions

$$(-1)^{\mathcal{K}_{\mathsf{aa}}} = (-1)^{\mathcal{Q}_{\mathsf{a}}}, \qquad \mathsf{a} = 1, \cdots, MN, \tag{5.3c}$$

must hold. As we are after the effects of interactions between electrons, we choose $\mathcal{Q}_{\mathsf{a}} = 1$ so that

$$\mathcal{L}_{\mathsf{aa}'} \coloneqq \operatorname{sgn}(\mathsf{a} - \mathsf{a}')\, (\mathcal{K}_{\mathsf{aa}'} + 1)\,, \qquad \mathsf{a}, \mathsf{a}' = 1, \cdots, MN. \tag{5.3d}$$

Third, one verifies that, for any pair $\mathsf{a}, \mathsf{a}' = 1, \cdots, MN$, the Hermitean fields $\hat{\phi}_{\mathsf{a}}$ and $\hat{\phi}_{\mathsf{a}'}$, defined by the Mandelstam formula

$$\hat{\psi}_{\mathsf{a}}(x) \equiv\ :\exp\left(+\mathrm{i}\mathcal{K}_{\mathsf{aa}'}\, \hat{\phi}_{\mathsf{a}'}(x)\right): \tag{5.4a}$$

as they are, obey the bosonic equal-time algebra

$$\left[\hat{\phi}_{\mathsf{a}}(x), \hat{\phi}_{\mathsf{a}'}(x')\right] = -\mathrm{i}\pi \left[\mathcal{K}^{-1}_{\mathsf{aa}'} \operatorname{sgn}(x - x') + \mathcal{K}^{-1}_{\mathsf{ab}}\, \mathcal{L}_{\mathsf{bc}}\, \mathcal{K}^{-1}_{\mathsf{ca}'}\right]. \tag{5.4b}$$

Here, the notation $:(\cdots):$ stands for normal ordering of the argument $(\cdots)$ and the summation convention over repeated indices is implied. In line with Eq. (5.1b), the notation

$$\widehat{\Phi}^{\mathsf{T}}(x) \equiv \left(\hat{\phi}_1(x) \cdots \hat{\phi}_{MN}(x)\right), \quad \widehat{\Phi}(x) \equiv \begin{pmatrix} \hat{\phi}_1(x) \\ \vdots \\ \hat{\phi}_{MN}(x) \end{pmatrix}, \tag{5.4c}$$

for the operator-valued row (i.e., $\widehat{\Phi}^{\mathsf{T}}$) and column (i.e., $\widehat{\Phi}$) vector fields is used. Periodic boundary conditions along the x direction parallel to the wires are imposed by demanding that

$$\mathcal{K}\, \widehat{\Phi}(x + L) = \mathcal{K}\, \widehat{\Phi}(x) + 2\pi\, \mathcal{N}, \qquad \mathcal{N} \in \mathbb{Z}^{MN}. \tag{5.4d}$$

Equipped with Eqs. (5.2)–(5.4), the many-body Hamiltonian $\widehat{H}$ for the MN interacting fermions all carrying the same electric charge e and propagating on the array of wires is decomposed additively into

$$\widehat{H} = \widehat{H}_{\mathcal{V}} + \widehat{H}_{\{\mathcal{T}\}} + \widehat{H}_{\{\mathcal{Q}\}}. \tag{5.5a}$$

Hamiltonian

$$\widehat{H}_{\mathcal{V}} \coloneqq \int \mathrm{d}x \, \left(\partial_x \widehat{\Phi}^{\mathsf{T}}\right)(t,x) \, \mathcal{V}(x) \, \left(\partial_x \widehat{\Phi}\right)(t,x), \tag{5.5b}$$

even though quadratic in the bosonic field, encodes both local one-body terms as well as contact many-body interactions between the M fermionic channels in any given wire from the array through the block-diagonal, real-valued, and symmetric $MN \times MN$ matrix

$$\mathcal{V}(x) \coloneqq \left(\mathcal{V}_{\mathsf{a}\mathsf{a}'}(x)\right) \equiv \left(\mathcal{V}_{(i,\gamma)(i',\gamma')}(x)\right) = \mathbb{1}_N \otimes \left(V_{\gamma\gamma'}(x)\right). \tag{5.5c}$$

Hamiltonian

$$\begin{aligned} \widehat{H}_{\{\mathcal{T}\}} \coloneqq& \int \mathrm{d}x \sum_{\mathcal{T}} \frac{h_{\mathcal{T}}(x)}{2} \left(e^{+\mathrm{i}\alpha_{\mathcal{T}}(x)} \prod_{\mathsf{a}=1}^{MN} \hat{\psi}_{\mathsf{a}}^{\mathcal{T}_{\mathsf{a}}}(t,x) + \mathrm{H.c.} \right) \\ =& \int \mathrm{d}x \sum_{\mathcal{T}} h_{\mathcal{T}}(x) \; :\cos\left(\mathcal{T}^{\mathsf{T}} \, \mathcal{K} \, \widehat{\Phi}(t,x) + \alpha_{\mathcal{T}}(x)\right): \end{aligned} \tag{5.5d}$$

is not quadratic in the bosonic fields. With the understanding that the operator-multiplication of identical fermion fields at the same point x along the wire requires point splitting, and with the short-hand notation $\hat{\psi}_{\mathsf{a}}^{-1}(x) \equiv \hat{\psi}_{\mathsf{a}}^{\dagger}(x)$, $\widehat{H}_{\{\mathcal{T}\}}$ is interpreted as a sum of all (possibly many-body) tunnelings between the fermionic channels. The set $\{\mathcal{T}\}$ comprises here of *all* integer-valued tunneling vectors

$$\mathcal{T} \equiv (\mathcal{T}_{\mathsf{a}}) \tag{5.5e}$$

obeying the condition

$$\sum_{\mathsf{a}=1}^{MN} \mathcal{T}_{\mathsf{a}} = \begin{cases} 0 \bmod 2, & \text{for D, DIII, C, and CI,} \\ \\ 0, & \text{otherwise.} \end{cases} \tag{5.5f}$$

Moreover, each $\mathcal{T}$ from the set $\{\mathcal{T}\}$ is assigned the real-valued functions

$$h_{\mathcal{T}}(x) = h_{\mathcal{T}}^{*}(x) \geq 0 \tag{5.5g}$$

and

$$\alpha_{\mathcal{T}}(x) = \alpha_{\mathcal{T}}^{*}(x). \tag{5.5h}$$

The condition (5.5f) ensures that these tunneling events preserve the parity of the total fermion number for the superconducting symmetry classes (symmetry classes D, DIII, C, and CI in Table 5.1), while they preserve the total fermion number for the non-superconducting symmetry classes (symmetry classes A, AIII, AI, AII, BDI, and CII in Table 5.1). The integer

$$q := \sum_{\mathsf{a}=1}^{MN} \frac{|\mathcal{T}_{\mathsf{a}}|}{2} \tag{5.5i}$$

dictates that $\mathcal{T}$ encodes a q-body interaction in the fermion representation. Hamiltonian

$$\widehat{H}_{\{\mathcal{Q}\}} := \int \mathrm{d}x \, \frac{1}{2\pi} \, A_0(x) \, \mathcal{Q}^{\mathsf{T}} \left(\partial_x \widehat{\Phi}\right)(t,x) \tag{5.5j}$$

encodes the response to a static scalar potential A_0 through the charge vector $\mathcal{Q}$ chosen to be

$$\mathcal{Q} = \begin{pmatrix} 1 & \cdots & 1 \end{pmatrix}^{\mathsf{T}} \tag{5.5k}$$

in units of the electron charge e.

Hamiltonian (5.5) and the commutators (5.4b) are form invariant under the transformation

$$\widehat{\Phi}(t,x) =: \mathcal{W}\,\widetilde{\Phi}(t,x), \tag{5.6a}$$

$$\widetilde{\mathcal{V}}(x) := \mathcal{W}^{\mathsf{T}}\,\mathcal{V}(x)\,\mathcal{W}, \tag{5.6b}$$

$$\widetilde{\mathcal{K}} := \mathcal{W}^{\mathsf{T}}\,\mathcal{K}\,\mathcal{W}, \tag{5.6c}$$

$$\widetilde{\mathcal{T}} := \mathcal{W}^{-1}\,\mathcal{T}, \tag{5.6d}$$

$$\widetilde{\mathcal{Q}} := \mathcal{W}^{\mathsf{T}}\,\mathcal{Q}, \tag{5.6e}$$

where the $MN\times MN$ integer-valued matrix $\mathcal{W}$ is assumed to be invertible, but not necessarily orthogonal! Observe that the tunneling and charge vectors transform differently whenever $\mathcal{W}^{-1} \neq \mathcal{W}^{\mathsf{T}}$ as they enter the Hamiltonian (5.5) with and without the matrix $\mathcal{K}$, respectively. [1]

Even if the deviation of the matrix $\mathcal{W}$ from the $MN \times MN$ unit matrix is small, the relationship between the vertex operators

$$\begin{aligned} \tilde{\psi}_{\tilde{\mathsf{a}}}(t,x) \equiv &\; :\exp\left(+\mathrm{i}\left(\widetilde{\mathcal{K}}\,\widetilde{\Phi}\right)_{\tilde{\mathsf{a}}}(t,x)\right): \\ = &\; :\exp\left(+\mathrm{i}\left(\mathcal{W}^{\mathsf{T}}\,\mathcal{K}\,\widehat{\Phi}\right)_{\tilde{\mathsf{a}}}(t,x)\right):, \quad \tilde{\mathsf{a}} = 1,\cdots,MN, \end{aligned} \tag{5.7}$$

and the vertex operators (5.4a) is non-perturbative. Performing a transformation of the form (5.6) to interpret a specific choice of interactions encoded by the tunneling matrices $\{\mathcal{T}\}$ will play an essential role below.

Because of the transformation laws (5.6c) and (5.6e), the dimensionless Hall conductivity is invariant under the (not necessarily orthogonal) transformation (5.6). Indeed,

$$\sigma_{\mathrm{H}} := \frac{1}{2\pi}\left(\mathcal{Q}^{\mathsf{T}}\,\mathcal{K}^{-1}\,\mathcal{Q}\right) = \frac{1}{2\pi}\left(\widetilde{\mathcal{Q}}^{\mathsf{T}}\,\left(\mathcal{W}^{-1}\,\mathcal{W}\right)\,\widetilde{\mathcal{K}}^{-1}\,\left(\mathcal{W}^{-1}\,\mathcal{W}\right)^{\mathsf{T}}\,\widetilde{\mathcal{Q}}\right) \tag{5.8a}$$

equals

$$\widetilde{\sigma}_{\mathrm{H}} := \frac{1}{2\pi}\left(\widetilde{\mathcal{Q}}^{\mathsf{T}}\,\widetilde{\mathcal{K}}^{-1}\,\widetilde{\mathcal{Q}}\right). \tag{5.8b}$$

In the sequel, we shall choose a non-orthogonal integer-valued $\mathcal{W}$ with $|\det\mathcal{W}| = 1$ when studying SRE phases of matter outside of the tenfold way, while we shall choose a non-orthogonal integer-valued $\mathcal{W}$ with $|\det\mathcal{W}| \neq 1$ in order to construct LRE phases of matter.

[1] Alternatively, $\mathcal{K}$ and $\mathcal{Q}\,\mathcal{Q}^{\mathsf{T}}$ must transform in the same way because of the Klein factors (5.3b).

5.3 Strategy for constructing topological phases

The many-body Hamiltonian $\widehat{H}_{\mathcal{V}}+\widehat{H}_{\{\mathcal{T}\}}$ defined in Eq. (5.5) is to be chosen so that (i) it belongs to any one of the ten symmetry classes from the tenfold way (with the action of symmetries defined in Sec. 5.3.1) and (ii) all excitations in the bulk are gapped by a *specific* choice of the tunneling vectors $\{\mathcal{T}\}$ entering $\widehat{H}_{\{\mathcal{T}\}}$ (with the condition for a spectral gap given in Sec. 5.3.3). The energy scales in $\widehat{H}_{\{\mathcal{T}\}}$ are assumed sufficiently large compared to those in $\widehat{H}_{\mathcal{V}}$ so that it is $\widehat{H}_{\mathcal{V}}$ that may be thought of as a perturbation of $\widehat{H}_{\{\mathcal{T}\}}$ and not the converse.

It will be shown that, for five of the ten symmetry classes, there can be protected gapless edge states because of locality and symmetry. Step (ii) for each of the five symmetry classes supporting gapless edge states is represented pictorially as is shown in the fourth and fifth columns of Table 5.1. In each symmetry class, topologically trivial states that do not support protected gapless edge states in the tenfold classification can be constructed by gapping all states in each individual wire from the array.

5.3.1 Representation of symmetries

The classification is based on the presence or the absence of the TRS and the PHS that are represented by the antiunitary many-body operator $\widehat{\Theta}$ and the unitary many-body operator $\widehat{\Pi}$, respectively. Each of $\widehat{\Theta}$ and $\widehat{\Pi}$ can exist in two varieties such that their single-particle representations Θ and Π square to the identity operator up to the multiplicative factor ± 1,

$$\Theta^2=\pm 1, \qquad \Pi^2=\pm 1, \tag{5.9}$$

respectively. By assumption, the set of all degrees of freedom in each given wire is invariant under the actions of $\widehat{\Theta}$ and $\widehat{\Pi}$. If so, the actions of $\widehat{\Theta}$ and $\widehat{\Pi}$ on the fermionic fields can be represented in two steps. First, two $M\times M$-dimensional matrix representations P_{Θ} and P_{Π} of the permutation group of M elements, which are combined into the block-diagonal $MN\times MN$ real-valued and orthogonal matrices

$$\mathcal{P}_{\Theta}:=\mathbb{1}_N\otimes P_{\Theta}, \qquad \mathcal{P}_{\Pi}:=\mathbb{1}_N\otimes P_{\Pi}, \tag{5.10a}$$

where $\mathbb{1}_N$ is the $N\times N$ unit matrix and P_{Θ} and P_{Π} represent products of transpositions so that

$$P_{\Theta}=P_{\Theta}^{-1}=P_{\Theta}^{\mathsf{T}}, \qquad P_{\Pi}=P_{\Pi}^{-1}=P_{\Pi}^{\mathsf{T}}, \tag{5.10b}$$

are introduced. Second, two column vectors $I_{\Theta}\in\mathbb{Z}^M$ and $I_{\Pi}\in\mathbb{Z}^M$, which are combined into the two column vectors

$$\mathcal{I}_{\Theta}:=\begin{pmatrix} I_{\Theta}\\ \vdots \\ I_{\Theta}\end{pmatrix}, \qquad \mathcal{I}_{\Pi}:=\begin{pmatrix} I_{\Pi}\\ \vdots \\ I_{\Pi}\end{pmatrix}, \tag{5.10c}$$

and the $MN\times MN$ diagonal matrices

$$\mathcal{D}_{\Theta}:=\operatorname{diag}(\mathcal{I}_{\Theta}), \qquad \mathcal{D}_{\Pi}:=\operatorname{diag}(\mathcal{I}_{\Pi}), \tag{5.10d}$$

with the components of the vectors $\mathcal{I}_{\Theta}$ and $\mathcal{I}_{\Pi}$ as diagonal matrix elements, are introduced. The vectors I_{Θ} and I_{Π} are not chosen arbitrarily. Demand that the vectors $(1+\mathcal{P}_{\Theta})\,\mathcal{I}_{\Theta}$ and

$(1+\mathcal{P}_\Pi)\,\mathcal{I}_\Pi$ are made of even [for the $+1$ in Eq. (5.9)] and odd [for the -1 in Eq. (5.9)] integer entries only, while

$$e^{+\mathrm{i}\pi\,\mathcal{D}_\Theta}\,\mathcal{P}_\Theta = \pm\mathcal{P}_\Theta\,e^{+\mathrm{i}\pi\,\mathcal{D}_\Theta} \tag{5.10e}$$

and

$$e^{+\mathrm{i}\pi\,\mathcal{D}_\Pi}\,\mathcal{P}_\Pi = \pm\mathcal{P}_\Pi\,e^{+\mathrm{i}\pi\,\mathcal{D}_\Pi}, \tag{5.10f}$$

in order to meet $\Theta^2=\pm1$ and $\Pi^2=\pm1$, respectively. The operations of reversal of time and interchanges of particles and holes are then represented by

$$\widehat{\Theta}\,\widehat{\Psi}\,\widehat{\Theta}^{-1} = e^{+\mathrm{i}\,\pi\,\mathcal{D}_\Theta}\,\mathcal{P}_\Theta\,\widehat{\Psi}, \tag{5.10g}$$

$$\widehat{\Pi}\,\widehat{\Psi}\,\widehat{\Pi}^{-1} = e^{+\mathrm{i}\pi\,\mathcal{D}_\Pi}\,\mathcal{P}_\Pi\,\widehat{\Psi}, \tag{5.10h}$$

for the fermions and

$$\widehat{\Theta}\,\widehat{\Phi}\,\widehat{\Theta}^{-1} = \mathcal{P}_\Theta\,\widehat{\Phi} + \pi\,\mathcal{K}^{-1}\,\mathcal{I}_\Theta, \tag{5.10i}$$

$$\widehat{\Pi}\,\widehat{\Phi}\,\widehat{\Pi}^{-1} = \mathcal{P}_\Pi\,\widehat{\Phi} + \pi\,\mathcal{K}^{-1}\,\mathcal{I}_\Pi, \tag{5.10j}$$

for the bosons. One verifies that Eq. (5.9) is fulfilled.

Hamiltonian (5.5) is TRS if

$$\widehat{\Theta}\,\widehat{H}\,\widehat{\Theta}^{-1} = +\widehat{H}. \tag{5.11a}$$

This condition is met if

$$P_\Theta\,V\,P_\Theta^{-1} = +V, \tag{5.11b}$$

$$P_\Theta\,K\,P_\Theta^{-1} = -K, \tag{5.11c}$$

$$h_{\mathcal{T}}(x) = h_{-\mathcal{P}_\Theta\mathcal{T}}(x), \tag{5.11d}$$

$$\alpha_{\mathcal{T}}(x) = \alpha_{-\mathcal{P}_\Theta\mathcal{T}}(x) - \pi\,\mathcal{T}^{\mathsf{T}}\,\mathcal{P}_\Theta\,\mathcal{I}_\Theta. \tag{5.11e}$$

The Hamiltonian (5.5) is PHS if

$$\widehat{\Pi}\,\widehat{H}\,\widehat{\Pi}^{-1} = +\widehat{H}. \tag{5.12a}$$

This condition is met if

$$P_\Pi\,V\,P_\Pi^{-1} = +V, \tag{5.12b}$$

$$P_\Pi\,K\,P_\Pi^{-1} = +K, \tag{5.12c}$$

$$h_{\mathcal{T}}(x) = h_{+\mathcal{P}_\Pi\mathcal{T}}(x), \tag{5.12d}$$

$$\alpha_{\mathcal{T}}(x) = \alpha_{\mathcal{P}_\Pi\mathcal{T}}(x) + \pi\,\mathcal{T}^{\mathsf{T}}\,\mathcal{P}_\Pi\,\mathcal{I}_\Pi. \tag{5.12e}$$

5.3.2 Particle-hole symmetry in interacting superconductors

The total number of fermions is a good quantum number in any metallic or insulating phase of fermionic matter. This is not true anymore in the mean-field treatment of superconductivity. In a superconductor, within a mean-field approximation, charge is conserved modulo two as Cooper pairs can be created and annihilated. The existence of superconductors and the phenomenological success of the mean-field approximation suggest that the conservation of the total fermion number operator should be relaxed down to its parity in a superconducting phase of matter. If one only demands that the parity of the total fermion number is conserved, one may then decompose any fermionic creation operator in the position basis into its real and imaginary parts, thereby obtaining two Hermitean operators called Majorana operators. Any Hermitean Hamiltonian that is build out of even powers of Majorana operators necessarily preserves the parity of the total fermion number operator, but it might break the conservation of the total fermion number. By definition, any such Hamiltonian belongs to the symmetry class D.

The tool of Abelian bosonization allows to represent a fermion operator as a single exponential of a Bose field. In Abelian bosonization, a Majorana operator is the sum of two exponentials, and this fact makes it cumbersome to apply Abelian bosonization for Majorana operators. It is possible to circumvent this difficulty by representing any Hamiltonian from the symmetry class D in terms of the components of Nambu-Gorkov spinors obeying a reality condition. Indeed, one may double the dimensionality of the single-particle Hilbert space by introducing Nambu-Gorkov spinors with the understanding that (i) a reality condition on the Nambu-Gorkov spinors must hold within the physical subspace of the enlarged single-particle Hilbert space and (ii) the dynamics dictated by the many-body Hamiltonian must be compatible with this reality condition. The reality condition keeps track of the fact that there are many ways to express an even polynomial of Majorana operators in terms of the components of a Nambu-Gorkov spinor. The complication brought about by this redundancy is compensated by the fact that it is straightforward to implement Abelian bosonization in the Nambu-Gorkov representation.

To implement this particle-hole doubling, assign to every pair of fermionic operators $\hat{\psi}$ and $\hat{\psi}^{\dagger}$ (whose indices have been omitted for simplicity) related to each other by the reality condition

$$\widehat{\Pi}\,\hat{\psi}\,\widehat{\Pi}^{\dagger}=\hat{\psi}^{\dagger}, \tag{5.13a}$$

the pair of bosonic field operators $\hat{\phi}$ and $\hat{\phi}'$ related by the reality condition

$$\widehat{\Pi}\,\hat{\phi}\,\widehat{\Pi}^{\dagger}=-\hat{\phi}'. \tag{5.13b}$$

Invariance under this transformation has to be imposed on the (interacting) Hamiltonian in the doubled (Nambu-Gorkov) representation. In addition to the PHS, it is also demanded, when describing the superconducting symmetry classes, that the parity of the total fermion number is conserved. This discrete global symmetry, the symmetry of the Hamiltonian under the reversal of sign of all fermion operators, becomes a continuous $U(1)$ global symmetry that is responsible for the conservation of the electric charge in all non-superconducting symmetry classes. In this way, all nine symmetry classes from the tenfold way descend from the symmetry class D by imposing a composition of TRS, $U(1)$ charge conservation, and the chiral (sublattice) symmetry.

The combined effects of disorder and interactions in superconductors was studied in Refs [52, 30, 31, 32] starting from the Nambu-Gorkov formalism to derive a non-linear-sigma model for the Goldstone modes relevant to the interplay between the physics of Anderson localization and that of interactions. The stability of Majorana zero modes to interactions preserving the particle-hole symmetry was studied in Ref. [36].

5.3.3 Conditions for a spectral gap

Hamiltonian $\widehat{H}_{\mathcal{V}}$ in the decomposition (5.5) has MN gapless modes. However, $\widehat{H}_{\mathcal{V}}$ does not commute with $\widehat{H}_{\{\mathcal{T}\}}$ and the competition between $\widehat{H}_{\mathcal{V}}$ and $\widehat{H}_{\{\mathcal{T}\}}$ can gap some, if not all, the gapless modes of $\widehat{H}_{\mathcal{V}}$. For example, a tunneling amplitude that scatters the right mover into the left mover of each flavor in each wire will gap out the spectrum of $\widehat{H}_{\mathcal{V}}$.

A term in $\widehat{H}_{\{\mathcal{T}\}}$ has the potential to gap out a gapless mode of $\widehat{H}_{\mathcal{V}}$ if the condition (in the Heisenberg representation) [87, 45]

$$\partial_x \left[\mathcal{T}^{\mathsf{T}}\, \mathcal{K}\, \widehat{\Phi}(t,x) + \alpha_{\mathcal{T}}(x)\right] = C_{\mathcal{T}}(x) \tag{5.14}$$

holds for some time-independent real-valued functions $C_{\mathcal{T}}(x)$ on the canonical momentum

$$(4\pi)^{-1}\, \mathcal{K}\, (\partial_x \widehat{\Phi})(t,x) \tag{5.15}$$

that is conjugate to $\widehat{\Phi}(t,x)$, when applied to the ground state. The locking condition (5.14) removes a pair of chiral bosonic modes with opposite chiralities from the gapless degrees of freedom of the theory. However, not all scattering vectors $\mathcal{T}$ can simultaneously lead to such a locking due to quantum fluctuations. The set of linear combinations $\{\mathcal{T}^{\mathsf{T}}\, \mathcal{K}\, \widehat{\Phi}(t,x)\}$ that can satisfy the locking condition (5.14) simultaneously is labeled by the subset $\{\mathcal{T}\}_{\mathrm{locking}}$ of all tunneling matrices $\{\mathcal{T}\}$ defined by Eqs. (5.5e) and (5.5f) obeying the Haldane criterion (5.16) [87, 45]

$$\mathcal{T}^{\mathsf{T}}\, \mathcal{K}\, \mathcal{T} = 0 \tag{5.16a}$$

for any $\mathcal{T} \in \{\mathcal{T}\}_{\mathrm{locking}}$ and

$$\mathcal{T}^{\mathsf{T}}\, \mathcal{K}\, \mathcal{T}' = 0 \tag{5.16b}$$

pairwise for any $\mathcal{T} \neq \mathcal{T}' \in \{\mathcal{T}\}_{\mathrm{locking}}$.

5.4 Reproducing the tenfold way

The first goal is to apply the wire construction in order to reproduce the classification of non-interacting topological insulators (symmetry classes A, AIII, AI, AII, BDI, and CII in Table 5.1) and superconductors (symmetry classes D, DIII, C,and CI in Table 5.1) in $(2+1)$ dimensions (see Table 5.1). [106, 107, 103, 58] In this section, the classification scheme is carried out within the bosonized description of quantum wires. Here, the classification is restricted to one-body tunneling terms, i.e., $q = 1$ in Eq. (5.5i), for the non-superconducting symmetry classes, and to two-body tunneling terms, i.e., $q = 2$ in Eq. (5.5i), for the superconducting symmetry classes. In Sec. 5.5, this construction is generalized to the cases $q > 1$ and $q > 2$ of multi-particle tunnelings in the non-superconducting and superconducting symmetry classes, respectively. The topological stability of edge modes will be an immediate consequence of the observation that no symmetry-respecting local terms can be added to the models to be constructed below.

Within the classification of non-interacting Hamiltonians, superconductors are nothing but fermionic bilinears with a particle-hole symmetry. The physical interpretation of the degrees of freedom as Bogoliubov quasiparticles is of no consequence to the analysis. In particular, they still carry an effective conserved $U(1)$ charge in the non-interacting description.

5.4.1 Symmetry class A

SRE phases in the tenfold way

Topological insulators in symmetry class A can be realized without any symmetry aside from the $U(1)$ charge conservation. The wire construction starts from wires supporting spinless fermions, so that the minimal choice $M = 2$ only counts left- and right-moving degrees of freedom. The K-matrix reads

$$K \coloneqq \operatorname{diag}(+1, -1). \tag{5.17a}$$

The entry $+1$ of the K-matrix corresponds to a right mover. It is depicted by the symbol $\otimes$ in the first line of Table 5.1. The entry -1 of the K-matrix corresponds to a left mover. It is depicted by the symbol $\odot$ in the first line of Table 5.1. The operation for reversal of time in any one of the N wires is represented by [one verifies that Eq. (5.10e) holds]

$$P_{\Theta} \coloneqq \begin{pmatrix} 0 & 1 \\ 1 & 0 \end{pmatrix}, \qquad I_{\Theta} \coloneqq \begin{pmatrix} 0 \\ 0 \end{pmatrix}. \tag{5.17b}$$

Define $\widehat{H}_{\{\mathcal{T}\}}$ by choosing $(N-1)$ scattering vectors, whereby, for any $j = 1, \cdots, (N-1)$,

$$\mathcal{T}^{(j)}_{(i,\gamma)} \coloneqq \delta_{i,j}\,\delta_{\gamma,2} - \delta_{i-1,j}\,\delta_{\gamma,1} \tag{5.18a}$$

with $i = 1, \cdots, N$ and $\gamma = 1, 2$. In other words,

$$\mathcal{T}^{(j)} \coloneqq (0,0|\cdots|0,+1|-1,0|\cdots|0,0)^{\mathsf{T}} \tag{5.18b}$$

for $j = 1, \cdots, N-1$. Intent on helping with the interpretation of the tunneling vectors, the $|$'s in Eq. (5.18b) is used to compartmentalize the elements within a given wire. Henceforth, there are $M = 2$ vector components within each pair of $|$'s that encode the $M = 2$ degrees of freedom within a given wire. The jth scattering vector (5.18b) labels a one-body interaction in the fermion representation that fulfills Eq. (5.5f) and breaks TRS, since the scattering vector $(0,+1)^{\mathsf{T}}$ is mapped into the scattering vector $(+1,0)^{\mathsf{T}}$ by the permutation P_{Θ} that represents reversal of time in a wire by exchanging right- with left-movers. For any $j = 1, \cdots, (N-1)$, introduce the amplitude

$$h_{\mathcal{T}^{(j)}}(x) \geq 0 \tag{5.18c}$$

and the phase

$$\alpha_{\mathcal{T}^{(j)}}(x) \in \mathbb{R} \tag{5.18d}$$

according to Eqs. (5.11d) and (5.11e), respectively. The choices for the amplitude (5.18c) and the phase (5.18d) are arbitrary. In particular the amplitude (5.18c) can be chosen to be sufficiently large so that it is $\widehat{H}_{\mathcal{V}}$ that may be thought of as a perturbation of $\widehat{H}_{\{\mathcal{T}\}}$ and not the converse.

One verifies that all $(N-1)$ scattering vectors (5.18a) satisfy the Haldane criterion (5.16), i.e.,

$$\mathcal{T}^{(i)\mathsf{T}}\,\mathcal{K}\,\mathcal{T}^{(j)} = 0, \qquad i,j = 1, \cdots, N-1. \tag{5.19}$$

Correspondingly, the term $\widehat{H}_{\{\mathcal{T}\}}$ gaps out $2(N-1)$ of the $2N$ gapless modes of $\widehat{H}_{\mathcal{V}}$. Two modes of opposite chirality that propagate along the first and last wire, respectively, remain in the low energy sector of the theory. These edge states are localized on wire $i = 1$ and $i = N$, respectively, for their overlaps with the gapped states from the bulk decay exponentially fast as a function of the distance away from the first and end wires. The energy splitting between the edge state localized on wire $i = 1$ and the one localized on wire $i = N$ that is brought about by the bulk states vanishes exponentially fast with increasing N. Two gapless edge states with opposite chiralities emerge in the two-dimensional limit $N \to \infty$.

At energies much lower than the bulk gap, the effective $\mathcal{K}$-matrix for the edge modes is

$$\mathcal{K}_{\text{eff}} := \operatorname{diag}(+1, 0|0, 0| \cdots |0, 0|0, -1). \tag{5.20}$$

Here, $\mathcal{K}_{\text{eff}}$ follows from replacing the entries in the $2N \times 2N$ $\mathcal{K}$ matrix for all gapped modes by 0. The pictorial representation of the topological phase in the symmetry class A with one chiral edge state per end wire through the wire construction is shown on the first row and fourth column of Table 5.1. The generalization to an arbitrary number n of gapless edge states sharing a given chirality on the first wire that is opposite to that of the last wire is the following. Enlarge $M = 2$ to $M = 2n$ by making n identical copies of the model depicted in the first row and fourth column of Table 5.1. The stability of the n chiral gapless edge states in wire 1 and wire N is guaranteed because back-scattering among these gapless edges state is not allowed kinematically within wire 1 or within wire N, while back-scattering across the bulk is exponentially suppressed for N large by locality and the gap in the bulk. The number of robust gapless edge states of a given chirality is thus integer. This is the reason why $\mathbb{Z}$ is found in the third column on the first line of Table 5.1.

SRE phases beyond the tenfold way

It is imperative to ask whether the phases constructed so far exhaust all possible SRE phases in the symmetry class A. By demanding that one-body interactions are dominant over many-body interactions, all phases from the (exhaustive) classification for non-interacting fermions in class A and only those were constructed. In these phases, the same topological invariant controls the Hall and the thermal conductivities. However, it was observed that interacting fermion systems can host additional SRE phases in the symmetry class A where this connection is lost. [73] These phases are characterized by an edge that includes charge-neutral chiral modes. While such modes contribute to the quantized energy transport (i.e., the thermal Hall conductivity), they do not contribute to the quantized charge transport (i.e., the charge Hall conductivity). By considering the thermal and charge Hall conductivity as two independent quantized topological responses, this enlarges the classification of SPT phases in the symmetry class A to $\mathbb{Z} \times \mathbb{Z}$.

Starting from identical fermions of charge e, an explicit model for an array of wires will be constructed that stabilizes a SRE phase of matter in the symmetry class A carrying a non-vanishing Hall conductivity but a vanishing thermal Hall conductivity. In order to build a wire-construction of such a strongly interacting SRE phase in the symmetry class A, three spinless electronic wires are grouped into one unit cell, i.e.,

$$K := \operatorname{diag}(+1, -1, +1, -1, +1, -1). \tag{5.21a}$$

It will be useful to arrange the charges $Q_\gamma = 1$ measured in units of the electron charge e for each of the modes $\hat{\phi}_\gamma$, $\gamma = 1, \cdots, M$, into the vector

$$Q = (1,1,1,1,1,1)^{\mathsf{T}}. \tag{5.21b}$$

The physical meaning of the tunneling vectors (interactions) to be defined below is most transparent when employing the following linear transformation on the bosonic field variables

$$\begin{aligned} \widehat{\Phi}(x) &=: \mathcal{W}\,\widetilde{\Phi}(x), && (5.22a)\\ \widetilde{\mathcal{K}} &:= \mathcal{W}^{\mathsf{T}}\,\mathcal{K}\,\mathcal{W}, && (5.22b)\\ \widetilde{\mathcal{T}} &:= \mathcal{W}^{-1}\,\mathcal{T}, && (5.22c)\\ \widetilde{\mathcal{Q}} &:= \mathcal{W}^{\mathsf{T}}\,\mathcal{Q}, && (5.22d) \end{aligned}$$

where $\mathcal{W}$ is a $MN \times MN$ block-diagonal matrix with the non-orthogonal block W having integer entries and the determinant one in magnitude. The transformation W and its inverse W^{-1} are given by

$$W := \begin{pmatrix} 0 & -1 & -1 & 0 & 0 & 0\\ +1 & -1 & -1 & 0 & 0 & 0\\ +1 & 0 & -1 & 0 & 0 & 0\\ 0 & 0 & 0 & -1 & 0 & +1\\ 0 & 0 & 0 & -1 & -1 & +1\\ 0 & 0 & 0 & -1 & -1 & 0 \end{pmatrix}, \qquad W^{-1} := \begin{pmatrix} -1 & +1 & 0 & 0 & 0 & 0\\ 0 & -1 & +1 & 0 & 0 & 0\\ -1 & +1 & -1 & 0 & 0 & 0\\ 0 & 0 & 0 & -1 & +1 & -1\\ 0 & 0 & 0 & +1 & -1 & 0\\ 0 & 0 & 0 & 0 & +1 & -1 \end{pmatrix}, \tag{5.23}$$

respectively. It brings K to the form

$$\widetilde{K} := \begin{pmatrix} 0 & +1 & 0 & 0 & 0 & 0\\ +1 & 0 & 0 & 0 & 0 & 0\\ 0 & 0 & +1 & 0 & 0 & 0\\ 0 & 0 & 0 & -1 & 0 & 0\\ 0 & 0 & 0 & 0 & 0 & -1\\ 0 & 0 & 0 & 0 & -1 & 0 \end{pmatrix}. \tag{5.24}$$

As can be read off from Eq. (5.4b), the parity of $K_{\gamma\gamma}$ determines the self-statistics of particles of type $\gamma = 1, \cdots, N$. As Eq. (5.4b) is form invariant under the transformation (5.22), one concludes that, with the choice (5.23), the transformed modes $\gamma = 1, 2$ as well as the modes $\gamma = 5, 6$ are pairs of bosonic degrees of freedom, while the third and fourth mode remain fermionic. Furthermore, the charges transported by the transformed modes $\widetilde{\phi}_{\gamma}$ are given by

$$\widetilde{Q} = W^{\mathsf{T}}\,Q = (+2, -2, -3, -3, -2, +2)^{\mathsf{T}}. \tag{5.25}$$

Define the charge-conserving tunneling vectors ($j = 1, \cdots, N-1$)

$$\begin{aligned} \widetilde{\mathcal{T}}_1^{(j)} &:= (0,0,0,0,0,0|\cdots|0,0,+1,-1,0,0|\cdots|0,0,0,0,0,0)^{\mathsf{T}},\\ \widetilde{\mathcal{T}}_2^{(j)} &:= (0,0,0,0,0,0|\cdots|0,0,0,0,+1,0|0,-1,0,0,0,0|\cdots|0,0,0,0,0,0)^{\mathsf{T}},\\ \widetilde{\mathcal{T}}_3^{(j)} &:= (0,0,0,0,0,0|\cdots|0,0,0,0,0,+1|-1,0,0,0,0,0|\cdots|0,0,0,0,0,0)^{\mathsf{T}}. \end{aligned} \tag{5.26}$$

In the original basis, these three families of tunneling vectors are of order 3, 2, and 2, respectively. They are explicitly given by

$$\begin{aligned}
\mathcal{T}_1^{(j)} &\coloneqq (0,0,0,0,0,0|\cdots|-1,-1,-1,+1,+1,+1|\cdots|0,0,0,0,0,0)^{\mathsf{T}},\\
\mathcal{T}_2^{(j)} &\coloneqq (0,0,0,0,0,0|\cdots|0,0,0,0,-1,-1|+1,+1,0,0,0,0|\cdots|0,0,0,0,0,0)^{\mathsf{T}},\\
\mathcal{T}_3^{(j)} &\coloneqq (0,0,0,0,0,0|\cdots|0,0,0,+1,+1,0|0,-1,-1,0,0,0|\cdots|0,0,0,0,0,0)^{\mathsf{T}}.
\end{aligned} \tag{5.27}$$

The tunneling vectors (5.26) gap all modes in the bulk and the remaining gapless edge modes on the left edge are

$$\widetilde{K}_{\mathrm{eff,left}} = \begin{pmatrix} 0 & 1 \\ 1 & 0 \end{pmatrix}, \qquad \widetilde{Q}_{\mathrm{eff,left}} = \begin{pmatrix} +2 \\ -2 \end{pmatrix}. \tag{5.28}$$

The only charge-conserving tunneling vector that could gap out this effective edge theory, $\widetilde{T} = (1,1)^{\mathsf{T}}$, is not compatible with Haldane's criterion (5.16). Thus, the edge theory (5.28) is stable against charge conserving perturbations. The Hall conductivity supported by this edge theory is given by

$$\widetilde{Q}^{\mathsf{T}}_{\mathrm{eff,left}}\, \widetilde{K}^{-1}_{\mathrm{eff,left}}\, \widetilde{Q}_{\mathrm{eff,left}} = -8 \tag{5.29}$$

in units of e^2/h. This is the minimal Hall conductivity of a SRE phase of bosons, if each boson is interpreted as a pair of electrons carrying the electronic charge $2e$. [73] On the other hand, the edge theory (5.28) supports two modes with opposite chiralities, for the symmetric matrix $\widetilde{K}_{\mathrm{eff,left}}$ has the pair of eigenvalues ± 1. Thus, the net energy transported along the left edge, and with it the thermal Hall conductivity, vanishes.

5.4.2 Symmetry class AII

Topological insulators in symmetry class AII can be realized by demanding that $U(1)$ charge conservation holds and that TRS with $\Theta^2 = -1$ holds. The wire construction starts from wires supporting spin-$1/2$ fermions because $\Theta^2 = -1$, so that the minimal choice $M = 4$ counts two pairs of Kramers degenerate left- and right-moving degrees of freedom carrying opposite spin projections on the spin quantization axis, i.e., two pairs of Kramers degenerate helical modes. The K-matrix reads

$$K \coloneqq \operatorname{diag}(+1,-1,-1,+1). \tag{5.30a}$$

The entries in the K-matrix represent, from left to right, a right-moving particle with spin up, a left-moving particle with spin down, a left-moving particle with spin up, and a right-moving particle with spin down. The operation for reversal of time in any one of the N wires is represented by [one verifies that Eq. (5.10e) holds]

$$P_\Theta \coloneqq \begin{pmatrix} 0&1&0&0\\ 1&0&0&0\\ 0&0&0&1\\ 0&0&1&0 \end{pmatrix}, \qquad I_\Theta \coloneqq \begin{pmatrix} 0\\1\\0\\1 \end{pmatrix}. \tag{5.30b}$$

Define $\widehat{H}_{\mathcal{V}}$ by choosing any symmetric 4×4 matrix V that obeys

$$V = P_\Theta\, V\, P_\Theta^{-1}. \tag{5.30c}$$

Define $\widehat{H}_{\{\mathcal{T}_{\mathrm{SO}}\}}$ by choosing $2(N-1)$ scattering vectors as follows. For any $j = 1, \cdots, (N-1)$, introduce the pair of scattering vectors

$$\mathcal{T}_{\rm SO}^{(j)} := (0,0,0,0|\cdots|0,0,+1,0|-1,0,0,0|\cdots|0,0,0,0)^{\mathsf{T}} \tag{5.31a}$$

and

$$\overline{\mathcal{T}}_{\rm SO}^{(j)} := -\mathcal{P}_{\Theta}\,\mathcal{T}_{\rm SO}^{(j)}. \tag{5.31b}$$

The scattering vector (5.31a) labels a one-body interaction in the fermion representation that fulfills Eq. (5.5f). It scatters a left mover with spin up from wire j into a right mover with spin up in wire $j+1$. For any $j=1,\cdots,(N-1)$, introduce the pair of amplitudes

$$h_{\mathcal{T}_{\rm SO}^{(j)}}(x) = h_{\overline{\mathcal{T}}_{\rm SO}^{(j)}}(x) \geq 0 \tag{5.31c}$$

and the pair of phases

$$\alpha_{\mathcal{T}_{\rm SO}^{(j)}}(x) = \alpha_{\overline{\mathcal{T}}_{\rm SO}^{(j)}}(x) \in \mathbb{R} \tag{5.31d}$$

according to Eqs. (5.11d) and (5.11e), respectively. The choices for the amplitude (5.31c) and the phase (5.31d) are arbitrary. The subscript SO refers to the intrinsic spin-orbit coupling. The rational for using it shall be shortly explained.

One verifies that all $2(N-1)$ scattering vectors (5.30c) and (5.31a) satisfy the Haldane criterion (5.16), i.e.,

$$\mathcal{T}_{\rm SO}^{(i)\mathsf{T}}\,\mathcal{K}\,\mathcal{T}_{\rm SO}^{(j)} = \overline{\mathcal{T}}_{\rm SO}^{(i)\mathsf{T}}\,\mathcal{K}\,\overline{\mathcal{T}}_{\rm SO}^{(j)} = \mathcal{T}_{\rm SO}^{(i)\mathsf{T}}\,\mathcal{K}\,\overline{\mathcal{T}}_{\rm SO}^{(j)} = 0, \tag{5.32}$$

for $i,j=1,\cdots,N-1$. Correspondingly, the term $\widehat{H}_{\{\mathcal{T}_{\rm SO}\}}$ gaps out $4(N-1)$ of the $4N$ gapless modes of $\widehat{H}_{\mathcal{V}}$. Two pairs of Kramers degenerate helical edge states that propagate along the first and last wire, respectively, remain in the low energy sector of the theory. These edge states are localized on wire $i=1$ and $i=N$, respectively, for their overlaps with the gapped states from the bulk decay exponentially fast as a function of the distance away from the first and end wires. The energy splitting between the edge state localized on wire $i=1$ and wire $i=N$ brought about by the bulk states vanishes exponentially fast with increasing N. Two pairs of gapless Kramers degenerate helical edge states emerge in the two-dimensional limit $N\to\infty$.

At energies much lower than the bulk gap, the effective $\mathcal{K}$-matrix for the two pairs of helical edge modes is

$$\mathcal{K}_{\rm eff} := \mathrm{diag}(+1,-1,0,0|0,0,0,0|\cdots|0,0,0,0|0,0,-1,+1). \tag{5.33}$$

Here, $\mathcal{K}_{\rm eff}$ follows from replacing the entries in the $4N\times 4N$ $\mathcal{K}$ matrix for all gapped modes by 0. It will be shown that the effective scattering vector

$$\mathcal{T}_{\rm eff} := (+1,-1,0,0|0,0,0,0|\cdots)^{\mathsf{T}}, \tag{5.34}$$

with the potential to gap out the pair of Kramers degenerate helical edge modes on wire $i=1$ since it fulfills the Haldane criterion (5.16), is not allowed by TRS. [2] On the one hand, $\mathcal{T}_{\rm eff}$ maps to itself under reversal of time,

[2] Even integer multiples of $\mathcal{T}_{\rm eff}$ would gap the edge states, but they must also be discarded as explained in Ref. [87].

$$\mathcal{T}_{\text{eff}} = -\mathcal{P}_{\Theta}\,\mathcal{T}_{\text{eff}}. \tag{5.35}$$

On the other hand,

$$\mathcal{T}_{\text{eff}}^{\mathsf{T}}\,\mathcal{P}_{\Theta}\,\mathcal{I}_{\Theta} = -1. \tag{5.36}$$

Therefore, the condition (5.11e) for $\mathcal{T}_{\text{eff}}$ to be a TRS perturbation is not met, for the phase $\alpha_{\mathcal{T}_{\text{eff}}}(x)$ associated to $\mathcal{T}_{\text{eff}}$ then obeys

$$\alpha_{\mathcal{T}_{\text{eff}}}(x) = \alpha_{\mathcal{T}_{\text{eff}}}(x) - \pi, \tag{5.37}$$

a condition that cannot be satisfied.

Had a TRS with $\Theta = +1$ been imposed instead of $\Theta = -1$ as is suited for the symmetry class AI that describes spinless fermions with TRS, one would only need to replace I_{Θ} in Eq. (5.30b) by the null vector. If so, the scattering vector (5.34) is compatible with TRS since the condition (5.11e) for TRS then becomes

$$\alpha_{\mathcal{T}_{\text{eff}}}(x) = \alpha_{\mathcal{T}_{\text{eff}}}(x) \tag{5.38}$$

instead of Eq. (5.37). This is the reason why symmetry class AI is always topologically trivial in two-dimensional space from the point of view of the wire construction.

Note also that had one not insisted on the condition of charge neutrality (5.5f), the tunneling vector

$$\mathcal{T}'_{\text{eff}} := (+1,+1,0,0|0,0,0,0|\cdots)^{\mathsf{T}}, \tag{5.39}$$

that satisfies the Haldane criterion and is compatible with TRS could gap out the Kramers degenerate pair of helical edge states.

To address the question of what happens if $M = 4$ is changed to $M = 4n$ with n any strictly positive integer in each wire from the array, consider, without loss of generality, the case of $n = 2$. To this end, it suffices to repeat all the steps that lead to Eq. (5.34), except for the change

$$\begin{aligned}\mathcal{K}_{\text{eff}} := \operatorname{diag}\,(&+1,-1,0,0;+1,-1,0,0|0,0,0,0;0,0,0,0|\\ &\cdots|0,0,0,0;0,0,0,0|0,0,-1,+1;0,0,-1,+1).\end{aligned} \tag{5.40}$$

One verifies that the scattering vectors

$$\mathcal{T}'_{\text{eff}} := (+1,0,0,0;0,-1,0,0|0,0,0,0;0,0,0,0|\cdots)^{\mathsf{T}} \tag{5.41}$$

and

$$\mathcal{T}''_{\text{eff}} := (0,-1,0,0;+1,0,0,0|0,0,0,0;0,0,0,0|\cdots)^{\mathsf{T}} \tag{5.42}$$

are compatible with the condition that TRS holds in that the pair is a closed set under reversal of time,

$$\mathcal{T}'_{\text{eff}} = -\mathcal{P}_{\Theta}\,\mathcal{T}''_{\text{eff}}. \tag{5.43}$$

One verifies that these scattering vectors fulfill the Haldane criterion (5.16). Consequently, inclusion in $\widehat{H}_{\{\mathcal{T}_{\text{SO}}\}}$ of the two cosine potentials with $\mathcal{T}'_{\text{eff}}$ and $\mathcal{T}''_{\text{eff}}$ entering in their arguments, respectively, gaps out the pair of Kramers degenerate helical modes on wire $i = 1$. The same treatment of the wire $i = N$ leads to the conclusion that TRS does not protect the gapless pairs of Kramers degenerate edge states from perturbations when $n = 2$. The generalization to $M = 4n$ channels is that it is only when n is odd that a pair of Kramers degenerate helical edge modes is robust to the most generic $\widehat{H}_{\{\mathcal{T}_{\mathrm{SO}}\}}$ of the form depicted in the fourth column on line 3 of Table 5.1. Since it is the parity of n in the number $M = 4n$ of channels per wire that matters for the stability of the Kramers degenerate helical edge states, the group of two integers $\mathbb{Z}_2$ under addition modulo 2 in the third column on line 3 of Table 5.1 is used.

If conservation of the projection of the spin-$1/2$ quantum number on the quantization axis was imposed, then processes by which a spin is flipped must be precluded from all scattering vectors. In particular, the scattering vectors (5.41) and (5.42) are not admissible anymore. By imposing the $U(1)$ residual symmetry of the full $SU(2)$ symmetry group for a spin-$1/2$ degree of freedom, the group of integers $\mathbb{Z}$ under the addition that encodes the topological stability in the quantum spin Hall effect (QSHE) is recovered.

The discussion of the symmetry class AII is closed by justifying the interpretation of the index SO as an abbreviation for the intrinsic spin-orbit coupling. To this end, introduce a set of $(N-1)$ pairs of scattering vectors

$$\mathcal{T}^{(j)}_{\mathrm{R}} := (0,0,0,0|\cdots|0,+1,0,0|-1,0,0,0|\cdots|0,0,0,0)^{\mathsf{T}} \tag{5.44a}$$

and

$$\overline{\mathcal{T}}^{(j)}_{\mathrm{R}} := -\mathcal{P}_{\Theta}\,\mathcal{T}^{(j)}_{\mathrm{R}} \tag{5.44b}$$

for $j = 1,\cdots,N-1$. The scattering vector (5.44a) labels a one-body interaction in the fermion representation that fulfills Eq. (5.5f). The index R is an acronym for Rashba as it describes a backward scattering process by which a left mover with spin down from wire j is scattered into a right mover with spin up on wire $j+1$ and conversely. For any $j = 1,\cdots,(N-1)$, introduce the pair of amplitudes

$$h_{\mathcal{T}^{(j)}_{\mathrm{R}}}(x) = h_{\overline{\mathcal{T}}^{(j)}_{\mathrm{R}}}(x) \geq 0 \tag{5.44c}$$

and the pair of phases

$$\alpha_{\mathcal{T}^{(j)}_{\mathrm{R}}}(x) = \alpha_{\overline{\mathcal{T}}^{(j)}_{\mathrm{R}}}(x) + \pi \in \mathbb{R} \tag{5.44d}$$

according to Eqs. (5.11d) and (5.11e), respectively. In contrast to the intrinsic spin-orbit scattering vectors, the Rashba scattering vectors (5.44a) fail to meet the Haldane criterion (5.16) as

$$\mathcal{T}^{(j)\mathsf{T}}_{\mathrm{R}}\,\mathcal{K}\,\overline{\mathcal{T}}^{(j+1)}_{\mathrm{R}} = -1, \qquad j = 1,\cdots,N-1. \tag{5.45}$$

Hence, the Rashba scattering processes fail to open a gap in the bulk, as is expected of a Rashba coupling in a two-dimensional electron gas. On the other hand, the intrinsic spin-orbit coupling can lead to a phase with a gap in the bulk that supports the spin quantum Hall effect in a two-dimensional electron gas.

5.4.3 Symmetry class D

The simplest example among the topological superconductors can be found in the symmetry class D that is defined by the presence of a PHS with $\Pi^2 = +1$ and the absence of TRS.

With the understanding of PHS as discussed in Sec. 5.3.2, a representative phase in class D is constructed from identical wires supporting right- and left-moving spinless fermions, each of which carry a particle or a hole label, i.e., $M = 4$. The K-matrix reads

$$K := \operatorname{diag}(+1, -1, -1, +1). \tag{5.46a}$$

The entries in the K-matrix represent, from left to right, a right-moving particle, a left-moving particle, a left-moving hole, and a right-moving hole. The operation for the exchange of particles and holes in any one of the N wires is represented by [one verifies that Eq. (5.10f) holds]

$$P_{\Pi} := \begin{pmatrix} 0 & 0 & 0 & 1 \\ 0 & 0 & 1 & 0 \\ 0 & 1 & 0 & 0 \\ 1 & 0 & 0 & 0 \end{pmatrix}, \qquad I_{\Pi} := \begin{pmatrix} 0 \\ 0 \\ 0 \\ 0 \end{pmatrix}. \tag{5.46b}$$

Define $\widehat{H}_{\mathcal{V}}$ by choosing any symmetric 4×4 matrix V that obeys

$$V = +P_{\Pi}\, V\, P_{\Pi}^{-1}. \tag{5.46c}$$

Define $\widehat{H}_{\{\mathcal{T}\}}$ by choosing $2N - 1$ scattering vectors as follows. For any wire $j = 1, \cdots, N$, introduce the scattering vector

$$\mathcal{T}^{(j)} := (0,0,0,0|\cdots| +1, -1, -1, +1|\cdots|0,0,0,0)^{\mathsf{T}}. \tag{5.47a}$$

Between any pair of neighboring wires introduce the scattering vector

$$\overline{\mathcal{T}}^{(j)} := (0,0,0,0|\cdots|0,+1,-1,0|-1,0,0,+1|\cdots|0,0,0,0)^{\mathsf{T}}, \tag{5.47b}$$

for $j = 1, \cdots, (N-1)$. Observe that both $\mathcal{T}^{(j)}$ and $\overline{\mathcal{T}}^{(j)}$ are eigenvectors of the particle-hole transformation in that

$$\mathcal{P}_{\Pi}\, \mathcal{T}^{(j)} = +\mathcal{T}^{(j)}, \qquad \mathcal{P}_{\Pi}\, \overline{\mathcal{T}}^{(j)} = -\overline{\mathcal{T}}^{(j)}. \tag{5.47c}$$

Thus, to comply with PHS, demand that the phases

$$\alpha_{\overline{\mathcal{T}}^{(j)}}(x) = 0, \tag{5.47d}$$

while $\alpha_{\mathcal{T}^{(j)}}(x)$ are unrestricted. Similarly, the amplitudes $h_{\mathcal{T}^{(j)}}(x)$ and $h_{\overline{\mathcal{T}}^{(j)}}(x)$ can take arbitrary real values.

One verifies that the set of scattering vectors defined by Eqs. (5.47a) and (5.47b) satisfies the Haldane criterion. Correspondingly, the term $\widehat{H}_{\{\mathcal{T}\}}$ gaps out $(4N-2)$ of the $4N$ gapless modes of $\widehat{H}_{\mathcal{V}}$. Furthermore, one identifies with

$$\overline{\mathcal{T}}^{(0)} = (-1,0,0,+1|0,0,0,0|\cdots|0,0,0,0|0,+1,-1,0)^{\mathsf{T}} \tag{5.48}$$

a unique (up to an integer multiplicative factor) scattering vector that satisfies the Haldane criterion with all existing scattering vectors Eqs. (5.47a) and (5.47b) and could thus potentially gap out the remaining pair of modes. However, the tunneling $\overline{\mathcal{T}}^{(0)}$ is non-local for it connects the two edges of the system when open boundary conditions are chosen. One thus concludes that the two remaining modes are exponentially localized near wire $i = 1$ and wire $i = N$, respectively, and propagate with opposite chirality.

To give a physical interpretation of the resulting topological (edge) theory in this wire construction, one has to keep in mind that the degrees of freedom were artificially doubled. One finds, in this doubled theory, a single chiral boson (with chiral central charge $c = 1$). To interpret it as the edge of a chiral $(p_x + \mathrm{i}p_y)$ superconductor, the reality condition is imposed to obtain a single chiral Majorana mode with chiral central charge $c = 1/2$.

The pictorial representation of the topological phase in the symmetry class D through the wire construction is shown on the fifth row of Table 5.1. The generalization to an arbitrary number n of gapless chiral edge modes is analogous to the case discussed in symmetry class A. The number of robust gapless chiral edge states of a given chirality is thus integer. This is the reason why the group of integers $\mathbb{Z}$ is found in the third column on the fifth line of Table 5.1.

5.4.4 Symmetry classes DIII and C

The remaining two topological nontrivial superconducting classes DIII (TRS with $\Theta^2 = -1$ and PHS with $\Pi^2 = +1$) and C (PHS with $\Pi^2 = -1$) involve spin-1/2 fermions. Each wire thus features no less than $M = 8$ internal degrees of freedom corresponding to the spin-$1/2$, chirality, and particle/hole indices. The construction is very similar to the cases already presented. Details are relegated to Ref. [86].

The scattering vectors that are needed to gap out the bulk for each class of class DIII and C are represented pictorially in the fourth column on lines 4 and 9 of Table 5.1.

5.4.5 Summary

An explicit construction was provided by way of an array of wires supporting fermions that realizes all five insulating and superconducting topological phases of matter with a nondegenerate ground state in two-dimensional space according to the tenfold classification of band insulators and superconductors. The topological protection of edge modes in the bosonic formulation follows from imposing the Haldane criterion (5.16) along with the appropriate symmetry constraints. It remains to extend the wire construction to allow many-body tunneling processes that delivers fractionalized phases with degenerate ground states.

5.5 Fractionalized phases

The power of the wire construction goes much beyond what was used in Sec. 5.4 to reproduce the classification of the SRE phases. It is possible to construct models for interacting phases of matter with intrinsic topological order and fractionalized excitations by relaxing the condition on the tunnelings between wires that they be of the one-body type. While these phases are more complex, the principles for constructing the models and proving the stability of edge modes remain the same: All allowed tunneling vectors have to obey the Haldane criterion (5.16) and the respective symmetries.

5.5.1 Symmetry class A: Fractional quantum Hall states

First, the models of quantum wires that are topologically equivalent to the Laughlin state in the FQHE are reviewed, [68] following the construction in Ref. [56] for Abelian fractional quantum Hall states. Here, the choice of scattering vectors is determined by the Haldane criterion (5.16) and at the same time prepare the grounds for the construction of fractional topological insulators with TRS in Sec. 5.5.2.

Needed are the fermionic Laughlin states indexed by the positive odd integer m. [68] (By the same method, other fractional quantum Hall phases from the Abelian hierarchy could be constructed. [56]) The elementary degrees of freedom in each wire are spinless right- and left-moving fermions with the K-matrix

$$K = \mathrm{diag}\,(+1,-1), \tag{5.49a}$$

as is done in Eq. (5.17a). Reversal of time is defined through P_Θ and I_Θ given in Eq (5.17b). Instead of Eq (5.18), the scattering vectors that describe the interactions between the wires are now defined by

$$\mathcal{T}^{(j)} := \big(0,0\,\big|\cdots\big|m_+,-m_-\,\big|m_-,-m_+\,\big|\cdots\big|\,0,0\big)^{\mathsf{T}}, \tag{5.49b}$$

for any $j = 1,\cdots,N-1$, where $m_\pm = (m \pm 1)/2$ [see Table 5.1 for an illustration of the scattering process].

For any $j = 1,\cdots,N-1$, the scattering (tunneling) vectors (5.49b) preserve the conservation of the total fermion number in that they obey Eq. (5.5f), and they encode a tunneling interaction of order $q = m$, with q defined in Eq. (5.5i). As a set, all tunneling interactions satisfy the Haldane criterion (5.16), for

$$\mathcal{T}^{(i)\mathsf{T}}\,\mathcal{K}\,\mathcal{T}^{(j)} = 0, \quad i,j = 1,\cdots,N-1. \tag{5.50}$$

Note that the choice of tunneling vector in Eq. (5.49b) is unique (up to an integer multiplicative factor) if one insists on charge conservation, compliance with the Haldane criterion (5.16), and only includes scattering between neighboring wires.

The bare counting of tunneling vectors shows that the wire model gaps out all but two modes. However, one still needs to show that the remaining two modes (i) live on the edge, (ii) cannot be gapped out by other (local) scattering vectors and (iii) are made out of fractionalized quasiparticles.

To address (i) and (ii), note that the remaining two modes can be gapped out by a unique (up to an integer multiplicative factor) charge-conserving scattering vector that satisfies the Haldane criterion (5.16) with all existing scatterings, namely

$$\mathcal{T}^{(0)} := \big(\,m_-,-m_+\big|\,0,0\big|\cdots\big|0,0\,\big|m_+,-m_-\,\big)^{\mathsf{T}}. \tag{5.51}$$

Connecting the opposite ends of the array of wires through the tunneling $\mathcal{T}^{(0)}$ is not an admissible perturbation, for it violates locality in the two-dimensional thermodynamic limit $N \to \infty$. Had periodic boundary conditions corresponding to a cylinder geometry (i.e., a tube as in Fig. 5.1) by which the first and last wire are nearest neighbors been chosen, $\mathcal{T}^{(0)}$ would be admissible. Hence, the gapless nature of the remaining modes when open boundary conditions are chosen depends on the boundary conditions. These gapless modes have support near the boundary only and are topologically protected.

Applying the transformation (5.6) with

$$W := \begin{pmatrix} -m_- & m_+ \\ m_+ & -m_- \end{pmatrix}, \qquad \det W = -m, \qquad W^{-1} = \frac{1}{m}\begin{pmatrix} m_- & m_+ \\ m_+ & m_- \end{pmatrix}, \tag{5.52a}$$

transforms the matrix K into

$$\widetilde{K} = W^{\mathsf{T}}\, K\, W = \begin{pmatrix} -m_- & m_+ \\ m_+ & -m_- \end{pmatrix} \begin{pmatrix} +1 & 0 \\ 0 & -1 \end{pmatrix} \begin{pmatrix} -m_- & m_+ \\ m_+ & -m_- \end{pmatrix} = \begin{pmatrix} -m & 0 \\ 0 & +m \end{pmatrix}. \tag{5.52b}$$

As its determinant is not unity, the linear transformation (5.52a) changes the compactification radius of the new field $\widetilde{\Phi}(x)$ relative to the compactification radius of the old field $\widehat{\Phi}(x)$ accordingly. Finally, the transformed tunneling and charge vectors are given by

$$\widetilde{\mathcal{T}}^{(j)} = \mathcal{W}^{-1}\, \mathcal{T}^{(j)} = (0,0|\cdots|0,0|0,+1|-1,0|0,0|\cdots|0,0)^{\mathsf{T}} \neq \mathcal{T}^{(j)}, \tag{5.52c}$$

$$\widetilde{\mathcal{Q}} = \mathcal{W}^{\mathsf{T}}\, \mathcal{Q} = (1,1|\cdots|1,1|1,1|1,1|1,1|\cdots|1,1)^{\mathsf{T}} = \mathcal{Q}, \tag{5.52d}$$

respectively, where $\mathcal{W} := \mathbb{1}_N \otimes W$ and $j = 1, \cdots, N-1$. Contrary to the tunneling vectors, the charge vector is invariant under the non-orthogonal linear transformation (5.52a).

In view of Eq. (5.52c), the remaining effective edge theory is described by

$$\widetilde{\mathcal{K}}_{\text{eff}} = \operatorname{diag}(-m, 0|0,0|\cdots|0,0|0,+m). \tag{5.53}$$

This is a chiral theory at each edge that cannot be gapped by local perturbations. In combination with Eq. (5.52d), Eq. (5.53) is precisely the edge theory for anyons with statistical angle $1/m$ and charge e/m, [128] where e is the charge of the original fermions.

5.5.2 Symmetry Class AII: Fractional topological insulators

Having understood how fractionalized quasiparticles emerge out of a wire construction, it is imperative to ask what other phases can be obtained when symmetries are imposed on the topologically ordered phase. Such symmetry enriched topological phases have been classified by methods of group cohomology. [17] Here, the case of TRS with $\Theta^2 = -1$ will provide an example for how the wire construction can be used to build up an intuition for these phases and to study the stability of their edge theory.

The elementary degrees of freedom in each wire are spin-$1/2$ right- and left-moving fermions with the K-matrix

$$K := \operatorname{diag}(+1, -1, -1, +1), \tag{5.54a}$$

as is done in Eq. (5.30a). Reversal of time is defined through P_Θ and I_Θ given in Eq (5.30b). Instead of Eq (5.31a), the scattering vectors that describe the interactions between the wires are now defined by

$$\mathcal{T}^{(j)} := \big(0,0,0,0\,\big|\cdots\big|-m_-,0,+m_+,0\,\big|-m_+,\ 0,+m_-,0\big|\cdots\big|\,0,0,0,0\big)^{\mathsf{T}} \tag{5.54b}$$

and

$$\overline{\mathcal{T}}^{(j)} := -\mathcal{P}_\Theta\, \mathcal{T}^{(j)}, \tag{5.54c}$$

for any $j = 1, \cdots, N-1$, m a positive odd integer, and $m_\pm = (m \pm 1)/2$.

For any $j = 1, \cdots, N-1$, the scattering (tunneling) vectors (5.54b) preserve conservation of the total fermion number in that they obey Eq. (5.5f), and they encode a tunneling interaction of order $q = m$ with q defined in Eq. (5.5i). They also satisfy the Haldane criterion (5.16) as a set [see Table 5.1 for an illustration of the scattering process].

Applying the transformation (5.6) with

$$W := \begin{pmatrix} -m_- & 0 & m_+ & 0 \\ 0 & -m_- & 0 & m_+ \\ m_+ & 0 & -m_- & 0 \\ 0 & m_+ & 0 & -m_- \end{pmatrix} \tag{5.55}$$

to the bosonic fields, leaves the representation of time-reversal invariant

$$W^{-1}\, P_\Theta\, W = P_\Theta, \tag{5.56}$$

while casting the theory in a new form with the transformed matrix $\widetilde{K}$ given by

$$\widetilde{K} = \mathrm{diag}\,(-m, +m, +m, -m), \tag{5.57}$$

and, for any $j = 1, \cdots, N-1$, with the transformed pair of scattering vectors $(\widetilde{\mathcal{T}}^j, \widetilde{\widetilde{\mathcal{T}}}^j)$ given by

$$\widetilde{\mathcal{T}}^{(j)} = (0,0,0,0|\cdots|+1,0,0,0|0,0,-1,0|\cdots|0,0,0,0)^{\mathsf{T}} \tag{5.58}$$

and

$$\widetilde{\widetilde{\mathcal{T}}}^{(j)} = (0,0,0,0|\cdots|0,-1,0,0|0,0,0,+1|\cdots|0,0,0,0)^{\mathsf{T}}. \tag{5.59}$$

When these scattering vectors have gapped out all modes in the bulk, the effective edge theory is described by

$$\widetilde{\mathcal{K}}_{\text{eff}} = \mathrm{diag}\,(0,0,+m,-m|0,0,0,0|\cdots|0,0,0,0|-m,+m,0,0). \tag{5.60}$$

This effective K-matrix describes a single Kramers degenerate pair of $1/m$ anyons propagating along the first wire and another single Kramers degenerate pair of $1/m$ anyons propagating along the last wire. Their robustness to local perturbations is guaranteed by TRS.

Unlike in the tenfold way, the correspondence between the bulk topological phase and the edge theories of LRE phases is not one-to-one. For example, while a bulk topological LRE phase supports fractionalized topological excitations in the bulk, its edge modes may be gapped out by symmetry-allowed perturbations. For the phases discussed in this section, namely the Abelian and TRS fractional topological insulators, it was shown in Refs. [87] and [70] that the edge, consisting of Kramers degenerate pairs of edge modes, supports at most one stable Kramers degenerate pair of delocalized quasiparticles that are stable against disorder. (Note that this does not preclude the richer edge physics of non-Abelian TRS fractional topological insulators. [105])

It turns out that the wire constructions with edge modes given by Eq. (5.60) exhaust all stable edge theories of Abelian topological phases which are protected by TRS with $\Theta^2 = -1$ alone.

Let the single protected Kramers degenerate pair be characterized by the linear combination of bosonic fields

$$\hat{\varphi}(x) \coloneqq \mathcal{T}^{\mathsf{T}}\,\mathcal{K}'\,\widehat{\Phi}(x) \tag{5.61}$$

and its time-reversed partner

$$\hat{\bar{\varphi}}(x) \coloneqq \overline{\mathcal{T}}^{\mathsf{T}}\,\mathcal{K}'\,\widehat{\Phi}(x), \tag{5.62}$$

where the tunneling vector $\mathcal{T}$ was constructed from the microscopic information from the theory in Ref. [87] and $\mathcal{K}'$ is the K-matrix of a TRS bulk Chern-Simons theory from the theory in Ref. [87]. [In other words, the theory encoded by $\mathcal{K}'$ has nothing to do a priory with the array of quantum wires defined by Eq. (5.54).] The Kramers degenerate pair of modes $(\hat{\varphi}, \hat{\bar{\varphi}})$ is stable against TRS perturbations supported on a single edge if and only if

$$\frac{1}{2}|\mathcal{T}^{\mathsf{T}}\,\mathcal{Q}| \tag{5.63}$$

is an odd number. Here, $\mathcal{Q}$ is the charge vector with integer entries that determines the coupling of the different modes to the electromagnetic field. Provided $(\hat{\varphi}, \hat{\bar{\varphi}})$ is stable, its equal-time commutation relations follow from Eq. (5.4b) as

$$[\hat{\varphi}(x), \hat{\varphi}(x')] = -\,\mathrm{i}\pi\,\left(\mathcal{T}^{\mathsf{T}}\,\mathcal{K}'\,\mathcal{T}\,\mathrm{sgn}(x-x') + \mathcal{T}^{\mathsf{T}}\,\mathcal{L}\,\mathcal{T}\right), \tag{5.64a}$$

$$\left[\hat{\bar{\varphi}}(x), \hat{\bar{\varphi}}(x')\right] = -\,\mathrm{i}\pi\,\left(-\mathcal{T}^{\mathsf{T}}\,\mathcal{K}'\,\mathcal{T}\,\mathrm{sgn}(x-x') + \overline{\mathcal{T}}^{\mathsf{T}}\,\mathcal{L}\,\overline{\mathcal{T}}\right), \tag{5.64b}$$

where the fact that $\mathcal{K}'$ anticommutes with $\mathcal{P}_{\Theta}$ according to Eq. (5.11c) was used. By the same token, one can show that the fields $\hat{\varphi}$ and $\hat{\bar{\varphi}}$ commute, for

$$\mathcal{T}^{\mathsf{T}}\,\mathcal{K}'\,\overline{\mathcal{T}} = \mathcal{T}^{\mathsf{T}}\,\mathcal{P}_{\Theta}\,\mathcal{K}'\,\mathcal{T} = -\overline{\mathcal{T}}^{\mathsf{T}}\,\mathcal{K}'\,\mathcal{T} = 0. \tag{5.65}$$

One concludes that the effective edge theory for <u>any</u> Abelian TRS fractional topological insulator build from fermions has the effective form of one Kramers degenerate pairs

$$\mathcal{K}_{\text{eff}} = \begin{pmatrix} \mathcal{T}^{\mathsf{T}}\mathcal{K}'\mathcal{T} & 0 \\ 0 & -\mathcal{T}^{\mathsf{T}}\mathcal{K}'\mathcal{T} \end{pmatrix}, \tag{5.66}$$

and is thus entirely defined by the single integer

$$m \coloneqq \mathcal{T}^{\mathsf{T}}\mathcal{K}'\mathcal{T}. \tag{5.67}$$

With the scattering vectors (5.54c) An explicit wire construction for each of these cases was given, thus exhausting all possible stable edge theories for Abelian fractional topological insulators.

For each positive odd integer m, the fractionalized mode has a $\mathbb{Z}_2$ character. It can have either one or none stable Kramers degenerate pair of m quasiparticles.

5.5.3 Symmetry Class D: Fractional superconductors

In Sec. 5.5.2 TRS was imposed on the wire construction of fractional quantum Hall states from which the fractional topological insulators in symmetry class AII followed. In complete analogy, one may impose PHS with $\Pi^2 = +1$ on the wire construction of a fractional quantum

Hall state, thereby promoting it to symmetry class D. Physically, there follows a model for a superconductor with "fractionalized" Majorana fermions or Bogoliubov quasiparticles.

Lately, interest in this direction has been revived by the investigation of exotic quantum dimensions of twist defects embedded in an Abelian fractional quantum Hall liquid, [8, 7, 6] along with heterostructures of superconductors combined with fractional quantum Hall effect, [72, 120, 21] or fractional topological insulators. [20] Furthermore, the Kitaev quantum wire has been generalized to $\mathbb{Z}_n$ clock models hosting parafermionic edge modes, [59, 27] along with efforts to transcend the Read-Rezayi quantum Hall state [98] to spin liquids [38,37] and superconductors, [79] all of which exhibit parafermionic quasiparticles.

As in the classification of non-interacting insulators, the Bogoliubov quasiparticles are treated with Abelian bosonization as if they were Dirac fermions. The fractional phase is driven by interactions among the Bogoliubov quasiparticles.

The elementary degrees of freedom in each wire are spinless right- and left-moving fermions and holes as was defined for symmetry class D in Eqs. (5.46a)-(5.46c). Construct the fractional topological insulator using the set of PHS scattering vectors $\mathcal{T}^{(j)}$, for $j = 1, \cdots, N$ with $\mathcal{T}^{(j)}$ as defined in Eq. (5.47a) in each wire and the PHS as defined in Eq. (5.46b). Complement them with the set of PHS scattering vectors $\overline{\mathcal{T}}^{(j)}$, for $j = 1, \cdots, N-1$ defined by ($m_{\pm} = (m \pm 1)/2$)

$$\overline{\mathcal{T}}^{(j)} = \big(0,0,0,0\,\big|\cdots\big|-m_{-},m_{+},-m_{+},m_{-}\big|-m_{+},m_{-},-m_{-},m_{+}\big|\cdots\big|\,0,0,0,0\big)^{\mathsf{T}}, \tag{5.68}$$

with m an odd positive integer. Notice that $\overline{\mathcal{T}}^{(j)} \coloneqq -\mathcal{P}_{\Pi}\,\overline{\mathcal{T}}^{(j)}$ so that one has to demand that $\alpha_{\overline{\mathcal{T}}^{(j)}} = 0$ has to comply with PHS. Thus, together the $\mathcal{T}^{(j)}$ and $\overline{\mathcal{T}}^{(j)}$ gap out $(4N-2)$ of the $4N$ chiral modes in the wire. Identify the unique (up to an integer multiplicative factor) scattering vector ($m_{\pm} = (m \pm 1)/2$)

$$\overline{\mathcal{T}}^{(0)} = \big(-m_{+},m_{-},-m_{-},m_{+}\big|\,0,0,0,0\big|\cdots\big|0,0,0,0\,\big|-m_{-},m_{+},-m_{+},m_{-}\,\big)^{\mathsf{T}}, \tag{5.69}$$

with m the same odd positive integer as in Eq. (5.68) that satisfies the Haldane criterion with all $\mathcal{T}^{(j)}$ and $\overline{\mathcal{T}}^{(j)}$ and thus can potentially gap out the 2 remaining modes. However, it is physically forbidden for it represents a non-local scattering from one edge to the other. It is concluded that each boundary supports a single remaining chiral mode that is an eigenstate of PHS.

To understand the nature of the single remaining chiral mode on each boundary, the local linear transformation W of the bosonic fields

$$W = \begin{pmatrix} -m_{-} & +m_{+} & 0 & 0 \\ +m_{+} & -m_{-} & 0 & 0 \\ 0 & 0 & -m_{-} & +m_{+} \\ 0 & 0 & +m_{+} & -m_{-} \end{pmatrix}, \quad m_{\pm} = \frac{m \pm 1}{2}, \tag{5.70}$$

with determinant $\det W = m^4$ is used. When applied to the non-local scattering vector $\overline{\mathcal{T}}^{(0)}$ that connects the two remaining chiral edge modes,

$$\begin{aligned} \tilde{\overline{\mathcal{T}}}^{(0)} &= \mathcal{W}^{-1}\,\overline{\mathcal{T}}^{(0)} \\ &= (0,-1,+1,0|0,0,0,0|\cdots|0,0,0,0|+1,0,0,-1), \end{aligned} \tag{5.71}$$

while the matrix K changes under this transformation to

$$\widetilde{K} = \mathrm{diag}\,(-m, m, m, -m). \tag{5.72}$$

Noting that the representation of PHS is unchanged

$$W^{-1}\,P_{\Pi}\,W = P_{\Pi}, \tag{5.73}$$

one may interpret the remaining chiral edge mode as a PHS superposition of a Laughlin quasiparticle and a Laughlin quasihole. It thus describes a fractional chiral edge mode on either side of the two-dimensional array of quantum wires. The definite chirality is an important difference to the case of the fractional $\mathbb{Z}_2$ topological insulator discussed in Sec. 5.5.2. It guarantees that any integer number $n \in \mathbb{Z}$ layers of this theory is stable, for no tunneling vector that acts locally on one edge can satisfy the Haldane criterion (5.16). For each m, one may thus say that the parafermion mode has a $\mathbb{Z}$ character, as does the SRE phase in symmetry class D.

5.5.4 Symmetry classes DIII and C: More fractional superconductors

The construction is very similar for classes DIII and C. to the cases already presented. Details are relegated to Ref. [86]. For class DIII, the edge excitations (and bulk quasiparticles) of the phase are TRS fractionalized Bogoliubov quasiparticles that have also been discussed in one-dimensional realizations. (In the latter context, these TRS fractionalized Bogoliubov quasiparticles are rather susceptible to perturbations. [60, 94])

5.6 Summary

In this section, a wire construction was developed to build models of short-range entangled and long-range entangled topological phases of two-dimensional quantum matter, so as to yield immediate information about the topological stability of their edge modes. As such, the periodic table for integer topological phases was promoted to its fractional counterpart. The following paradigms were applied.

(1) Each Luttinger liquid wire describes (spinfull or spinless) electrons. Abelian bosonization was used.

(2) Back-scattering and short-range interactions within and between wires are added. Modes are gapped out if these terms acquire a finite expectation value.

(3) A mutual compatibility condition, the Haldane criterion, is imposed among the terms that acquire an expectation value. It is an incarnation of the statement that the operators have to commute if they are to be replaced simultaneously by their expectation values.

(4) A set of discrete and local symmetries are imposed on all terms in the Hamiltonian. When modes become massive, they may not break these symmetries.

(5) The model was analyzed in a strong-coupling limit, instead of the weak coupling limit in which one derives the renormalization group flows for the interactions.

It has become fashionable to write papers in condensed matter physics that take Majorana fermions as the building blocks of lattice models. Elegant mathematical results have been obtained in this way, some of which having the added merit for bringing conceptual clarity. However, the elementary building blocks of condensed matter are ions and electrons whose interactions are governed by quantum electrodynamics. Majorana fermions in condensed matter physics can only emerge in a non-perturbative way through (i) the interactions between the electrons from the valence bands of a material, or (ii) as the low-energy excitations of exotic quantum magnets. For Majorana fermions to be observable in condensed matter physics, a deconfining transition must have taken place, a notoriously non-perturbative phenomenon. One of the challenges that was undertaken in this section is to find interacting models for itinerant electrons with local interactions that support Majorana fermions at low energies and long wave lengths. This goal was achieved, starting from non-interacting itinerant electrons, by constructing local many-body interactions that conserve the electron charge and that stabilize two-dimensional bulk superconductors supporting gapless Majorana fermions along their two-dimensional boundaries. This is why strictly many-body interactions are needed in the symmetry classes D, DIII, and C to realize SRE topological phases in the fourth column of Table 5.1.

Acknowledgments

I am grateful to Claudio Chamon, Titus Neupert, Luiz Santos, Shinsei Ryu, and Ronnie Thomale with whom our collaborations have shaped Secs. 4 and 5. I am also grateful to Maurizio Storni for his help with Sec. 3.

References

[1] Takahiro Morimoto, Akira Furusaki, and Christopher Mudry, *"Anderson localization and the topology of classifying spaces,"* unpublished.

[2] More precisely, to guarantee that there are N_{K} Kramers degenerate pairs of electrons in the theory, demand that there exists a space and time independent transformation

$$O = +\Sigma_1\, O\, \Sigma_1 \in \mathrm{SL}(2N, \mathbb{Z})$$

such that

$$K \mapsto O^{\mathsf{T}}\, K\, O, \qquad V \mapsto O^{\mathsf{T}}\, V\, O,$$

and

$$Q \mapsto O^{\mathsf{T}}\, Q$$

with the transformed charge vector containing $2N_{\mathrm{K}}$ odd integers.

[3] Abrahams, E., Anderson, P. W., Licciardello, D. C., and Ramakrishnan, T. V. (1979). Scaling theory of localization: Absence of quantum diffusion in two dimensions. Phys. Rev. Lett., **42**, 673–676.

[4] Altland, Alexander and Zirnbauer, Martin R. (1997). Nonstandard symmetry classes in mesoscopic normal-superconducting hybrid structures. Phys. Rev. B, **55**, 1142–1161.

[5] Anderson, P. W. (1958). Absence of Diffusion in Certain Random Lattices. Phys. Rev., **109**, 1492–1505.

[6] Barkeshli, Maissam, Jian, Chao-Ming, and Qi, Xiao-Liang (2013). Theory of defects in abelian topological states. Phys. Rev. B, **88**, 235103.

[7] Barkeshli, Maissam, Jian, Chao-Ming, and Qi, Xiao-Liang (2013). Twist defects and projective non-abelian braiding statistics. Phys. Rev. B, **87**, 045130.

[8] Barkeshli, Maissam and Qi, Xiao-Liang (2012). Topological nematic states and non-abelian lattice dislocations. Phys. Rev. X, **2**, 031013.

[9] Berezinskiǐ, V. L. (1971). Destruction of Long-range Order in One-dimensional and Two-dimensional Systems having a Continuous Symmetry Group I. Classical Systems. Soviet Journal of Experimental and Theoretical Physics, **32**, 493.

[10] Bernevig, B. Andrei, Hughes, Taylor L., and Zhang, Shou-Cheng (2006). Quantum spin hall effect and topological phase transition in hgte quantum wells. Science, **314**(5806), 1757–1761.

[11] Bernevig, B. A. and Zhang, S.-C. (2006). Quantum Spin Hall Effect. Phys. Rev. Lett., **96**(10), 106802.

[12] Brouwer, P. W., Furusaki, A., Gruzberg, I. A., and Mudry, C. (2000). Localization and delocalization in dirty superconducting wires. Phys. Rev. Lett., **85**, 1064–1067.

[13] Brouwer, P. W., Furusaki, A., Mudry, C., and Ryu, S. (2005). Disorder-induced critical phenomena–new universality classes in Anderson localization. BUTSURI **60**, 935 (2005) (in Japanese, english version arXiv:cond-mat/0511622).

[14] Brouwer, P. W., Mudry, C., and Furusaki, A. (2000). Density of states in coupled chains with off-diagonal disorder. Phys. Rev. Lett., **84**, 2913–2916.
[15] Brouwer, P. W., Mudry, C., Simons, B. D., and Altland, A. (1998). Delocalization in coupled one-dimensional chains. Phys. Rev. Lett., **81**, 862–865.
[16] Budich, Jan Carl, Thomale, Ronny, Li, Gang, Laubach, Manuel, and Zhang, Shou-Cheng (2012). Fluctuation-induced topological quantum phase transitions in quantum spin-hall and anomalous-hall insulators. Phys. Rev. B, **86**, 201407.
[17] Chen, Xie, Gu, Zheng-Cheng, Liu, Zheng-Xin, and Wen, Xiao-Gang (2013). Symmetry protected topological orders and the group cohomology of their symmetry group. Phys. Rev. B, **87**, 155114.
[18] Chen, Xie, Gu, Zheng-Cheng, and Wen, Xiao-Gang (2011). Classification of gapped symmetric phases in one-dimensional spin systems. Phys. Rev. B, **83**, 035107.
[19] Chen, Xie, Gu, Zheng-Cheng, and Wen, Xiao-Gang (2011). Complete classification of one-dimensional gapped quantum phases in interacting spin systems. Phys. Rev. B, **84**, 235128.
[20] Cheng, Meng (2012). Superconducting proximity effect on the edge of fractional topological insulators. Phys. Rev. B, **86**, 195126.
[21] Clarke, David J., Alicea, J., and Shtengel, K. (2013). Nature Comm., **4**, 1348.
[22] Coleman, S. (1975). Quantum sine-Gordon equation as the massive Thirring model. Phys. Rev. D, **11**, 2088–2097.
[23] Deser, S., Jackiw, R., and Templeton, S. (1982). Three-Dimensional Massive Gauge Theories. Phys. Rev. Lett., **48**, 975–978.
[24] Dirac, P. A. M. (1931). Quantised Singularities in the Electromagnetic Field. Royal Society of London Proceedings Series A, **133**, 60–72.
[25] Dyson, F. J. (1953). The Dynamics of a Disordered Linear Chain. Phys. Rev., **92**, 1331–1338.
[26] Dyson, F. J. (1962). The Threefold Way. Algebraic Structure of Symmetry Groups and Ensembles in Quantum Mechanics. Journal of Mathematical Physics, **3**, 1199–1215.
[27] Fendley, P. (2012). J. Stat. Mech., P11020.
[28] Fidkowski, Lukasz and Kitaev, Alexei (2010). Effects of interactions on the topological classification of free fermion systems. Phys. Rev. B, **81**, 134509.
[29] Fidkowski, Lukasz and Kitaev, Alexei (2011). Topological phases of fermions in one dimension. Phys. Rev. B, **83**, 075103.
[30] Foster, Matthew S. and Ludwig, Andreas W. W. (2006). Interaction effects on two-dimensional fermions with random hopping. Phys. Rev. B, **73**, 155104.
[31] Foster, Matthew S. and Ludwig, Andreas W. W. (2008). Metal-insulator transition from combined disorder and interaction effects in hubbard-like electronic lattice models with random hopping. Phys. Rev. B, **77**, 165108.
[32] Foster, Matthew S., Xie, Hong-Yi, and Chou, Yang-Zhi (2014). Topological protection, disorder, and interactions: Survival at the surface of three-dimensional topological superconductors. Phys. Rev. B, **89**, 155140.
[33] Freedman, M., Nayak, C., Shtengel, K., Walker, K., and Wang, Z. (2004). A class of P, T-invariant topological phases of interacting electrons. Annals of Physics, **310**, 428–492.
[34] Fröhlich, J. and Gabbiani, F. (1990). Braid Statistics in Local Quantum Theory. Reviews in Mathematical Physics, **2**, 251–353.

[35] Fu, Liang, Kane, C. L., and Mele, E. J. (2007). Topological insulators in three dimensions. Phys. Rev. Lett., **98**, 106803.
[36] Goldstein, G. and Chamon, C. (2012). Exact zero modes in closed systems of interacting fermions. Phys. Rev. B, **86**, 115122.
[37] Greiter, Martin, Schroeter, Darrell F., and Thomale, Ronny (2014). Parent hamiltonian for the non-abelian chiral spin liquid. Phys. Rev. B, **89**, 165125.
[38] Greiter, Martin and Thomale, Ronny (2009). Non-abelian statistics in a quantum antiferromagnet. Phys. Rev. Lett., **102**, 207203.
[39] Gu, Zheng-Cheng and Wen, Xiao-Gang (2009). Tensor-entanglement-filtering renormalization approach and symmetry-protected topological order. Phys. Rev. B, **80**, 155131.
[40] Gu, Z.-C. and Wen, X.-G. (2012). Symmetry-protected topological orders for interacting fermions – fermionic topological non-linear sigma-models and a group supercohomology theory. ArXiv e-prints.
[41] Gurarie, V. (2011). Single-particle green's functions and interacting topological insulators. Phys. Rev. B, **83**, 085426.
[42] Haldane, F. D. M. (1983). Continuum dynamics of the 1-D Heisenberg antiferromagnet: Identification with the O(3) nonlinear sigma model. Phys. Lett. A, **93**, 464–468.
[43] Haldane, F. D. M. (1983). Fractional quantization of the Hall effect - A hierarchy of incompressible quantum fluid states. Phys. Rev. Lett., **51**, 605–608.
[44] Haldane, F. D. M. (1983). Nonlinear Field Theory of Large-Spin Heisenberg Antiferromagnets: Semiclassically Quantized Solitons of the One-Dimensional Easy-Axis Néel State. Phys. Rev. Lett., **50**, 1153–1156.
[45] Haldane, F. D. M. (1988). Model for a quantum Hall effect without Landau levels: Condensed-matter realization of the "parity anomaly". Phys. Rev. Lett., **61**, 2015–2018.
[46] Haldane, F. D. M. (1995). Stability of Chiral Luttinger Liquids and Abelian Quantum Hall States. Phys. Rev. Lett., **74**, 2090–2093.
[47] Halperin, B. I. (1982). Quantized Hall conductance, current-carrying edge states, and the existence of extended states in a two-dimensional disordered potential. Phys. Rev. B, **25**, 2185–2190.
[48] Hansson, T. H., Oganesyan, V., and Sondhi, S. L. (2004). Superconductors are topologically ordered. Annals of Physics, **313**, 497–538.
[49] Heinzner, P., Huckleberry, A., and Zirnbauer, M. R. (2005). Symmetry Classes of Disordered Fermions. Communications in Mathematical Physics, **257**, 725–771.
[50] Hikami, S. (1980). Renormalization Group Functions of Orthogonal and Symplectic Non-Linear σ Models. Progress of Theoretical Physics, **64**, 1466–1469.
[51] Jackiw, R. and Rebbi, C. (1976). Solitons with fermion number 1/2. Phys. Rev. D, **13**, 3398–3409.
[52] Jeng, M., Ludwig, A. W. W., Senthil, T., and Chamon, C. (2001). Interaction Effects on Quasiparticle Localization in Dirty Superconductors. eprint arXiv:cond-mat/0112044.
[53] Kane, C. L., Fisher, M. P. A., and Polchinski, J. (1994). Randomness at the edge: Theory of quantum Hall transport at filling ν=2/3. Phys. Rev. Lett., **72**, 4129–4132.
[54] Kane, C L and Mele, E J (2005). Quantum spin hall effect in graphene. Phys. Rev. Lett., **95**(22), 226801.
[55] Kane, Charles L and Mele, Eugene J (2005). Z_ {2} topological order and the quantum spin hall effect. Phys. Rev. Lett., **95**(14), 146802.

[56] Kane, C. L., Mukhopadhyay, Ranjan, and Lubensky, T. C. (2002). Fractional quantum hall effect in an array of quantum wires. Phys. Rev. Lett., **88**, 036401.
[57] Khmelnitskii, D. E. (1983). Quantization of Hall conductivity. ZhETF Pisma Redaktsiiu, **38**, 454–458.
[58] Kitaev, Alexei (2009). Periodic table for topological insulators and superconductors. AIP Conf. Proc., **1134**, 22.
[59] Kitaev, A. Y. (2001). Phys.-Usp., **44**, 131.
[60] Klinovaja, J. and Loss, D. (2013). Time-Reversal Invariant Parafermions in Interacting Rashba Nanowires. ArXiv e-prints.
[61] Klinovaja, Jelena and Loss, Daniel (2013). Topological edge states and fractional quantum hall effect from umklapp scattering. Phys. Rev. Lett., **111**, 196401.
[62] Klinovaja, J. and Loss, D. (2014). Integer and fractional quantum Hall effect in a strip of stripes. European Physical Journal B, **87**, 171.
[63] Klitzing, K. V., Dorda, G., and Pepper, M. (1980). New Method for High-Accuracy Determination of the Fine-Structure Constant Based on Quantized Hall Resistance. Phys. Rev. Lett., **45**, 494–497.
[64] König, Markus, Wiedmann, Steffen, Brüne, Christoph, Roth, Andreas, Buhmann, Hartmut, Molenkamp, Laurens W, Qi, Xiao-Liang, and Zhang, Shou-Cheng (2007). Quantum spin hall insulator state in hgte quantum wells. Science, **318**(5851), 766–770.
[65] Kosterlitz, J. M. (1974). The critical properties of the two-dimensional xy model. Journal of Physics C Solid State Physics, **7**, 1046–1060.
[66] Kosterlitz, J. M. and Thouless, D. J. (1973). Ordering, metastability and phase transitions in two-dimensional systems. Journal of Physics C Solid State Physics, **6**, 1181–1203.
[67] Laughlin, R. B. (1981). Quantized Hall conductivity in two dimensions. Phys. Rev. B, **23**, 5632–5633.
[68] Laughlin, R. B. (1983). Anomalous quantum Hall effect - An incompressible quantum fluid with fractionally charged excitations. Phys. Rev. Lett., **50**, 1395–1398.
[69] Lee, Dung-Hai (1994). Network models of quantum percolation and their field-theory representations. Phys. Rev. B, **50**, 10788–10791.
[70] Levin, M. and Stern, A. (2009). Fractional Topological Insulators. Phys. Rev. Lett., **103**(19), 196803.
[71] Levine, H., Pruisken, A. M. M., and Libby, S. B. (1983). Electron delocalization by a magnetic field in two dimensions. Phys. Rev. Lett., **51**, 1915–1918.
[72] Lindner, Netanel H., Berg, Erez, Refael, Gil, and Stern, Ady (2012). Fractionalizing majorana fermions: Non-abelian statistics on the edges of abelian quantum hall states. Phys. Rev. X, **2**, 041002.
[73] Lu, Yuan-Ming and Vishwanath, Ashvin (2012). Theory and classification of interacting integer topological phases in two dimensions: A chern-simons approach. Phys. Rev. B, **86**, 125119.
[74] Lu, Y.-M. and Vishwanath, A. (2013). Classification and Properties of Symmetry Enriched Topological Phases: A Chern-Simons approach with applications to Z2 spin liquids. ArXiv e-prints.
[75] Ludwig, A. W. W., Fisher, M. P. A., Shankar, R., and Grinstein, G. (1994). Integer quantum Hall transition: An alternative approach and exact results. Phys. Rev. B, **50**, 7526–7552.

[76] Luther, A. and Peschel, I. (1975). Calculation of critical exponents in two dimensions from quantum field theory in one dimension. Phys. Rev. B, **12**, 3908–3917.
[77] Mandelstam, S. (1975). Soliton operators for the quantized sine-Gordon equation. Phys. Rev. D, **11**, 3026–3030.
[78] Manmana, Salvatore R., Essin, Andrew M., Noack, Reinhard M., and Gurarie, Victor (2012). Topological invariants and interacting one-dimensional fermionic systems. Phys. Rev. B, **86**, 205119.
[79] Mong, Roger S. K., Clarke, David J., Alicea, Jason, Lindner, Netanel H., Fendley, Paul, Nayak, Chetan, Oreg, Yuval, Stern, Ady, Berg, Erez, Shtengel, Kirill, and Fisher, Matthew P. A. (2014). Universal topological quantum computation from a superconductor-abelian quantum hall heterostructure. Phys. Rev. X, **4**, 011036.
[80] Moore, G. and Read, N. (1991). Nonabelions in the fractional quantum hall effect. Nucl. Phys. B, **360**, 362–396.
[81] Moore, J. E. and Balents, L. (2007). Topological invariants of time-reversal-invariant band structures. Phys. Rev. B, **75**, 121306.
[82] Moore, J. E. and Wen, X.-G. (1998). Classification of disordered phases of quantum Hall edge states. Phys. Rev. B, **57**, 10138–10156.
[83] Mudry, Christopher and Fradkin, Eduardo (1994). Separation of spin and charge quantum numbers in strongly correlated systems. Phys. Rev. B, **49**, 5200–5219.
[84] Naud, J. D., Pryadko, L. P., and Sondhi, S. L. (2000). Quantum Hall bilayers and the chiral sine-Gordon equation. Nucl. Phys. B, **565**, 572–610.
[85] Naud, J. D., Pryadko, L. P., and Sondhi, S. L. (2001). Edge dynamics in quantum Hall bilayers: Exact results with disorder and parallel fields. Phys. Rev. B, **63**(11), 115301.
[86] Neupert, T., Chamon, C., Mudry, C., and Thomale, R. (2014). Wire deconstructionism of two-dimensional topological phases. Phys. Rev. B, **90**(20), 205101.
[87] Neupert, T., Santos, L., Chamon, C., and Mudry, C. (2011). Fractional Quantum Hall States at Zero Magnetic Field. Phys. Rev. Lett., **106**(23), 236804.
[88] Neupert, T., Santos, L., Ryu, S., Chamon, C., and Mudry, C. (2011). Fractional topological liquids with time-reversal symmetry and their lattice realization. Phys. Rev. B, **84**(16), 165107.
[89] Nielsen, H. B. and Ninomiya, M. (1981). A no-go theorem for regularizing chiral fermions. Phys. Lett. B, **105**, 219–223.
[90] Nielsen, H. B. and Ninomiya, M. (1981). Absence of neutrinos on a lattice (I). Proof by homotopy theory. Nucl. Phys. B, **185**, 20–40.
[91] Nielsen, H. B. and Ninomiya, M. (1981). Absence of neutrinos on a lattice (II). Intuitive topological proof. Nucl. Phys. B, **193**, 173–194.
[92] Niu, Q. and Thouless, D. J. (1984). Quantised adiabatic charge transport in the presence of substrate disorder and many-body interaction. Journal of Physics A Mathematical General, **17**, 2453–2462.
[93] Niu, Q., Thouless, D. J., and Wu, Y.-S. (1985). Quantized Hall conductance as a topological invariant. Phys. Rev. B, **31**, 3372–3377.
[94] Oreg, Yuval, Sela, Eran, and Stern, Ady (2014). Fractional helical liquids in quantum wires. Phys. Rev. B, **89**, 115402.
[95] Pollmann, Frank, Turner, Ari M., Berg, Erez, and Oshikawa, Masaki (2010). Entanglement spectrum of a topological phase in one dimension. Phys. Rev. B, **81**, 064439.

[96] Pruisken, A. M. M. (1984). On localization in the theory of the quantized hall effect: A two-dimensional realization of the θs-vacuum. Nucl. Phys. B, **235**, 277–298.
[97] Raghu, S., Qi, Xiao-Liang, Honerkamp, C., and Zhang, Shou-Cheng (2008). Topological mott insulators. Phys. Rev. Lett., **100**, 156401.
[98] Read, N. and Rezayi, E. (1999). Beyond paired quantum hall states: Parafermions and incompressible states in the first excited landau level. Phys. Rev. B, **59**, 8084–8092.
[99] Roy, Rahul (2009). Topological phases and the quantum spin hall effect in three dimensions. Phys. Rev. B, **79**, 195322.
[100] Ryu, S., Mudry, C., Hou, C.-Y., and Chamon, C. (2009). Masses in graphenelike two-dimensional electronic systems: Topological defects in order parameters and their fractional exchange statistics. Phys. Rev. B, **80**(20), 205319.
[101] Ryu, S., Mudry, C., Ludwig, A. W. W., and Furusaki, A. (2012). Global phase diagram of two-dimensional dirac fermions in random potentials. Phys. Rev. B, **85**, 235115.
[102] Ryu, S., Mudry, C., Obuse, H., and Furusaki, A. (2007). Z_2 Topological Term, the Global Anomaly, and the Two-Dimensional Symplectic Symmetry Class of Anderson Localization. Phys. Rev. Lett., **99**(11), 116601.
[103] Ryu, S., Schnyder, A. P., Furusaki, A., and Ludwig, A. W. W. (2010). Topological insulators and superconductors: tenfold way and dimensional hierarchy. New J. Phys., **12**(6), 065010.
[104] Sachdev, Subir and Read, Nick (1991). Large n expansion for frustrated and doped quantum antiferromagnets. Int. J. Mod. Phys. B, **05**, 219–249.
[105] Scharfenberger, Burkhard, Thomale, Ronny, and Greiter, Martin (2011). Non-abelian statistics and a hierarchy of fractional spin liquids in spin-s antiferromagnets. Phys. Rev. B, **84**, 140404.
[106] Schnyder, A. P., Ryu, S., Furusaki, A., and Ludwig, A. W. W. (2008). Classification of topological insulators and superconductors in three spatial dimensions. Phys. Rev. B, **78**(19), 195125.
[107] Schnyder, A. P., Ryu, Shinsei, Furusaki, Akira, and Ludwig, A. W. W. (2009). Advances in theoretical physics: Landau memorial conference. AIP Conf. Proc., **1134**, 10.
[108] Schuch, Norbert, Perez-Garcia, David, and Cirac, Ignacio (2011). Classifying quantum phases using matrix product states and projected entangled pair states. Phys. Rev. B, **84**, 165139.
[109] Seroussi, I., Berg, E., and Oreg, Y. (2014). Topological superconducting phases of weakly coupled quantum wires. Phys. Rev. B, **89**(10), 104523.
[110] Shockley, W. (1939). On the Surface States Associated with a Periodic Potential. Phys. Rev., **56**, 317–323.
[111] Simon, B. (1983). Holonomy, the Quantum Adiabatic Theorem, and Berry's Phase. Phys. Rev. Lett., **51**, 2167–2170.
[112] Sondhi, S. L. and Yang, Kun (2001). Sliding phases via magnetic fields. Phys. Rev. B, **63**, 054430.
[113] Stormer, H. L., Chang, A., Tsui, D. C., Hwang, J. C. M., Gossard, A. C., and Wiegmann, W. (1983). Fractional quantization of the hall effect. Phys. Rev. Lett., **50**, 1953–1956.
[114] Su, W. P., Schrieffer, J. R., and Heeger, A. J. (1980). Soliton excitations in polyacetylene. Phys. Rev. B, **22**, 2099–2111.
[115] Tamm, I. (1932). On the possible bound states of electrons on a crystal surface. Phys.

Z. Soviet Union, **1**, 733.
[116] Teo, Jeffrey C. Y. and Kane, C. L. (2014). From luttinger liquid to non-abelian quantum hall states. Phys. Rev. B, **89**, 085101.
[117] Thouless, D. J., Kohmoto, M., Nightingale, M. P., and den Nijs, M. (1982). Quantized Hall Conductance in a Two-Dimensional Periodic Potential. Phys. Rev. Lett., **49**, 405–408.
[118] Tsui, D. C., Stormer, H. L., and Gossard, A. C. (1982). Two-Dimensional Magnetotransport in the Extreme Quantum Limit. Phys. Rev. Lett., **48**, 1559–1562.
[119] Turner, Ari M., Pollmann, Frank, and Berg, Erez (2011). Topological phases of one-dimensional fermions: An entanglement point of view. Phys. Rev. B, **83**, 075102.
[120] Vaezi, Abolhassan (2013). Fractional topological superconductor with fractionalized majorana fermions. Phys. Rev. B, **87**, 035132.
[121] Vaezi, Abolhassan (2014). Superconducting analogue of the parafermion fractional quantum hall states. Phys. Rev. X, **4**, 031009.
[122] Wang, Zhong and Zhang, Shou-Cheng (2012). Simplified topological invariants for interacting insulators. Phys. Rev. X, **2**, 031008.
[123] Wegner, F. J. (1976). Electrons in disordered systems. Scaling near the mobility edge. Zeitschrift fur Physik B Condensed Matter, **25**, 327–337.
[124] Wen, X. G. (1990). Electrodynamical properties of gapless edge excitations in the fractional quantum Hall states. Phys. Rev. Lett., **64**, 2206–2209.
[125] Wen, X. G. (1990). Topological Orders in Rigid States. International Journal of Modern Physics B, **4**, 239–271.
[126] Wen, X. G. (1991). Edge Excitations in the Fractional Quantum Hall States at General Filling Fractions. Modern Physics Letters B, **5**, 39–46.
[127] Wen, X.-G. (1991). Edge transport properties of the fractional quantum Hall states and weak-impurity scattering of a one-dimensional charge-density wave. Phys. Rev. B, **44**, 5708–5719.
[128] Wen, X.-G. (1991). Topological Orders and Chern-Simons Theory in Strongly Correlated Quantum Liquid. International Journal of Modern Physics B, **5**, 1641–1648.
[129] Wen, X. G. and Niu, Q. (1990). Ground-state degeneracy of the fractional quantum Hall states in the presence of a random potential and on high-genus Riemann surfaces. Phys. Rev. B, **41**, 9377–9396.
[130] Witten, E. (1984). Non-abelian bosonization in two dimensions. Communications in Mathematical Physics, **92**, 455–472.
[131] Xu, C. and Moore, J. E. (2006). Stability of the quantum spin Hall effect: Effects of interactions, disorder, and Z_2 topology. Phys. Rev. B, **73**(4), 045322.
[132] Yakovenko, Victor M. (1991). Quantum hall effect in quasi-one-dimensional conductors. Phys. Rev. B, **43**, 11353–11366.
[133] Zirnbauer, M. R. (1996). Riemannian symmetric superspaces and their origin in random-matrix theory. Journal of Mathematical Physics, **37**, 4986–5018.